Metabolic PET Tracers for Neuroendocrine Tumors

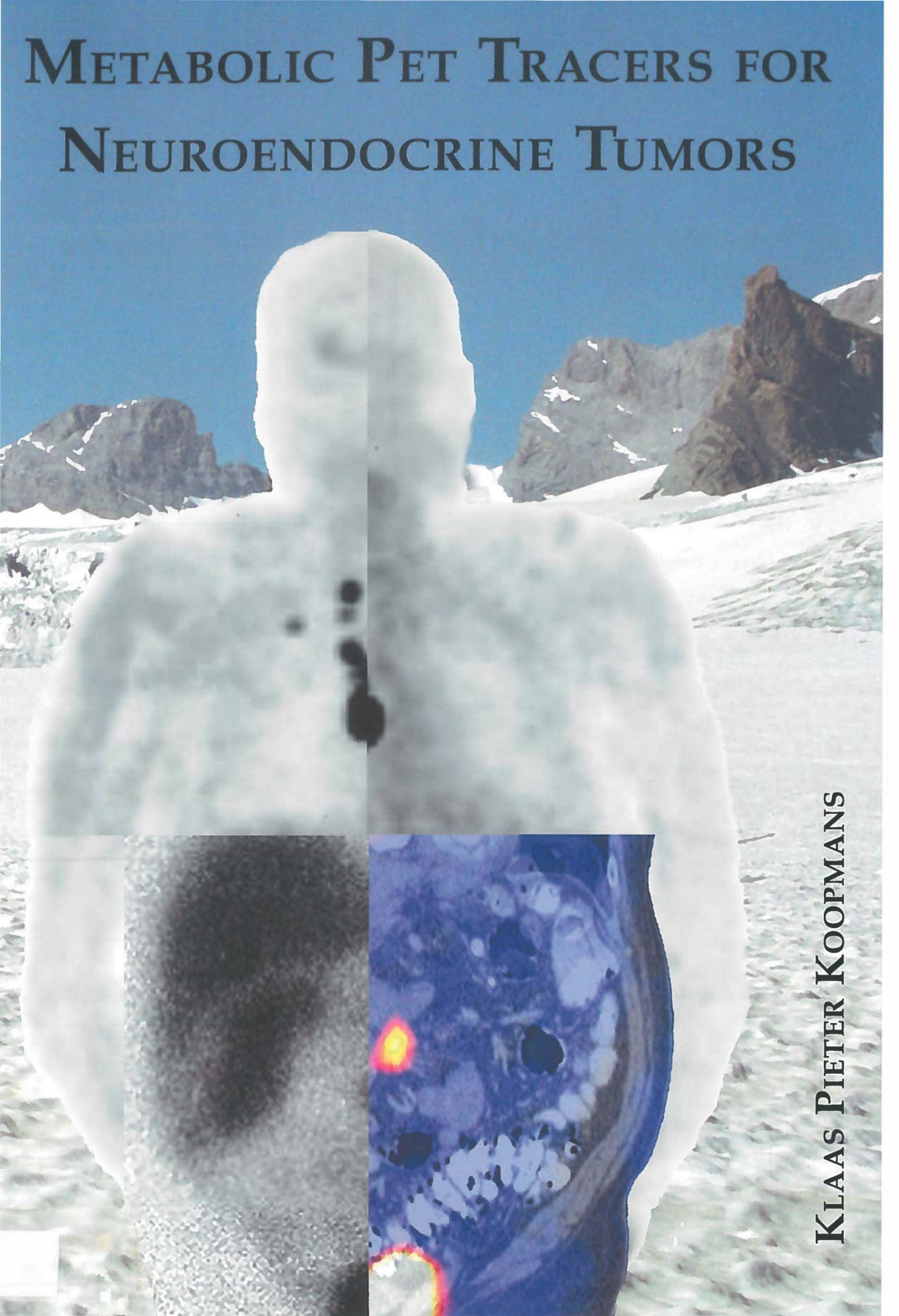

Klaas Pieter Koopmans

Metabolic PET tracers for neuroendocrine tumors

Klaas Pieter Koopmans

Stellingen behorende bij het proefschrift

Metabolic PET tracers for neuroendocrine tumors

1. Voor stadiëring van een patient met een carcinoid is de ^{18}F-DOPA PET scan de eerste keus voor beeldvorming. (dit proefschrift)

2. Voor het stadiëren van patiënten met medullair schildkliercarcinoom en verhoogde tumormarkers is de ^{18}FDOPA PET scan beter dan de ^{18}F-FDG PET scan. (dit proefschrift)

3. Het verschil in opname tussen ^{18}F-DOPA en ^{11}C-HTP bij carcinoiden en eilandjesceltumoren wordt verklaard door de verschillen in het intracellulaire tracermetabolisme en de traceropslag. (dit proefschrift)

4. Patiënten met eilandjesceltumoren moeten gestadieerd worden middels een PET-CT met ^{11}C-5-HTP als tracer. (dit proefschrift)

5. Alleen voor de diagnostiek van het medullair schildkliercarcinoom is er nog een beperkte plek voor de ^{99m}Tc-V-DMSA scan. (dit proefschrift)

6. De MIBG scan heeft een beperkte waarde bij paragangliomen. (dit proefschrift)

7. Ook bij de PET-CT machines heeft softwarematige beeldfusie middels elastische vervorming ("warping") meerwaarde voor de thorax en lever.

8. Om patiënten met neuroendocriene tumoren optimaal te kunnen behandelen, moeten deze patienten uitsluitend in gespecialiseerde centra gestadieerd en behandeld worden.

9. Juist voor astmatici is het van belang bij bergbeklimmingen tot >3200m acetazolamide te gebruiken om hunverhoogde risico op acute mountain sickness en/of High Altitude Pulmonary Edema te minimaliseren.

10. Om hoogte acclimatisatie bij bergsporters goed in te kunnen schatten moeten zowel psychische als lichamelijke factoren worden afgewogen met bijvoorbeeld de DARIX index.

11. Door het uitlogen van zware metalen uit vliegas (afvalproduct van de huisvuilverbranding) in de bodem wordt het milieu belast. De mate van uitlogen is te voorspellen middels complexe theoretische modellen.

12. Nucleaire geneeskunde is als fotografie: de kwaliteit en beoordeling van de afbeeldingen is niet volledig afhankelijk van de prijs en complexiteit van de apparatuur, maar met name van de mensen die de apparatuur bedienen.

13. "Ook het schrijven van een proefschrift begint met een enkel woord." (vrij naar Laozi, grondlegger van het Taoisme, 600 v Chr - 470 v Chr)

14. De General Aviation (ook wel kleine luchtvaart genoemd) is de kraamkamer voor de grote luchtvaart en dient meer door de lokale en landelijke overheden ondersteund te worden.

Klaas Pieter Koopmans
23 januari 2008

The research presented in this thesis was part of the research project named "Metabolic characterization and localization of neuroendocrine tumors and their metastases using positron emission tomography", funded by the Dutch Cancer Society, grant 2003-2936

Financial support was kindly provided by:
Siemens Medical Solutions, Den Haag
Veenstra Instruments Joure

ISBN:	978-90-367-3327-4
ISBN:	978-90-367-3328-1 (electronic version)
Printed by:	Gildeprint Drukkerijen B.V., Enschede - www.gildeprint.nl
layout:	Gildeprint Drukkerijen B.V., Enschede en www.estherontwerpt.nl

RIJKSUNIVERSITEIT GRONINGEN

Metabolic PET tracers for neuroendocrine tumors

Proefschrift

ter verkrijging van het doctoraat in de
Medische Wetenschappen
aan de Rijksuniversiteit Groningen
op gezag van de
Rector Magnificus, dr. F. Zwarts,
in het openbaar te verdedigen op
woensdag 23 januari 2008
om 14:45 uur

door

Klaas Pieter Koopmans
geboren op 11 mei 1973
te Leeuwarden

Promotores

prof. dr. E.G.E. de Vries

prof. dr. P.L. Jager

Co-promotores

dr. I.P. Kema

dr. P.H. Elsinga

Beoordelingscommissie

prof. dr. C.J.M. Lips

prof. dr. M.J.H. Slooff

prof. dr. W.J.G. Oyen

"Opgedragen aan mijn vader, Pieter Klaas Koopmans
29 juni 1944 - 25 december 1997
die deze wereld helaas veel te vroeg heeft verlaten."

Paranimfen
Jeroen Dijkstra
Ali Agool

Contents

Chapter one

Introduction

INTRODUCTION

Neuroendocrine tumors originate from the diffuse neuroendocrine system. Embryologically the diffuse neuroendocrine system is derived from the neuroectoderm and the endoderm (gut).[1,2] The function of diffuse neuroendocrine system cells is to regulate neighbouring cells (paracrine regulation) by the excretion of biologically active amines and hormones. For the production of these hormones, the diffuse neuroendocrine system cells are specialized to be able to take up amino acids precursors and decarboxylate them. This process, also known amino precursor uptake and decarboxylation (APUD), is a common biochemical property of neuroendocrine (tumor-) cells. Neuroendocrine tissues and cells are involved in the regulation of numerous processes within the body and can be found in almost every organ. A large variety of biologically active substances can be produced depending on the required function. Important active pathways are the catecholamine and serotonin pathway.

Neuroendocrine tumors are often slowly growing and well differentiated tumors that can produce a large variety of biologically active products. They are rare tumors, which form only approximately 0.49% of all malignancies.[3] Most neuroendocrine tumors arise in the gut (these are also known as carcinoids, of which approximately 60% have their primary localization in the intestine), but all other organ sites are possible. Originally carcinoids were classified based on the embryologic origin of their 'parent tissue' and divided into three groups (table 1); foregut, midgut and hindgut. Each subgroup has a characteristic hormonal secretion pattern. Until recently there was no classification system for other neuroendocrine tumor types. However, the World Health Organization has proposed a new classification method for all neuroendocrine tumors. This classification is based on histopathologic characteristics consisting of cellular grading, primary tumor size, primary tumor localization, proliferation markers, degree of invasiveness and the production of biologically active substances. The main categories defined by this classification are the well differentiated endocrine tumors with a low grade of malignancy, well differentiated, more aggressive carcinomas, poorly differentiated endocrine carcinomas with a high grade of malignancy and a poor prognosis and finally mixed exocrine–endocrine tumors. In this WHO classification the term carcinoid is abandoned and replaced by neuroendocrine tumor. [4]

Due to the slow growth and vague non-specific symptoms caused by carcinoids and many other neuroendocrine tumors, these tumors are frequently extensively metastasized at first presentation. The only curative treatment for most neuroendocrine tumors is surgery. There has been a trend to more aggressive surgical treatment including debulking and even liver transplantation. When cure is not possible, reducing tumor bulk can still be of interest for these patients.[5] Substances produced by carcinoid tumors can cause severe symptoms, such as diarrhea, flushing, hypo- or hypertensive crisis, etc. For curative treatment of carcinoids, no systemic treatment options are currently available. In these indolent tumors

Table 1. Classical classification of carcinoids based on embryologic origin

Embryologic origin	Tumor types	Secretion products
Foregut carcinoids	Bronchopulmonary neuroendocrine tumor Thymic neuroendocrine tumor Esophageal carcinoid Gastric carcinoid Duodenal carcinoid Pancreatic neuroendocrine tumor	5-HTP, histamine, multiple peptides
Midgut carcinoids	Small intestine carcinoids Appendiceal carcinoids Carcinoids of ascending colon Liver	Serotonin (5-HT), catecholamines, bradykinin, prostaglandin, substance p, neurokinin A, other peptides
Hindgut carcinoids	Carcinoids of transverse and descending colon Rectal carcinoids	Usually non-secretory

somatostatin analogs and interferon can be used to control symptoms caused by hormone secretion and to slow down tumor growth.[6] For certain subtypes, such as pancreatic islet cell tumors, curative systemic treatment in the form of chemotherapy is available.[6] Currently several new targeted drugs are available and are expected to find their place in standard treatment in the future.

For the right treatment choices optimal insight in the extent of the disease is of utmost importance. Morphologic imaging methods for assessing tumor spread, such as CT, MRI and ultrasound, are almost always used in conjunction with nuclear medicine imaging techniques. Several well-known tracers, such as ^{111}In-octreotide (SRS), ^{123}I-meta-iodo-benzylguanidine (MIBG), ^{18}FDG and ^{99m}Tc-V-Dimercapto succinyl acid (DMSA), are used for this purpose. However availability of ^{18}F-dihydroxyphenylalanine (^{18}F-DOPA) tracer(7) and development of the ^{11}C-5-Hydroxy-tryptophan (HTP) tracer [8] in our center allowed us to study neuroendocrine tumors with these new tracers. The rationale for the use of these tracers is the biochemical activity of neuroendocrine tumors and their active production of catecholamines and serotonin. ^{18}F-DOPA is used as a precursor for the catecholamine pathway [9], whereas ^{11}C-5-HTP [10] is used as a precursor for the serotonin pathway. Both tracers are taken up actively via large amino acid transporters and subsequently metabolized by their respective pathways to end products. These end products (such as noradrenalin and dopamine for the catecholamine pathway and serotonin for the serotonin pathway) are stored in vesicles, ready for secretion. This is in contrast to the receptor approach in which the overexpression of somatostatin receptors on the cellular membrane is exploited. [11] Somatostatin can be labeled with isotopes and these molecules will then bind to the extracellular receptors.[12] The thus formed complexes are taken up (interiorized) in

lysosomes where these receptor-tracer complexes are broken down.[13] However, the receptor density between tumor cells can vary within an individual, which can lead to false negative results.

Accurate knowledge of biochemical behavior and tumor localization is of interest for patient tailored therapy. Since somatostatin receptor scintigraphy is unable to detect all tumor lesions, other imaging methods are warranted. Exploiting the metabolic properties by using precursors for the metabolic pathways as tracers seems to be a potential interesting approach.

Aim of this thesis

The aim of this thesis is to study the value of new tracers for scanning neuroendocrine tumors in comparison with established imaging methods with an emphasis on the metabolic PET tracers 6-[F-18]fluoro-L-dihydroxyphenylalanin (^{18}F-DOPA) and β-[11C]-5-hydroxy-L-tryptophan (^{11}C-5-HTP). For this purpose several neuroendocrine tumor subtypes were studied.

Outline of this thesis

Chapter 2 gives an extensive literature overview of tracers used in nuclear medicine to detect neuroendocrine tumors. First, it describes the mechanisms of tracer uptake in neuroendocrine tumors. Secondly, it gives an overview of the diagnostic value of these tracers for most neuroendocrine tumor subtypes. This review tries to position the currently used nuclear medicine techniques such as somatostatin receptor scintigraphy (SRS) with the newly available metabolic tracers. These data can potentially be used for better treatment choices in these patients.

Chapter 3 describes the study which aims to compare the value of ^{18}F-DOPA PET imaging in patients with carcinoid tumors with the results of morphological imaging using CT, and functional whole body imaging using SRS. A total of 53 patients were studied. These results were compared with biochemical parameters of the catecholamine and serotonin pathways.

Chapter 3a . In this chapter a patient is described in which the intravenous injection of ^{18}F-DOPA resulted in a carcinoid crisis. The implications of this finding are addressed.

In **Chapter 4 the** study is described which aims to establish the diagnostic value of tracers ^{18}F-DOPA and ^{11}C-5-HTP for patients with carcinoid disease and islet cell tumors.

Patients with carcinoid (n=24) and patients with pancreatic islet cell tumors (n=23) all underwent PET imaging with the ^{18}F-DOPA and ^{11}C-5-HTP tracer as well as, CT and functional imaging with SRS Carcinoid tumors and pancreatic islet cell tumors differ in metabolic behavior. Carcinoid tumors are often biochemically active and can produce large amounts of serotonin and catecholamine metabolites. Of all pancreatic islet cell tumors, approximately 60 % are hormonal active and can produce a variety of products.[14]

Chapter 5 aims to detect the value of ^{18}F-DOPA PET and FDG PET in 21 patients with recurrent medullary thyroid carcinoma as defined by rising tumor markers Results of morphologic imaging, ^{18}F- FDG PET, ^{99m}Tc-V-DMSA scintigraphy and ^{18}F-DOPA PET were compared. We hypothesized that tumor marker kinetics for medullary thyroid carcinoma and markers for the catecholamine and serotonin pathway might be useful to analyze whether the course of the disease progression can tailor imaging for individual patients.

Chapter 6 focuses on the value of SRS and ^{123}I-MIBG for the detection of paraganglioma. In 29 patients SRS, MIBG and CT were compared. Biochemical markers for the catecholamine pathway were collected to establish any possible relationship between tracer uptake and hormone production by the tumor.

Chapter 7 contains the summary and addresses future perspectives.

In **Chapter 8** an outline of this thesis is given in Dutch together with introductory information for those unfamiliar with nuclear medicine and neuroendocrine tumors.

REFERENCES

1. Rawdon BB, Andrew A: Origin and differentiation of gut endocrine cells. Histol Histopathol 8:567-580, 1993
2. Andrew A, Kramer B, Rawdon BB: The origin of gut and pancreatic neuroendocrine (APUD) cells-the last word? J Pathol 186:117-118, 1998
3. Modlin IM, Lye KD, Kidd M: A 5-decade analysis of 13,715 carcinoid tumors. Cancer 97:934-959, 2003
4. Solcia E, Kloppel G, Sobin LH, et al: Histological typing of endocrine tumours. Heidelberg, World Health Organization, 2000,
5. Akerstrom G, Hellman P: Surgery on neuroendocrine tumours. Best Pract Res Clin Endocrinol Metab 21:87-109, 2007
6. Oberg K: Chemotherapy and biotherapy in the treatment of neuroendocrine tumours. Ann Oncol 12 Suppl 2:S111-S114, 2001
7. Vries EFJ, Luurtsema G, Brussermann M, et al: Fully automated synthesis module for the high yield one-pot preparation of 6-[18F]-fluoro-L-DOPA. Appl Radiat Isot 51:389-419, 1999
8. Neels OC, Jager P.L., Koopmans K.P., et al: Development of a reliable remote-controlled synthesis of β-[^{11}C]-5-hydroxy-L-tryptophan on a Zymark robotic system. J Labelled Comp Radiopharm 49:889-895, 2006
9. Boyes BE, Cumming P, Martin WR, et al: Determination of plasma [18F]-6-fluorodopa during positron emission tomography: elimination and metabolism in carbidopa treated subjects. Life Sci 39:2243-2252, 1986
10. Sundin A, Eriksson B, Bergstrom M, et al: Demonstration of [11C] 5-hydroxy-L-tryptophan uptake and decarboxylation in carcinoid tumors by specific positioning labeling in positron emission tomography. Nucl Med Biol 27:33-41, 2000
11. Reubi JC, Hacki WH, Lamberts SW: Hormone-producing gastrointestinal tumors contain a high density of somatostatin receptors. J Clin Endocrinol Metab 65:1127-1134, 1987
12. Krenning EP, Kwekkeboom DJ, Bakker WH, et al: Somatostatin receptor scintigraphy with [111In-DTPA-D-Phe1]- and [123I-Tyr3]-octreotide: the Rotterdam experience with more than 1000 patients. Eur J Nucl Med 20:716-731, 1993
13. Hofland LJ, Lamberts SW: The pathophysiological consequences of somatostatin receptor internalization and resistance. Endocr Rev 24:28-47, 2003
14. Heitz PU, Komminoth P, Perren A: Pancreatic endocrine tumours: introduction, In: RA DeLellis, RV Lloyd, PU Heitz, and et al. (ed): Pathology and genetics: tumours of endocrine organs. WHO classification of tumors. Lyon, IARC Press, 2004, pp 177-182

Chapter two

Molecular imaging in neuroendocrine tumors: molecular uptake mechanisms and clinical results

Klaas P. Koopmans[1], Oliver N. Neels[1], Ido P. Kema[2], Philip H. Elsinga[1], Thera P. Links[3], Elisabeth G.E. de Vries[4], Pieter L. Jager[1]

Departments of Nuclear Medicine and Molecular Imaging[1], Clinical Chemistry[2], Endocrinology[3], Medical Oncology[4], University of Groningen and University Medical Centre Groningen, P.O. Box 30.001, 9700 RB Groningen, The Netherlands

This work was supported by project grant 2003-2936 from the Dutch Cancer Society.

Provisionally accepted

ABSTRACT

Neuroendocrine tumors can originate almost everywhere in the body and consist of a great variety of subtypes. This paper focuses on molecular imaging methods using nuclear medicine techniques in neuroendocrine tumors, coupling molecular uptake mechanisms of radiotracers with clinical results. A non-systematic review is presented on receptor based and metabolic imaging methods. Receptor-based imaging covers the molecular backgrounds of somatostatin, vaso-intestinal peptide (VIP), bombesin and cholecystokinin (CCK) receptors and their link with nuclear imaging. Imaging methods based on specific metabolic properties include meta-iodo-benzylguanide (MIBG) and dimercapto-sulphuric acid (DMSA-V) scintigraphy as well as more modern positron emission tomography (PET) based methods using radiolabeled analogues of amino acids, glucose, dihydroxyphenylalanine (DOPA), dopamine and tryptophan. Diagnostic sensitivities are presented for each imaging method and for each neuroendocrine tumor subtype. Finally, a Forest plot analysis of diagnostic performance is presented for each tumor type in order to provide a comprehensive overview for clinical use.

1. INTRODUCTION

Neuroendocrine tumors are unique and rare tumors originating from neuroendocrine cells. These neuroendocrine cells are postulated to arise from common precursor cells of the embryologic neural crest and are dispersed throughout the human body. Characteristic is a common phenotype consisting of the simultaneous expression of general protein markers of neuroendocrine cells and hormonal products specific to each cell type.[1] The main function of neuroendocrine cells is to regulate a large variety of body functions through paracrine action with dedicated amines and peptides, of which the "biogenic amines", such as serotonin and catecholamines, are most prominent. In order to be able to synthesize these amines, neuroendocrine cells have the ability to take-up and decarboxylate amine precursors (APUD; amine precursor uptake and decarboxylation). Other biogenic amines, substances such as adrenocorticotrophic hormone, growth hormone, neuropeptide K, substance P, bradykinin, kallikrein and prostaglandins can also be secreted.[2,3] Neuroendocrine tumors arise in nearly every organ but primary sites in gastrointestinal (56%) and bronchopulmonary (12%) tracts are most frequent.[4]

Due to the slow growth of most neuroendocrine tumors and the long time span between the onset of symptoms, many patients present with metastases (figure 1).

Even with advanced disease, patients may survive for many years. However, there are also subtypes, which behave more aggressively. The diagnosis is based on histology and can be considered when specific symptoms induced by tumor products are present, such as diarrhea

or flushing. Apart from clinical symptoms, determination of tumor secretory products using biochemical assays can assist in obtaining a diagnosis.

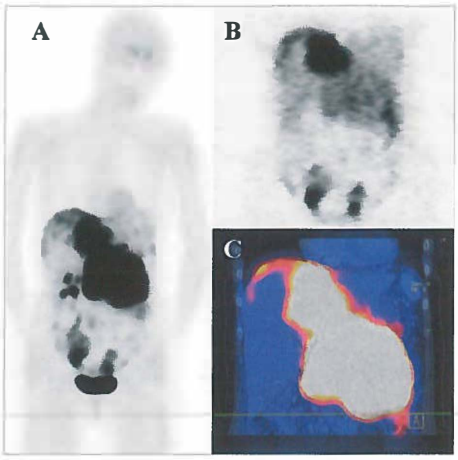

Figure 1. Metastasized carcinoid.
^{18}F-DOPA PET scan (A), Octreotide scan (B) and ^{18}F-DOPA PET-CT fusion image (C) of a female patient presenting with a metastasized carcinoid. This patient illustrates the intra-individual heterogeneity in the uptake of different tracers by tumor metastases (arrows).

A division based on the embryological origin of the organs in which neuroendocrine tumors arise has been made in the past. This division classifies these tumors as foregut, midgut and hindgut tumors. However, the recent World Health Organization (WHO) classification of the different subtypes of neuroendocrine tumors of gastro-intestinal and pancreatic origin is based on histopathologic characteristics consisting of cellular grading, primary tumor size, primary tumor localization, proliferation markers, degree of invasiveness and the production of biologically active substances. The main categories defined by this classification are the well differentiated endocrine tumors with a low grade of malignancy, well differentiated, more aggressive carcinomas, poorly differentiated endocrine carcinomas with a high grade of malignancy and a poor prognosis and finally mixed exocrine–endocrine tumors. In this WHO classification the term carcinoid is abandoned and replaced by neuroendocrine tumor. [5]

Currently, there is a broad variety of treatment options for patients with neuroendocrine tumors. Surgery is the only curative option. When cure is not possible, palliative treatment aims to control symptoms, maintain local tumor control and prolong life. Palliative procedures include surgical debulking, correction of bowel obstruction, chemo-embolizations, or systemic treatment using interferon-α or somatostatin analogues.[2] Other treatment options

are chemotherapy and radionuclide therapy. New targeted therapies such as anti-angiogenic therapies are currently being explored.[4,6,7]

Accurate localization of tumor lesions can guide treatment decisions. In general, radiological techniques such as CT, ultrasound or MRI are applied in staging and restaging, but also nuclear medicine techniques, such as somatostatin receptor scintigraphy (SRS), have proven to be of great value. The presence of somatostatin receptors on many neuroendocrine tumors was the driving force that enabled the development of SRS. Besides receptors, the remarkable metabolic activity of specific biochemical pathways used in substance synthesis provides possibilities for molecular nuclear medicine imaging.

The unique characteristics of neuroendocrine tumors have led to the development of interesting new diagnostic methods for these tumors over the last years, both in receptor imaging and metabolic imaging. Especially the increase in positron emission tomography (PET) facilities allows developments of tracers for new molecular targets with a high-resolution method for imaging. In addition new insights in the genetic, biochemical and metabolic aspects of subtypes of the neuroendocrine tumor family have arisen over the last years. It is therefore important to understand the receptor and metabolic targets for neuroendocrine tumors, as the molecular mechanisms that drive tracer uptake, translate into images and determine the final clinical applicability.

The unique characteristics of neuroendocrine tumors are increasingly exploited to successfully enhance our imaging and therapeutical options for these tumors. Three directions can be seen in the development of new tracers for imaging use. The first uses tumor receptor expression, the second uses the metabolic properties and the last method uses antibodies. Therefore, the purpose of this review is to describe the receptor and metabolic imaging methods of neuroendocrine tumors and translate the molecular uptake mechanisms into clinical parameters such as sensitivity and specificity. For this purpose, a review of current literature is presented, both for imaging methods and for tumor types.

2. SEARCH STRATEGY AND SELECTION CRITERIA

For this non-systematic review, a Medline and PubMed search was performed. Due to the many subtypes of neuroendocrine tumor and imaging methods a multitude of different search terms was necessary. A detailed list is available on request. Only papers with an English abstract published over the last 10 years (1995) were included. Material from review articles also referring to older studies was evaluated and was used if relevant. Reference lists of individual papers were also analyzed for study selection. Only studies from which a clear description of sensitivity or specificity for individual tumor subgroups could be derived, were included. Data from all sources were sorted and divided over subcategories

of tracer and tumor type. In general, studies with fewer than 10 subjects were excluded, however, due to the rarity of a number of tumor types, some of these reports or small studies were included. The number of patients included in the studies was used as a weight factor in summarizing results for different tracers and is represented by a square in the Forest plot analysis. The size of the square represents the weight that the studies exert in the analysis. Sensitivity values given in the figures denote a lesion-based sensitivity for the detection of all types of tumor deposits.

3. NUCLEAR IMAGING METHODS

The methods for nuclear imaging of neuroendocrine tumors can be divided in three main categories, namely tracers based on a) the selective expression of different receptors, b) metabolic properties of tumors and c) tracers which exploit antigens expressed by the tumors. For each category, currently available tracers will be described and their clinical impact. A schematic overview of the uptake mechanisms of these tracers can be found in figure 2.

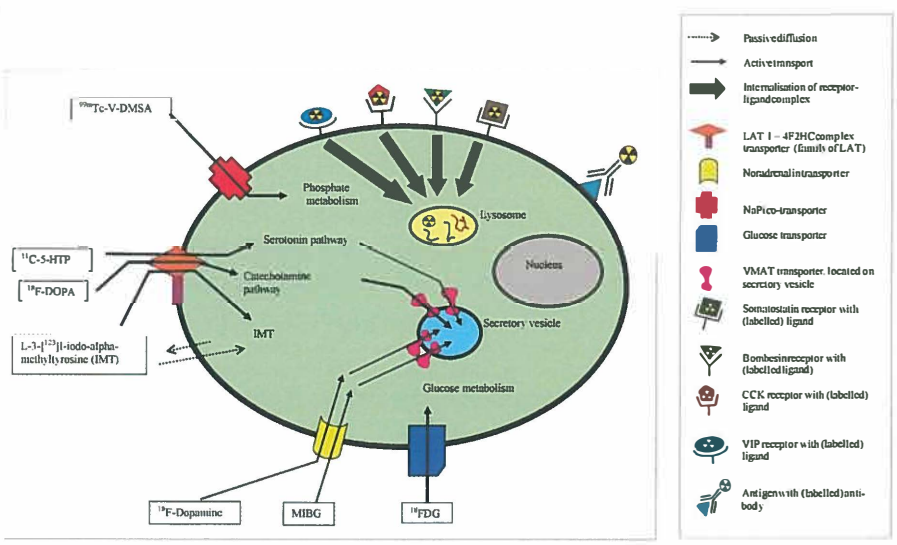

Figure 2. Metabolic pathways.
In this figure the different metabolic pathways by which neuroendocrine tumors can be visualized using nuclear medicine imaging techniques are schematically depicted. Three major routes can be identified: receptor based techniques, techniques which use the metabolic properties of these tumors and labeled antibody based techniques.

A general principle in nuclear medicine is that detectability of lesions primarily depends on the amount of tracer localized in a lesion, and only indirectly on the size of that lesion. In theory a 1 mm lesion can be detected as long as there is enough tracer uptake. On the images, such a lesion will result in a 'hot-spot' with larger dimensions and vague borders. This is especially true for imaging with gamma cameras, such as SPECT, which have a considerable lower spatial resolution than methods based on PET. A prerequisite for molecular uptake mechanisms therefore is that the magnitude of tracer uptake is high and the background uptake low. In daily practice of commonly used tracer methods, these principles translate into a detection limit of 1-2 cm for conventional gamma camera imaging and 0.5-1 cm for PET imaging.

3.1 Receptor based imaging methods

3.1.1. *Somatostatin receptor imaging*

Currently somatostatin receptor imaging is the method of choice for the staging of neuroendocrine tumors.[8] Somatostatin is a small regulatory peptide, which is widely distributed in the human body. Besides its function as a neurotransmitter in the hypothalamus, it has an inhibitory effect on the production of several exocrine hormones in the gastrointestinal tract and anti-proliferative effects.[9] Somatostatin receptors are G protein coupled receptors on the cell membrane which recognize the ligand and generate a trans-membrane signal. The resulting hormone-receptor complexes have the ability to be internalized. Once internalized, these vesicles fuse with lysosomes, resulting in hormone degradation or receptor recycling.[10] Thus far, 6 different somatostatin receptors have been cloned, namely sst_1-sst_5 (sst_2 can be alternately spliced to yield two products, sst_{2A} and sst_{2B}).

Neuroendocrine tumors frequently express a high density of somatostatin receptors, which is exploited by imaging techniques using somatostatin analogues. These analogues have been developed because somatostatin itself has a very short plasma half life (~ 3 min). For most somatostatin analogues internalization of the ^{111}In-octreotide complex with residualization of the ^{111}In label is the most likely mechanism accounting for the good scintigraphic tumor to background ratio observed 24 h after injection.[11] Currently radio-labeled analogues of somatostatin such as octreotide, vapreotide and MK678, are in clinical use for imaging. All octreotide analogues bind with high affinity to sst2 and sst5 and with varying affinity to the sst3 and sst4 receptors. When chelators such as DTPA or DOTA are coupled to somatostatin analogues, these molecules can thereafter be labeled with for instance ^{111}In or ^{99m}Tc for scintigraphic purposes. When labeled with positron emitting isotopes, such as ^{18}F, ^{64}Cu or ^{68}Ga the somatostatin analogues can be used for PET imaging.[12,13] There are many new developments in newer better chelators (i.e. DOTA, EDDA or HYNIC) and analogues with more rapid internalization properties.[14]

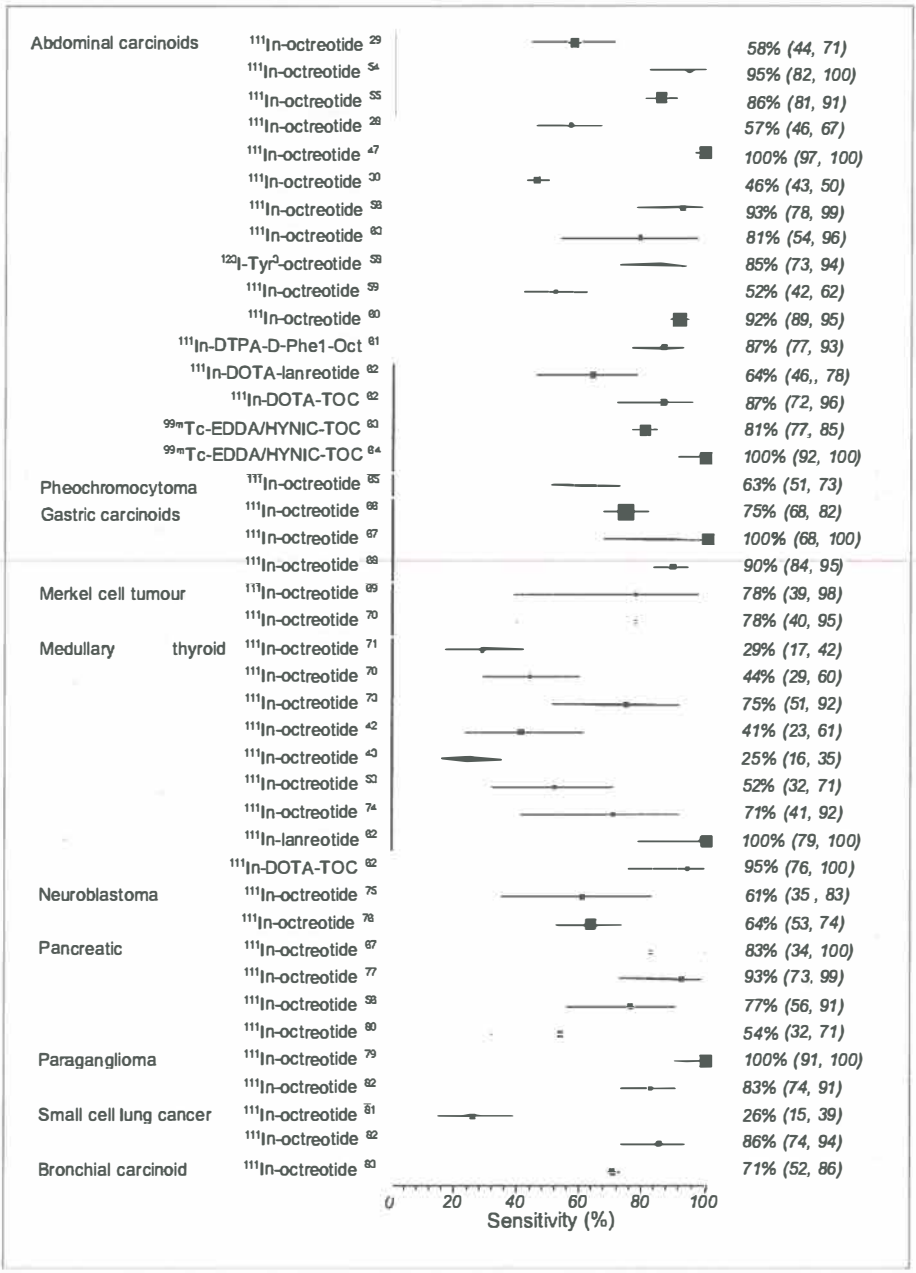

Figure 3. Forest plot analysis of SRS imaging per tumor type.

Results of SRS imaging sorted per tumor type in a Forest plot analysis. On the left side of this plot the tumor type is given with the tracers used in the presented studies. On the right side sensitivities from literature data are given with their calculated confidence interval. The size of the solid black square represents the weight the corresponding study exerts in this analysis and is calculated using the number of patients included (Mantel-Haenszel weight).

Based on the high receptor expression, somatostatin receptor imaging using ^{111}In-octreotide provides important information on tumor localizations of many neuroendocrine tumors. SRS is now widely available, and yields the best results in paragangliomas and neuroendocrine gastrointestinal tumors (87 and 88% sensitivity). SRS is least suitable for medullary thyroid carcinoma (44% sensitivity). In general the SRS whole body scan information is complementary to the more focal information given by CT or MRI. In figure 3 literature results are summarized in a Forest plot.

The three imaging methods described below, namely VIP, bombesin and CCK receptor imaging, are still experimental and are not yet available for routine clinical use. In figure 4 results for VIP, CCK and antibody imaging are presented.

3.1.2. *Vasoactive intestinal peptide receptor imaging (VIP)*

VIP and pituitary adenylate cyclase activating peptide (PACAP), both member of the secretin like peptides, are neuropeptides which regulate a broad spectrum of biological activities, including vasodilatation, stimulation of secretion of various hormones, immunomodulation and promotion of cell proliferation. There are two groups of receptors, namely $VPAC_1$ and $VPAC_2$, which are receptors with high affinity for VIP, PACAP and PAC_1, which is characterized, by a high affinity for PACAP but a low affinity for VIP. These receptors function through two distinct G-protein-coupled receptor subtypes that can also be internalized.[15] $VPAC_1$ is expressed in most epithelial tissues and the brain, while $VPAC_2$ is only present in smooth muscle. Subsequently, these receptors are expressed in tumors derived from these tissues.

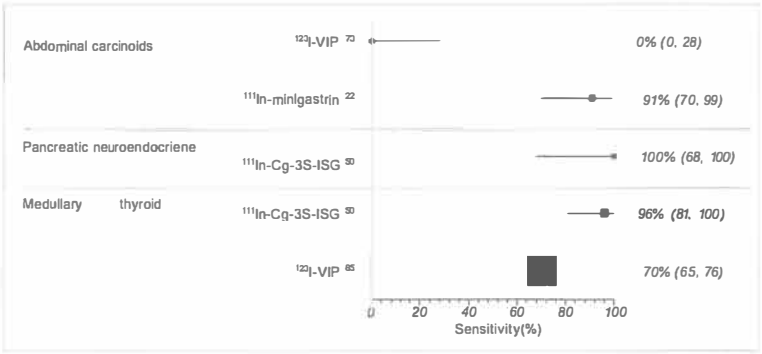

Figure 4. Forest plot analysis of VIP, CCK and anti-body imaging per tumor type.
Results of VIP, CCK and anti-body imaging sorted per tumor type in a Forest plot analysis. On the left side of this plot the tumor type is given with the tracers used in the presented studies. On the right side sensitivities from literature data are given with their calculated confidence interval. The size of the solid black square represents the weight the corresponding study exerts in this analysis and is calculated using the number of patients included (Mantel-Haenszel weight).

The PAC_1 receptor is the only VIP/PACAP receptor found on catecholamine producing tumor cells of neuroendocrine origin and neuroblastomas. Interestingly VIP/PACAP receptors are absent in medullary thyroid cancers.[16] Proteolytic degradation of VIP in vivo as well as high $VPAC_1$ receptor expression in normal epithelial tissues and $VPAC_2$ expression in smooth muscle hampers the applicability of this target for neuroendocrine tumor imaging. Recently a ^{64}Cu labeled VIP analogue has been developed, which is more stable and has been shown to have a higher tumor uptake then the ^{99m}Tc labeled VIP analogue. Therefore this analogue might become of interest to study over expression of VIP receptors.[17] Clinical application is however still limited.

3.1.3 Bombesin receptor imaging

Bombesin and gastrin releasing peptides (GRP) are members of the brain-gut peptides present in the nervous system, gastrointestinal tract and the pulmonary tract.[18] GRP regulates several physiologic processes in the central and enteric nerve systems. An autocrine feedback mechanism involving the expression of bombesin, GRP receptors and the production of peptides in tumor cells (i.e. small cell lung cancer or neuroblastoma), can stimulate growth of neighboring tumor cells.[16] The bombesin receptor family consists of four receptor subtypes; gastrin releasing peptide receptor (BB_2), neuromedin B receptors (BB_1 or NMB), and bombesin receptors BB_3 and BB_4. GRP receptor proteins are over expressed in tumors such as prostate, breast, renal cell and small cell lung cancer. The bombesin and GRP receptors are G protein coupled and can internalize after a receptor-agonist complex has been formed. In neuroendocrine tumors GRP receptors are preferentially expressed by gastrinomas. Ileal carcinoids express NMB receptors whereas small cell lung carcinomas and bronchial carcinoids express the BB_3 receptors.[19] Bombesin analogues for the GRP receptor have been successfully labeled and seem to be interesting candidates for tumor imaging, especially in prostate cancer imaging to possibly improve lymph node staging and recurrence detection.[20]

3.1.4 CCK receptor imaging

Cholecystokinin and gastrin, both members of the cholecystokinin peptide family, play an important role in the neurotransmission in the central nervous system as well as in the gastrointestinal physiology. In the gastrointestinal tract they play a role as a growth factor for physiologic processes, but also for several neoplasms, i.e. colon and brain tumors [16]. Three G protein-coupled CCK receptors have been identified, namely CCK_1, CCK_2 and CCK_c. These CCK receptors have the same internalization mechanisms as somatostatin receptors. This internalization is limited to receptor ligands with agonistic activity.[21] CCK_1 receptors have been detected in i.e. meningioma and neuroblastoma. The CCK_2 receptor was identified in medullary thyroid carcinoma, astrocytomas, and some neuroendocrine gastroenteropancreatic tumors (especially insulinomas) and several soft tissue tumors. In pheochromocytomas and

paragangliomas CCK_2 receptors are rarely expressed. This CCK_2 receptor can be targeted by radiolabeled CCK octapeptides.[21] The last family member, the CCK_C receptor, seems to be mainly involved in gastrin mediated proliferation in tumors of the nervous system.
Only a few clinical studies with CCK imaging have been published. CCK-2 imaging is feasible with ^{111}In-DTPA-D-GLU^1-minigastrin in patients with metastatic medullary thyroid cancer. In 32 patients, the sensitivity for this tracer was 91%.[22]

3.2 Metabolic imaging

The production of different peptides distinguishes neuroendocrine tumors of other malignancies. Therefore the metabolic pathways by which neuroendocrine tumors synthesize these peptides and the intracellular processes which are essential to be able to sustain production of these peptides are ideal candidates for the development of tracers specific for neuroendocrine tumors. These pathways can be targeted at different levels. Tracers can be developed as a marker for the transporter proteins, which are necessary to supply the substrate into the cell (or intracellular vesicle), as a true substrate for the involved pathway, as a substrate which irreversibly binds to an enzyme involved in the pathway or as a marker for (re-)uptake of the end product.
The thus far targeted metabolic pathways and the large amino acid transporter system (LAT, which is responsible for the uptake of precursors for both the serotonin and catecholamine pathway) will be described below in order of clinical importance. In figure 5 literature results of metabolic imaging methods for PET are presented.

3.2.1. Catecholamine pathway

In the catecholamine pathway phenylalanine and intermediate products such as L-3,4 -di-hydroxy-phenylalanine (L-DOPA) are taken up via the LAT system into the cytoplasm of the cell.[23] Here these precursors can be metabolized to dopamine, which is transported into secretory vesicles via the vesicular monoamine transporter (VMAT) system.[24] In these vesicles dopamine can be further metabolized to noradrenalin and adrenalin. The secretory vesicles are responsible for the secretion of end products. Finally, these end products can be transported back via i.e. dopamine and noradrenalin transporters. Tracers developed for this pathway are the precursor 6-^{18}F -L-3,4 -di-hydroxy-phenylalanine (^{18}F-DOPA), the end product 6-^{18}F-dopamine and Metaiodobenzylguanidine (MIBG), which is a substrate for the noradrenalin transporter.

3.2.1.1. ^{18}F-DOPA PET

^{18}F-DOPA is an ^{18}F labeled variant of L-DOPA used for PET imaging (figure 6).
Although the presence of the ^{18}F atom in ^{18}F -DOPA influences the metabolism, it has no or little effect for the transport into the intracellular environment via the cell membrane

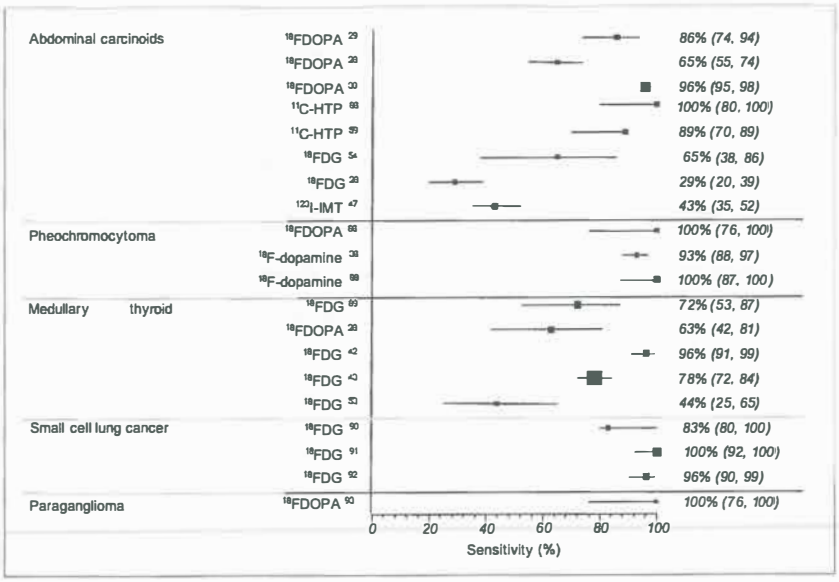

Figure 5. Forest plot analysis of metabolic PET tracer imaging per tumor type.
Results of ^{18}F-FDG PET, ^{18}F-DOPA PET, ^{18}F-Dopamine PET and ^{11}C-5-HTP PET sorted per tumor type in a Forest plot analysis. On the left side of this plot the tumor type is given with the tracers used in the presented studies. On the right side sensitivities from literature data are given with their calculated confidence interval. The size of the solid black square represents the weight the corresponding study exerts in this analysis and is calculated using the number of patients included (Mantel-Haenszel weight).

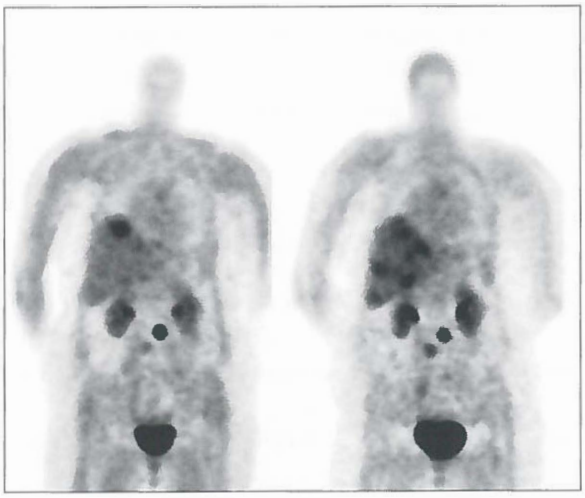

Figure 6. Patient with metastatic pancreatic islet cell tumor.
^{18}F-DOPA PET (left) and ^{11}C-5-HTP PET (right) in a patient with metastatic pancreatic islet cell tumor.

bound LAT2 transporter.[25] ^{18}F -DOPA is decarboxylated to ^{18}F-dopamine via the enzyme aromatic acid decarboxylase (AADC) at a faster rate then L-DOPA. The thus formed dopamine is then probably transported into secretory vesicles by VMAT transporters. Although the precise uptake mechanism is not fully understood, it appears that the high^{18}F-DOPA uptake in neuroendocrine tumors is the result of increased LAT2 transporter activity to satisfy a high precursor turnover due to an increased catecholamine pathway or at least increased AADC activity.[26]

Somewhat paradoxically, the AADC inhibitor carbidopa is sometimes used in conjunction with ^{18}F-DOPA PET imaging. In the proximal tubuli of the kidney ^{18}F-DOPA is rapidly converted by AADC to ^{18}F-dopamine, which is then excreted. This leads to rapid loss of ^{18}F-DOPA and may generate renal, ureter or bladder artifacts in ^{18}F-DOPA PET imaging. The use of oral carbidopa as pre-treatment for ^{18}F-DOPA PET studies improves image quality by reducing the conversion of ^{18}F-DOPA and the excretion of ^{18}F-dopamine in the kidney in urine. The use of carbidopa also lowers physiological ^{18}F-DOPA uptake in the pancreas. The combined effect is a higher availability of ^{18}F-DOPA for tumor uptake.[27]

Only a few studies with ^{18}F-DOPA PET in neuroendocrine tumors have thus far been published. ^{18}F-DOPA PET yields a very high sensitivity in the detection of carcinoid tumors, paragangliomas and pheochromocytomas. For example, in the detection of gastrointestinal neuroendocrine tumors, the average sensitivity of ^{18}F-DOPA PET is very high (89%, figure 5), whereas in these studies the currently used standard methods (CT and SRS imaging) performed not nearly as good (sensitivities of 56% for CT versus 47% for SRS imaging).[28,29,30] When comparing the thus far published results, ^{18}F-DOPA PET enabled best localization of primary tumors and lymph node staging.[28,29,30]

There is a very small risk that the use of a catecholamine precursor in patients with a carcinoid syndrome can lead to the development of a carcinoid crisis. Only one case has thus far been published. This complication can be prevented by a slow tracer injection and if necessary an intravenous injection of octreotide.[31]

3.2.1.2. ^{123}I and ^{131}I- Metaiodobenzylguanidine (MIBG)

The precise uptake and retention mechanism in neuroendocrine tumors for MIBG has not been clarified, but the noradrenalin transporter seems to play an important role for MIBG uptake (figure 3). Reports indicate that MIBG acts as an intracellular substrate for the vesicular monoamine transporters $VMAT_1$ and $VMAT_2$.[32] These transporters are located on the membrane of secretory vesicles of neuroendocrine cells. It seems likely that, once MIBG has passed the cell membrane, the VMAT transporters transport MIBG into secretory chromaffin granules.[32] MIBG can be labeled with ^{123}I and ^{131}I. ^{123}I labeled MIBG yields the best image quality, due to the superior physical qualities for imaging. It has high photon energy of 159 KeV, a half life of 13 hours and it can be administered in a higher dose then ^{131}I-MIBG. These

properties enable the use of ^{123}I-MIBG for SPECT.[33]
MIBG scintigraphy has become the imaging method of choice for neuroblastoma and pheochromocytomas (for an example see figure 7).

MIBG scintigraphy has a lower sensitivity for the detection of other neuroendocrine tumors, such as carcinoid (averaging 50%) (figure 8).Its specificity in detecting pheochromocytoma and neuroblastoma is superior to other imaging modalities. There is however no explanation for the variation in uptake of MIBG by the different neuroendocrine tumors (figure 4). Most studies report specificities for MIBG ranging from 80-100% for the detection of pheochromocytoma, but less then 80% for the detection its malignant variant. Specificity for neuroblastomas is 84%. But, since other neuroendocrine tumors in childhood are rare, a positive MIBG scan is nearly diagnostic for a neuroblastoma.[34]

3.2.1.3. 6-^{18}F-Dopamine PET

6-^{18}F-Dopamine is a substrate for the monoamine transporters DAT (dopamine transporter) and the norepinephrine transporter. After this trans-membrane transport, ^{18}F-dopamine is stored in cytoplasmatic secretory vesicles through the VMAT system. However, ^{18}F-dopamine plasma levels decline rapidly after injection due to metabolization.[35]
The PET tracer 6-^{18}F-dopamine was developed to visualize sympathiconeuronal innervation. This tracer is actively taken up, stored and metabolized by cells from organs with a sympathetic innervation. Organs which have a high ^{18}F-dopamine uptake are the heart, liver, spleen, salivary glands and chest wall. ^{18}F-dopamine does not cross the blood-brain barrier, and therefore virtually no uptake is seen in the brain.
^{18}F-dopamine PET is a useful imaging method for the detection of pheochromocytomas. [36] These tumors have a high expression of monoamine transporters, which makes these tumors ideal candidates for ^{18}F-dopamine imaging. Due to a low specific activity and the pharmacological activity of both labeled and unlabelled dopamine, the maximum injectable dose of ^{18}F-dopamine is limited.

3.2.2. Serotonin pathway

The serotonin and catecholamine pathway have many common features. Precursors for the serotonin pathway (tryptophan and 5-hydroxytryptophan, 5-HTP) are taken up via the same LAT transport system as utilized by the catecholamine pathway. The conversion from 5-HTP to serotonin is performed by the same enzyme, which decarboxylizes L-DOPA to dopamine, namely the AADC enzyme. The end product, serotonin, is also transported via the same VMAT transporter system into secretory vesicles.

Figure 7. Double side pheochromocytoma.
18F-DOPA PET (left) and 123I-MIBG (right) of a patient with double-sided pheochromocytoma.

3.2.2.1. ^{11}C-5-Hydroxytryptophan (^{11}C-5-HTP) PET

Thus far, ^{11}C-5-HTP PET is the only tracer for this pathway, which has reached clinical application (figure 6). In neuroendocrine tumors, the high uptake via the over expressed system L transporter, the rapid decarboxylation by AADC and the subsequent storage in secretory granules allow for an excellent discrimination of these tumors with ^{11}C-5-HTP and ^{18}F-DOPA as compared with normal tissue.[37] Due to low organ uptake of ^{11}C-5-HTP, scans are characterized by a low background activity. ^{11}C-5-HTP uptake by the kidneys and metabolization to serotonin by the AADC enzyme followed by subsequent urinary excretion, result in an intense signal in these organ systems. There is also some physiologic pancreatic uptake noticeable. This can lead to difficulties in the interpretation of lesions in the direct vicinity of these organs. However, the oral pre-medication with carbidopa lowers the metabolization to serotonin thereby reducing the signal intensity in this area, thus improving image quality and interpretability.[38]

There are however two draw-backs for this tracer. The tracer synthesis is very complex since it relies on two complex multi-enzyme steps. Also the short half life of 20 min for ^{11}Carbon limits the use of this tracer to specialized centers with their own cyclotron facilities. Nevertheless, the published results with this tracer justify the use of this tracer.

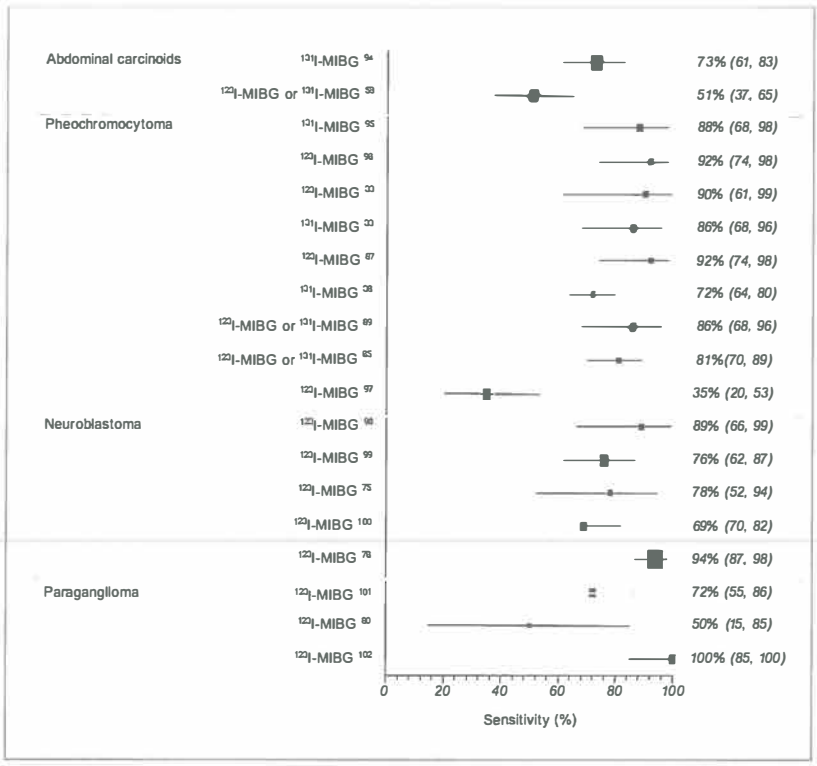

Figure 8. Forest plot analysis of MIBG imaging per tumor type.
Results of MIBG imaging sorted per tumor type in a Forest plot analysis. On the left side of this plot the tumor type is given with the tracers used in the presented studies. On the right side sensitivities from literature data are given with their calculated confidence interval. The size of the solid black square represents the weight the corresponding study exerts in this analysis and is calculated using the number of patients included (Mantel-Haenszel weight).

3.3. Phosphate metabolism

Inorganic phosphate (Pi) molecules and Na+ ions are taken up by cells via the Na^+/Pi co-transporters.[39]. Three different families of Na^+/Pi co-transporters have been reported, type I, II and III. These transporters are involved in the inorganic phosphate transport in cells. Type II and III are regulated by extra cellular pH whereas type I is indifferent to pH. Type II activity is decreased by acidic pH and increased with an alkaline pH. Type III functions in the opposite way, i.e. acidic pH increases its activity. The physiologic function of the Na^+/Pi transporters is still not entirely clear. These transporters are predominantly expressed in kidney, liver and brain. The three families of this transporter are expressed differently in these organs and within the tissues of these organs.[39, 40].

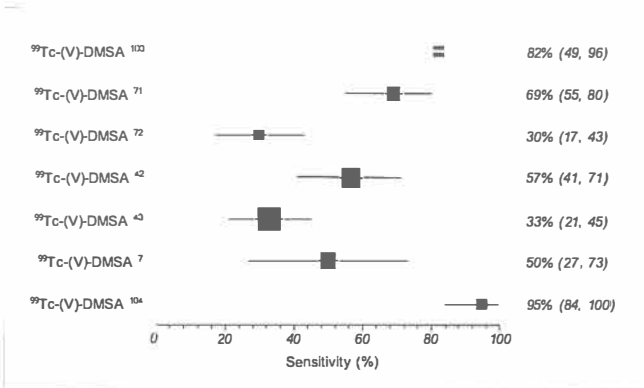

Figure 9. Forest plot analysis of ^{99m}Tc-(V)-DMSA imaging for medullary thyroid tumors.
Results of DMSA imaging for medullary thyroid carcinoma in a Forest plot analysis. On the left side of this plot the tumor type is given with the tracers used in the presented studies. On the right side sensitivities from literature data are given with their calculated confidence interval. The size of the solid black square represents the weight the corresponding study exerts in this analysis and is calculated using the number of patients included (Mantel-Haenszel weight).

3.3.1. ^{99m}Tc -(V)-Dimercaptosuccinic acid (^{99m}Tc-(V)-DMSA)

The uptake mechanism for ^{99m}Tc-(V)-DMSA is based on the resemblance between the TcO_4^{3-} complex in labeled DMSA and the phosphate molecule PO_4^{3-} [40]. Due to the over expression of type III Na^+/Pi transporters, lack of Type II Na^+/Pi transporters and a more acidic extra cellular pH in tumor cells than normal tissue, tumor cells have a higher phosphate uptake. As ^{99m}Tc (V)-DMSA resembles the phosphate molecule, it is also actively taken up. ^{99m}Tc-(V)-DMSA is therefore a marker for the phosphate metabolism [41].
This tracer has thus far mainly been used for imaging medullary thyroid tumors. For the detection of this tumor type, ^{99m}Tc-(V)-DMSA is the routinely used tracer with the best

results (figure 3). It has an average sensitivity of 76 % for medullary thyroid tumors (figure 9). In these tumors, morphological imaging (CT/MRI) performs equally (sensitivity ranging from 67% to 87%).[42,43]

3.4 Glucose metabolism

Cells rely mostly on their glucose metabolism to obtain ATP as their energy source. After uptake by glucose transporters, glucose is phosphorylated by the hexokinase enzyme to a phosphorylated intermediate, which is eventually metabolized to pyruvate and lactate. This step does not require oxygen (anaerobic glycolysis). The next step, the citric acid cycle, requires oxygen (aerobic) and produces most of the ATP molecules. In the citric cycle, pyruvate is eventually metabolized to

CO2. Tumor cells rely mainly on the anaerobic glycolysis with its relatively low energy yield, and therefore require much more glucose.

3.4.1. ^{18}F-Fluor-2-deoxy-D-Glucose PET

^{18}F-2-deoxy-D-glucose (FDG) is transported into the cells and then phosphorylated by hexokinase. This results in a polar intermediate (FDG-6p), which crosses the cell membrane poorly. The increased expression of the glucose transporter molecules and the hexokinase enzyme result in an increased uptake and retention of FDG in tumor cells compared to normal cells.[44] In general, FDG uptake increases when tumors behave more aggressively.[45]

However, neuroendocrine tumors do not have a high glycolysis rate. Results of FDG imaging in neuroendocrine tumors are inferior to these obtained for metabolically active tumors. Neuroendocrine tumors which have a high uptake, such as small cell lung cancer, are characterized by a more aggressive behavior.[46] The use of the FDG PET scan in neuroendocrine tumors is therefore more or less limited to imaging small cell lung cancer (with approximately 93% sensitivity) and medullary thyroid carcinoma (76% sensitivity).

3.5 Large amino acid transport system

To import large branched and aromatic neutral amino acids cells rely on the plasma membrane bound system L transporters. This system consists of two heterodimers composed of a large glycoprotein part and a variable light chain, thus forming the LAT 1 to 5. System L transporters, which are amino acid transporters, are obligatory exchange transporters which can only function by exchanging an intracellular amino acid for an extra-cellular one. In combination with other unidirectional transporters with overlapping amino acid sensitivities, cells can control the activity of the system L transport. Over expression of amino acid transporters helps to satisfy the metabolic needs, but tumor cells can consume more nutrients than required for the metabolic needs. In neuroendocrine tumors the LAT2 transporters play an important role, due to their ability to take up large neutral amino acids such as phenylalanine and tryptophan. Thus far only L-3-^{123}I-alpha-methyl-tyrosine (^{123}I-IMT) has been developed to exploit the over expression of the LAT system for imaging purposes in neuroendocrine tumors.[46,47]

3.5.1. L-3-^{123}I-alpha-methyl-tyrosine (^{123}I-IMT)

^{123}I-IMT, an artificial amino acid derived from tyrosine, was initially developed as a functional imaging agent for neutral amino acid transport in brain tumors. ^{123}I-IMT accumulates fast in neuroendocrine tumor cells due to uptake via LAT1, but is not further metabolized intra-cellularly .[48] Therefore, it can be regarded as a true marker for transport capabilities of neuroendocrine tumor cells. A study in 22 carcinoid patients showed an overall lesion detection of 43% with a lower lesion contrast and image quality than ^{111}In-octreotide.[49] ^{123}I-IMT is not generally available.

3.6 Radio labeled monoclonal antibodies

Only a few reports of patient studies with radio labeled monoclonal antibodies against antigens expressed on neuroendocrine tumors used for nuclear medicine imaging are available. Described applications are anti-CEA for paragangliomas, anti CgA for medullary thyroid carcinoma and anti- UJ13A and anti GD2 for neuroblastoma.[49-52] These reports should be seen as experimental, due to the limited data available and the fact that these methods have not yet been adapted for clinical use.

4. CONCLUSION

Most receptor-based tracers have been developed for scintigraphic use, and changing to positron emitting labels (i.e. ^{18}F, ^{64}Cu, ^{68}Ga) could make these tracers suitable for PET imaging. For SRS, different somatostatin analogues are investigated which are more stable and bind more receptor subtypes with a higher affinity.

Most neuroendocrine tumors share common metabolic pathways, such as the catecholamine and serotonin pathways. Different strategies in the development of tracers suitable to visualize the metabolic pathways are possible. For example, three different tracers for the catecholamine pathway have been developed: the tracer ^{18}FM-6-FmT is an aromatic L-AADC inhibitor, ^{18}F-DOPA is a substrate in the catecholamine synthesis, ^{18}F-dopamine is stored in vesicles where it is metabolized to ^{18}F-norepinephrin and ^{18}F-epinephrin. Several other tracers, which exploit the metabolic characteristics, are in development.

The use of antibodies specific for neuroendocrine tumors, has thus far not been as successful as the receptor and metabolic based imaging methods. It has been troubled by the high background uptake.

The developments in the area of image fusion are also of great interest for neuroendocrine tumors. Nuclear medicine techniques lack anatomical information, whereas morphological imaging lacks functional information. Co-registration of these modalities, either by software or by hardware, assists in tumor localization. The combined functional and anatomic images give surgeons essential information to guide surgical decision-making.

An enormous amount of expertise and knowledge has been gathered in the past years with somatostatin analogues, both for diagnostic and treatment purposes. It is more or less clear which tumor types can be visualized to what extend with this tracer. It can be expected that combining somatostatin analogues with positron emitting labels will secure its position within both diagnostic and therapeutic procedures in nuclear medicine in the near future. However, somatostatin receptors are not expressed evenly both in receptor subtypes and quantity of expressed receptors on the cellular membrane. Therefore other techniques will improve diagnostic imaging. Due to their common capability for the uptake of large amino

acids for the incorporation in metabolic pathways, precursors (i.e. ^{18}F-DOPA and ^{11}C-5-HTP) for these pathways are interesting candidates for diagnostic and therapeutic purposes. Although results are promising, experience with these PET tracers is still limited. It is foreseeable that in the future the first step in neuroendocrine tumor imaging will be with the use of PET tracers, such as ^{18}F-DOPA on a PET-CT machine. When this combination yields negative results, other techniques can be used for further analysis.

Conflict of interest statement

There are no conflicts of interest.

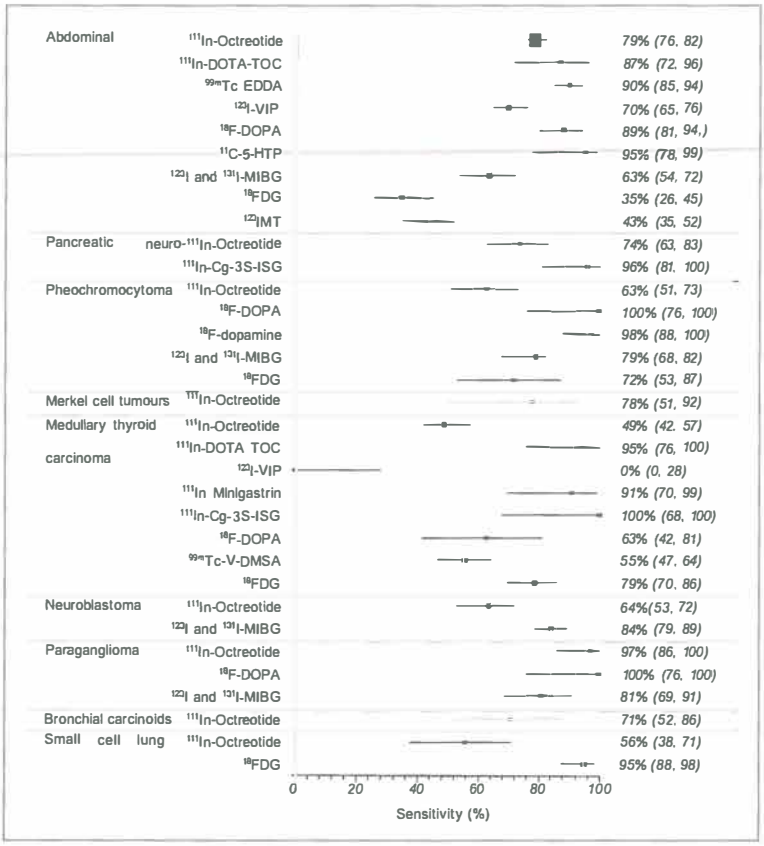

Figure 10. Summary of results.

Results of all described imaging methods sorted per tumor type in a Forest plot analysis. On the left side of this plot the tumor type is given with the tracers used in the presented studies. On the right side sensitivities from literature data are given with their calculated confidence interval. The size of the solid black square represents the weight the corresponding study exerts in this analysis and is calculated using the number of patients included (Mantel-Haenszel weight).

REFERENCES

1. Reubi JC. Neuropeptide receptors in health and disease: the molecular basis for in vivo imaging. J Nucl Med 1995;36:1825-35
2. Schnirer LL, Yao JC, Ajani JA. Carcinoid-a comprehensive review. Acta Oncol 2003;42:672-92
3. Kloppel G, Heitz PU, Capella C, Solcia E. Pathology and nomenclature of human gastrointestinal neuroendocrine (carcinoid) tumours and related lesions. World J Surg 1996;20:132-41
4. Modlin IM, Lye KD, Kidd M. A 5-decade analysis of 13,715 carcinoid tumours. Cancer 2003;97:934-59
5. Solcia E, Kloppel G, Sobin LH, et al. Histologic typing of endocrine tumours. WHO International Histological Classification of Tumours. 2nd ed. Heidelberg: Springer Verlag;2000
6. Oberg K. Chemotherapy and biotherapy in the treatment of neuroendocrine tumours. Ann Oncol 2001;12 Suppl 2:S111-S114
7. Warner RR, O'dorisio TM. Radiolabeled peptides in diagnosis and tumour imaging: clinical overview. Semin Nucl Med 2002;32:79-83
8. Plockinger U, Rindi G, Arnold R, et al. Guidelines for the diagnosis and treatment of neuroendocrine gastrointestinal tumours. A consensus statement on behalf of the European Neuroendocrine Tumour Society (ENETS). Neuroendocrinology 2004;80:394-424
9. Lamberts SW, de Herder WW, Hofland LJ. Somatostatin analogs in the diagnosis and treatment of cancer. Trends Endocrinol Metab 2002;13:451-7
10. Hofland LJ, Lamberts SW. The pathophysiological consequences of somatostatin receptor internalization and resistance. Endocr Rev 2003;24:28-47
11. Krenning EP, Kwekkeboom DJ, Bakker WH, et al. Somatostatin receptor scintigraphy with (111In-DTPA-D-Phe1)- and (123I-Tyr3)-octreotide: the Rotterdam experience with more than 1000 patients. Eur J Nucl Med 1993;20:716-31
12. Schottelius M, Poethko T, Herz M, et al. First (18)F-labeled tracer suitable for routine clinical imaging of sst receptor-expressing tumours using positron emission tomography. Clin Cancer Res 2004;10:3593-606
13. Lewis JS, Srinivasan A, Schmidt MA, Anderson CJ. In vitro and in vivo evaluation of 64Cu-TETA-Tyr3-octreotate. A new somatostatin analog with improved target tissue uptake. Nucl Med Biol 1999;26:267-73
14. Ginj M, Chen J, Walter MA, Eltschinger V, Reubi JC, Maecke HR. Preclinical evaluation of new and highly potent analogues of octreotide for predictive imaging and targeted radiotherapy. Clin Cancer Res 2005;11:1136-45
15. Shetzline MA, Walker JK, Valenzano KJ, Premont RT. Vasoactive intestinal polypeptide type-1 receptor regulation. Desensitization, phosphorylation, and sequestration. J Biol Chem 2002; 277:25519-26
16. Reubi JC. Peptide receptors as molecular targets for cancer diagnosis and therapy. Endocr Rev 2003;24:389-427
17. Thakur ML, Aruva MR, Gariepy J, et al. PET imaging of oncogene overexpression using 64Cu-vasoactive intestinal peptide (VIP) analog: comparison with 99mTc-VIP analog. J Nucl Med 2004;45:1381-9
18. Seretis E, Gavrill A, Agnantis N, Golematis V, Voloudakis-Baltatzis IE. Comparative study of serotonin and bombesin in adenocarcinomas and neuroendocrine tumours of the colon. Ultrastruct Pathol 2001;25:445-54

19. Reubi JC, Wenger S, Schmuckli-Maurer J, Schaer JC, Gugger M. Bombesin receptor subtypes in human cancers: detection with the universal radioligand (125)I-(D-TYR(6), beta-ALA(11), PHE(13), NLE(14)) bombesin(6-14). Clin Cancer Res 2002;8:1139-46
20. Reubi JC, Waser B. Concomitant expression of several peptide receptors in neuroendocrine tumours: molecular basis for in vivo multireceptor tumour targeting. Eur J Nucl Med Mol Imaging 2003;30:781-93
21. Behe M, Behr TM. Cholecystokinin-B (CCK-B)/gastrin receptor targeting peptides for staging and therapy of medullary thyroid cancer and other CCK-B receptor expressing malignancies. Biopolymers 2002;66:399-418
22. Behr TM, Behe MP. Cholecystokinin-B/Gastrin receptor-targeting peptides for staging and therapy of medullary thyroid cancer and other cholecystokinin-B receptor-expressing malignancies. Semin Nucl Med 2002;32:97-109
23. Soares-da-Silva P, Serrao MP. High- and low-affinity transport of L-leucine and L-DOPA by the hetero amino acid exchangers LAT1 and LAT2 in LLC-PK1 renal cells. Am.J.Physiol Renal Physiol 2004;2:F252-61
24. Ericksson JD, Schafer MK, Bonner TI, Eiden LE, Weihe E. Distinct pharmacological properties and distribution in neurons and endocrine cells of two isoforms of the human vesicular monoamine transporter. Proc.Natl.Acad.Sci.U.S.A 1996;93:5166-71
25. Uchino H, Kanai Y, Kim DK, et al. Transport of amino acid-related compounds mediated by L-type amino acid transporter 1 (LAT1): insights into the mechanisms of substrate recognition. Mol Pharmacol 2002;61:729-37
26. Firnau G, Sood S, Chirakal R, Nahmias C, Garnett ES. Metabolites of 6-(18F)fluoro-L-dopa in human blood. J Nucl Med 1988;29:363-9
27. Hoffman JM, Melega WP, Hawk TC, et al. The effects of carbidopa administration on 6-(18F)fluoro-L-dopa kinetics in positron emission tomography. J Nucl Med 1992; 33:1472-7
28. Hoegerle S, Altehoefer C, Ghanem N, et al. Whole-body 18F dopa PET for detection of gastrointestinal carcinoid tumours. Radiology 2001;220:373-80
29. Becherer A, Szabo M, Karanikas G, et al. Imaging of advanced neuroendocrine tumours with (18)F-FDOPA PET. J Nucl Med 2004;45:1161-7
30. Koopmans KP, de Vries EG, Kema IP, et al. Staging of carcinoid tumours using 18F-DOPA positron emission tomography: a diagnostic accuracy study. Lancet Oncol 2006;7:728-34
31. Koopmans KP, Brouwers AH, De Hooge MN, et al. Carcinoid crisis after injection of 6-18F-fluorodihydroxyphenylalanine in a patient with metastatic carcinoid. J Nucl Med 2005;46:1240-3
32. Kolby L, Bernhardt P, Levin-Jakobsen AM, et al. Uptake of meta-iodobenzylguanidine in neuroendocrine tumours is mediated by vesicular monoamine transporters. Br J Cancer 2003;89:1383-8
33. Furuta N, Kiyota H, Yoshigoe F, Hasegawa N, Ohishi Y. Diagnosis of pheochromocytoma using (123I)-compared with (131I)-metaiodobenzylguanidine scintigraphy. Int J Urol 1999;6:119-24
34. Hiorns MP, Owens CM. Radiology of neuroblastoma in children. Eur Radiol 2001;11:2071-81
35. Goldstein DS, Holmes C. Metabolic fate of the sympathoneural imaging agent 6-(18F)fluorodopamine in humans. Clin Exp Hypertens 1997;19:155-61
36. Ilias I, Yu J, Carrasquillo JA, et al. Superiority of 6-(18F)-fluorodopamine positron emission tomography versus (131I)-metaiodobenzylguanidine scintigraphy in the localization of metastatic

pheochromocytoma. J Clin Endocrinol Metab 2003;88:4083-7
37. Bergstrom M, Lu L, Eriksson B et al. Modulation of organ uptake of 11C-labelled 5-hydroxytryptophan. Biog Amines 1996;12:477-85
38. Orlefors H, Sundin A, Lu L, et al. Carbidopa pretreatment improves image interpretation and visualisation of carcinoid tumours with (11)C-5-hydroxytryptophan positron emission tomography. Eur J Nucl Med Mol Imaging 2006;33:60-5
39. Werner A, Dehmelt L, Nalbant P. Na+-dependent phosphate cotransporters: the NaPi protein families. J Exp Biol 1998;201:3135-42
40. Lam AS, Puncher MR, Blower PJ. In vitro and in vivo studies with pentavalent technetium-99m dimercaptosuccinic acid. Eur J Nucl Med 1996;23:1575-82
41. Denoyer D, Perek N, Le Jeune N, Frere D, Dubois F. Evidence that 99mTc-(V)-DMSA uptake is mediated by NaPi cotransporter type III in tumour cell lines. Eur J Nucl Med Mol Imaging 2004;31:77-84
42. De Groot JW, Links TP, Jager PL, Kahraman T, Plukker JT. Impact of 18F-fluoro-2-deoxy-D-glucose positron emission tomography (FDG-PET) in patients with biochemical evidence of recurrent or residual medullary thyroid cancer. Ann Surg Oncol 2004;11:786-94
43. Diehl M, Risse JH, Brandt-Mainz K, et al. Fluorine-18 fluorodeoxyglucose positron emission tomography in medullary thyroid cancer: results of a multicentre study. Eur J Nucl Med 2001;28:1671-6
44. Bar-Shalom R, Valdivia AY, Blaufox MD. PET imaging in oncology. Semin Nucl Med 2000;30:150-85
45. Adams S, Baum R, Rink T, Schumm-Drager PM, Usadel KH, Hor G. Limited value of fluorine-18 fluorodeoxyglucose positron emission tomography for the imaging of neuroendocrine tumours. Eur J Nucl Med 1998;25:79-83
46. Meier C, Ristic Z, KLauser S, Verrey F. Activation of system L heterodimeric amino acid exchangers by intracellular substrates. Embo J 2002;21:580-9
47. Jager PL, Meijer WG, Kema IP, Willemse PH, Piers DA, de Vries EG. L-3-(123I)Iodo-alpha-methyltyrosine scintigraphy in carcinoid tumours: correlation with biochemical activity and comparison with (111In-DTPA-D-Phe1)-octreotide imaging. J Nucl Med 2000;41:1793-800
48. Shikano N, Kanai Y, Kawai K, et al. Isoform selectivity of 3-125I-iodo-alpha-methyl-L-tyrosine membrane transport in human L-type amino acid transporters. J Nucl Med 2003;44:244-6
49. Kairemo KJ, Himi T, Hopsu EV, Ramsay HA. Radioimmunoimaging of glomus tympanicum tumours by In-111 labeled monoclonal antibody using single photon emission computed tomography. Am J Otol 1997;18:750-3
50. Siccardi AG, Paganelli G, Pontiroli AE, et al. In vivo imaging of chromogranin A-positive endocrine tumours by three-step monoclonal antibody targeting. Eur J Nucl Med 1996;23:1455-9
51. Goldman A, Vivian G, Gordon I, Pritchard J, Kemshead J. Immunolocalization of neuroblastoma using radiolabeled monoclonal antibody UJ13A. J Pediatr 1984;105:252-6
52. Larson SM, Pentlow KS, Volkow ND, et al. PET scanning of iodine-124-3F9 as an approach to tumour dosimetry during treatment planning for radioimmunotherapy in a child with neuroblastoma. J Nucl Med 1992;33:2020-3
53. Hoegerle S, Altehoefer C, Ghanem N, Brink I, Moser E, Nitzsche E. 18F-DOPA positron emission tomography for tumour detection in patients with medullary thyroid carcinoma and elevated calcitonin levels. Eur J Nucl Med 2001;28:64-71
54. Belhocine T, Foidart J, Rigo P, et al. Fluorodeoxyglucose positron emission tomography and

somatostatin receptor scintigraphy for diagnosing and staging carcinoid tumours: correlations with the pathological indexes p53 and Ki-67. Nucl Med Commun 2002;23:727-34

55. Chiti A, Fanti S, Savelli G, et al. Comparison of somatostatin receptor imaging, computed tomography and ultrasound in the clinical management of neuroendocrine gastro-entero-pancreatic tumours. Eur J Nucl Med 1998;25:1396-403
56. Krausz Y, Bar-Ziv J, de Jong RB, et al. Somatostatin-receptor scintigraphy in the management of gastroenteropancreatic tumours. Am J Gastroenterol 1998;93:66-70
57. Montravers F, Grahek D, Kerrou K. Can fluorodihydroxyphenylalanine PET replace somatostatin receptor scintigraphy in patients with digestive endocrine tumors? J Nucl Med 2006;47:1455-66
58. Nocaudie-Calzada M, Huglo D, Carnaille B, Proye C, Marchandise X. Comparison of somatostatin analogue and metaiodobenzylguanidine scintigraphy for the detection of carcinoid tumours. Eur J Nucl Med 1996;23:448-54
59. Orlefors H, Sundin A, Ahlstrom H, et al. Positron emission tomography with 5-hydroxytryprophan in neuroendocrine tumours. J Clin Oncol 1998;16:2534-41
60. Raderer M, Kurtaran A, Leimer M, et al. Value of peptide receptor scintigraphy using (123)I-vasoactive intestinal peptide and (111)In-DTPA-D-Phe1-octreotide in 194 carcinoid patients: Vienna University Experience, 1993 to 1998. J Clin Oncol 2000;18:1331-6
61. Shi W, Johnston CF, Buchanan KD, et al. Localization of neuroendocrine tumours with (111In) DTPA-octreotide scintigraphy (Octreoscan): a comparative study with CT and MR imaging. QJM 1998;91:295-301
62. Virgolini I, Patri P, Novotny C, et al. Comparative somatostatin receptor scintigraphy usingin-111-DOTA-lanreotide and in-111-DOTA-Tyr3-octreotide versus F-18-FDG-PET for evaluation of somatostatin receptor-mediated radionuclide therapy. Ann Oncol 2001;12 Suppl 2:S41-S45
63. Gabriel M, Muehllechner P, Decristoforo C, et al. 99mTc-EDDA/HYNIC-Tyr(3)-octreotide for staging and follow-up of patients with neuroendocrine gastro-entero-pancreatic tumours. J Nucl Med Mol Imaging 2005;49:237-44
64. Hubalewska-Dydejczyk A, Fross-Baron K, Mikolajczak R, et al. (99m)Tc-EDDA/HYNIC-octreotate scintigraphy, an efficient method for the detection and staging of carcinoid tumours: results of 3 years' experience. Eur J Nucl Med Mol Imaging 2006;33:1123-33
65. Tenenbaum F, Lumbroso J, Schlumberger M, et al. Comparison of radiolabeled octreotide and meta-iodobenzylguanidine (MIBG) scintigraphy in malignant pheochromocytoma. J Nucl Med 1995;36:1-6
66. Gibril F, Reynolds JC, Lubensky IA, et al. Ability of somatostatin receptor scintigraphy to identify patients with gastric carcinoids: a prospective study. J Nucl Med 2000;41:1646-56
67. Briganti V, Matteini M, Ferri P, Vaggelli L, Castagnoli A, Pieroni C. Octreoscan SPET evaluation in the diagnosis of pancreas neuroendocrine tumours. Cancer Biother Radiopharm 2001;16:515-24
68. Schillaci O, Spanu A, Scopinaro F, et al. Somatostatin receptor scintigraphy with 111In-pentetreotide in non-functioning gastroenteropancreatic neuroendocrine tumours. Int J Oncol 2003;23:1687-95
69. Durani BK, Klein A, Henze M, Haberkorn U, Hartschuh W. Somatostatin analogue scintigraphy in Merkel cell tumours. Br J Dermatol 2003;148:135-40
70. Guitera-Rovel P, Lumbroso J, Gautier-Gougis MS, et al. Indium-111 octreotide scintigraphy of Merkel cell carcinomas and their metastases. Ann Oncol 2001;12:807-11
71. Adams S, Baum RP, Hertel A, Schumm-Draeger PM, Usadel KH, Hor G. Comparison of metabolic and

receptor imaging in recurrent medullary thyroid carcinoma with histopathological findings. Eur J Nucl Med 1998;25:277-83

72. Arslan N, Ilgan S, Yuksel D, et al. Comparison of In-111 octreotide and Tc-99m (V) DMSA scintigraphy in the detection of medullary thyroid tumour foci in patients with elevated levels of tumour markers after surgery. Clin Nucl Med 2001;26:683-8
73. Berna L, Chico A, Matias-Guiu X, et al. Use of somatostatin analogue scintigraphy in the localization of recurrent medullary thyroid carcinoma. Eur J Nucl Med 1998;25:1482-8
74. Kurtaran A, Scheuba C, Kaserer K, Schima W, Czerny C, Angelberger P et al. Indium-111-DTPA-D-Phe-1-octreotide and technetium-99m-(V)-dimercaptosuccinic acid scanning in the preoperative staging of medullary thyroid carcinoma. J Nucl Med 1998;39:1907-9
75. Kropp J, Hofmann M, Bihl H. Comparison of MIBG and pentetreotide scintigraphy in children with neuroblastoma. Is the expression of somatostatin receptors a prognostic factor? Anticancer Res 1997;17:1583-8
76. Schilling FH, Bihl H, Jacobsson H, et al. Combined (111)In-pentetreotide scintigraphy and (123)I-mIBG scintigraphy in neuroblastoma provides prognostic information. Med Pediatr Oncol 2000;35:688-91
77. Corleto VD, Scopinaro F, Angeletti S, et al. Somatostatin receptor localization of pancreatic endocrine tumours. World J Surg 1996;20:241-4
78. Rickes S, Unkrodt K, Ocran K, Neye H, Wermke W. Differentiation of neuroendocrine tumours from other pancreatic lesions by echo-enhanced power Doppler sonography and somatostatin receptor scintigraphy. Pancreas 2003;26:76-81
79. Duet M, Sauvaget E, Petelle B, et al. Clinical impact of somatostatin receptor scintigraphy in the management of paragangliomas of the head and neck. J Nucl Med 2003;44:1767-74
80. Muros MA, Llamas-Elvira JM, Rodriguez A, et al. 111In-pentetreotide scintigraphy is superior to 123I-MIBG scintigraphy in the diagnosis and location of chemodectoma. Nucl Med Commun 1998;19:735-42
81. Bohuslavizki KH, Brenner W, Gunther M, et al. Somatostatin receptor scintigraphy in the staging of small cell lung cancer. Nucl Med Commun 1996;17:191-6
82. Bombardieri E, Crippa F, Cataldo I, et al. Somatostatin receptor imaging of small cell lung cancer (SCLC) by means of 111In-DTPA octreotide scintigraphy. Eur J Cancer 1995;31A:184-8
83. Fanti S, Farsad M, Battista G, et al. Somatostatin receptor scintigraphy for bronchial carcinoid follow-up. Clin Nucl Med 2003;28:548-52
84. Kurtaran A, Scheuba C, Kaserer K, et al. Indium-111-DTPA-D-Phe-1-octreotide and technetium-99m-(V)-dimercaptosuccinic acid scanning in the preoperative staging of medullary thyroid carcinoma. J Nucl Med 1998;39:1907-9
85. Raderer M, Kurtaran A, Leimer M, et al. Value of peptide receptor scintigraphy using (123)I-vasoactive intestinal peptide and (111)In-DTPA-D-Phe1-octreotide in 194 carcinoid patients: Vienna University Experience, 1993 to 1998. J Clin Oncol 2000;18:1331-6
86. Orlefors H, Sundin A, Ahlstrom H, et al. Positron emission tomography with 5-hydroxytryprophan in neuroendocrine tumours. J Clin Oncol 1998;16:2534-41
87. Hoegerle S, Nitzsche E, Altehoefer C, et al. Pheochromocytomas: detection with 18F DOPA whole body PET--initial results. Radiology 2002;222:507-12
88. Pacak K, Eisenhofer G, Carrasquillo JA, Chen CC, Li ST, Goldstein DS. 6-(18F)fluorodopamine positron emission tomographic (PET) scanning for diagnostic localization of pheochromocytoma.

Hypertension 2001;38:6-8
89. Shulkin BL, Thompson NW, Shapiro B, Francis IR, Sisson JC. Pheochromocytomas: imaging with 2-(fluorine-18)fluoro-2-deoxy-D-glucose PET. Radiology 1999;212:35-41
90. Chin R Jr, McCain TW, Miller AA, et al. Whole body FDG-PET for the evaluation and staging of small cell lung cancer: a preliminary study. Lung Cancer 2002;37:1-6
91. Pandit N, Gonen M, Krug L, Larson SM. Prognostic value of (18F)FDG-PET imaging in small cell lung cancer. Eur J Nucl Med Mol Imaging 2003;30:78-84
92. Schumacher T, Brink I, Mix M, et al. FDG-PET imaging for the staging and follow-up of small cell lung cancer. Eur J Nucl Med 2001;28:483-8
93. Hoegerle S, Ghanem N, Altehoefer C, et al. 18F-DOPA positron emission tomography for the detection of glomus tumours. Eur J Nucl Med Mol Imaging 2003; 30:689-94
94. Hoefnagel CA, Taal BG, Valdes Olmos RA. Role of (131I)metaiodobenzylguanidine therapy in carcinoids. J Nucl Biol Med 1991;35:346-8
95. Berglund AS, Hulthen UL, Manhem P, Thorsson O, Wollmer P, Tornquist C. Metaiodobenzylguanidine (MIBG) scintigraphy and computed tomography (CT) in clinical practice. Primary and secondary evaluation for localization of phaeochromocytomas. J Intern Med 2001;249:247-51
96. De Graaf JS, Dullaart RP, Kok T, Piers DA, Zwierstra RP. Limited role of meta-iodobenzylguanidine scintigraphy in imaging phaeochromocytoma in patients with multiple endocrine neoplasia type II. Eur J Surg 2000;166:289-92
97. van der Harst E, de Herder WW, Bruining HA, et al. ((123)I)metaiodobenzylguanidine and ((111)In)octreotide uptake in benign and malignant pheochromocytomas. J Clin Endocrinol Metab 2001;86:685-93
98. Hadj-Djilani NL, Lebtahi NE, Delaloye AB, Laurini R, Beck D. Diagnosis and follow-up of neuroblastoma by means of iodine-123 metaiodobenzylguanidine scintigraphy and bone scan, and the influence of histology. Eur J Nucl Med 1995;22:322-9
99. Hashimoto T, Koizumi K, Nishina T, Abe K. Clinical usefulness of iodine-123-MIBG scintigraphy for patients with neuroblastoma detected by a mass screening survey. Ann Nucl Med 2003;17:633-40
100. Pfluger T, Schmied C, Porn U, et al. Integrated imaging using MRI and 123I metaiodobenzylguanidine scintigraphy to improve sensitivity and specificity in the diagnosis of pediatric neuroblastoma. AJR Am J Roentgenol 2003;181:1115-24
101. Erickson D, Kudva YC, Ebersold MJ et al. Benign paragangliomas: clinical presentation and treatment outcomes in 236 patients. J Clin Endocrinol Metab 2001;86:5210-6
102. Virotta G, Medolago G, Zappone C et al. Meta-(123I)iodobenzylguanidine single photon emission computed tomography in chemodectomas. J Nucl Med 1995;39:9-12
103. Adalet I, Kocak M, Oguz H, Alagol F, Cantez S. Determination of medullary thyroid carcinoma metastases by 201Tl, 99Tcm(V)DMSA, 99Tcm-MIBI and 99Tcm-tetrofosmin. Nucl Med Commun 1999;20:353-9
104. Ugur O, Kostakglu L, Guler N, et al. Comparison of 99mTc(V)-DMSA, 201Tl and 99mTc-MIBI imaging in the follow-up of patients with medullary carcinoma of the thyroid. Eur J Nucl Med 1996;23:1367-71

Chapter three

Staging of carcinoid tumours using 18F-DOPA positron emission tomography

Klaas P Koopmans, MD, Elisabeth G E de Vries, MD, PhD, Ido P Kema, PhD, Philip H Elsinga, PhD, Oliver C Neels, ChemD, Wim J Sluiter, PhD, Anouk N A van der Horst-Schrivers, MD, Pieter L Jager, MD. PhD.

Departments of Nuclear Medicine and Molecular Imaging (K P K, O C N, P H E, P L J), Medical Oncology (E G E V, A N A H), Pathology and Laboratory Medicine (I P K), and Endocrinology (W J S). University Medical Centre Groningen, Groningen, The Netherlands

Lancet Oncol 2006; 7:728–34

SUMMARY

Background To assess individual treatment options for patients with carcinoid tumours, accurate knowledge of tumour localizations is essential. We aimed to test the diagnostic sensitivity of ^{18}F-DOPA PET, compared with conventional methods methods, in patients with carcinoid tumours.

Methods In a prospective, single-centre, diagnostic accuracy study ^{18}F-DOPA PET with carbidopa pre-treatment was compared with Somatostatin receptor scintigraphy (SRS), CT and combined SRS and CT in 53 patients with a metastatic carcinoid tumour. The performance of all imaging modalities was analysed for individual patients, for eight body regions and for detection of individual lesions. PET and CT images were fused to improve localization. To produce a composite reference standard, we used cytological and histological findings; all imaging tests, including secondary assessments for newly found lesions; follow-up; and biochemical data Sensitivities were calculated and compared.

Findings In a patient based analysis, we recorded sensitivities of 100% (95% CI 93-100) for ^{18}F-DOPA PET, 92% (82-98) for SRS, 87% (75-95) for CT, and 96% (87-100) for combined SRS and CT ($p=0.45$ for ^{18}F-DOPA PET vs combined SRS and CT) . However, ^{18}F-DOPA PET detected more lesions, more positive regions and more lesions per region than combined SRS and CT. In region- based analysis, sensitivity of ^{18}F-DOPA PET was 95% (90-98) versus 66% (57-74) for SRS, 57% (48-66) for CT and 79% (70-86) for combined SRS and CT ($p<0\cdot001$, PET vs combined SRS and CT). In lesion analysis, corresponding sensitivities were 96% (95-98), 46% (43-50), 54% (51-58) and 65% (62-69; $p<0.0001$ for PET vs combined SRS and CT).

Interpretation If the improved tumour localisation seen with ^{18}F-DOPA PET compared with conventional imaging is confirmed in future studies, this imaging method could replace use of SRS, help improve prediction of prognosis, and be used to assess patients' response to treatment for carcinoid tumours.

INTRODUCTION

Neuroendocrine tumours are a heterogeneous group of slowly growing lesions arising from neuroendocrine cells, of which carcinoid tumours are the most common. These tumours are often located in the abdomen and can produce and secrete a large variety of products because of their intrinsic ability to take up, accumulate and decarboxylate amine precursors.[1] In metastatic disease these products, such as serotonin and catecholamines, can bypass the first-pass metabolization and inactivation by the liver and cause symptoms. Treatment options for carcinoid tumours include curative or debulking surgery, medical treatment with somatostatin analogues and interferon.[(2)]

To assess individual treatment options, accurate knowledge of tumour localization,

biochemical activity and the rate of progression is essential. The initial work-up for patients with carcinoid tumours consists of morphological imaging methods such as CT, combined with functional whole body imaging using somatostatin receptor scintigraphy (SRS).[3-5] However, CT and MR imaging of the abdomen have difficulties in correctly separating tumours and mesenterial metastases from intestinal structures.[6-8] Furthermore, SRS can produce false negative findings, due to variable affinity and expression of somatostatin receptors and the restricted resolution of gammacameras and single photon emission tomography (SPECT) methods.[9,10]

PET using the catecholamine precursor 6-[F-18]fluoro-L-DOPA (^{18}F-DOPA) has recently emerged as a new imaging method for neuroendocrine tumours.[6] By contrast with other methods, this procedure is based on the intrinsic property of neuroendocrine tumours to take up amine precursors, such as ^{18}F-DOPA.[11-15] The combination of this specific tracer with the high resolution provided by PET, could lead to a clinically relevant improvement in detection and staging of neuroendocrine tumours. A few small studies have shown some potential of ^{18}F-DOPA PET in small and heterogeneous groups of patients with neuroendocrine tumours.[6,16-17]

Therefore, the aim of this study was to compare the diagnostic sensitivity of ^{18}F-DOPA PET with that of conventional imaging methods, such as SRS and CT, in a large and homogeneous population of patients with carcinoid tumours.

METHODS

Patients

Patients eligible for this prospective single-centre diagnostic accuracy study included: those who were newly referred to our centre (which serves the northern region of the Netherlands) with a carcinoid tumour, based on clinical or biochemical findings and at least one abnormal lesion detected on CT, MRI, sonography or on SRS, and those known to have a histopathologically proven carcinoid tumour, who had a clinical indication for restaging and who had at least one abnormal lesion on conventional imaging studies. We excluded patients younger than 18 years, those who were pregnant, and those in whom an additional non-carcinoid tumour had been diagnosed. Every consecutive patient underwent ^{18}F-DOPA PET, SRS, CT scanning of the abdomen and (if needed) the chest and biochemical analysis. Imaging methods were undertaken in a random order. The local medical ethics committee approved the study and all patients gave written informed consent.

Procedures

^{18}F-DOPA was produced in the radiochemical laboratory of our hospital as described

previously.[18] Patients fasted for 6 h before the examination and were allowed to continue all medication. Whole-body two-dimensional PET images were acquired 60 min after intravenous use of ^{18}F-DOPA (130–230 MBq, radiation dose 2.6–4.6 mSv)[19], on a Siemens ECAT HR+ (high-resolution) positron camera (Siemens, Knoxville, TN, USA) with attenuation correction (7–10 bedpositions of 5 min emission and 3 min transmission scan). For the reduction of tracer decarboxylation and subsequent renal clearance, all patients received 2 mg/kg carbidopa orally as pretreatment, 1 h before the 18F-DOPA injection, to increase tracer uptake in tumour cells.[19-21]

Two nuclear medicine physicians (KPK, PLJ), who were masked to the results of other imaging examinations and to the extension of tumour spread in study patients, interpreted the 18F-DOPA PET images independently. Only lesions in every body region that clearly showed more activity than that seen in patients and regions not known to contain tumours were regarded as abnormal. If discrepancies were found, a consensus reading was done. Since 18F-DOPA PET is a new test, these physicians built expertise in the first 20 cases, and then reviewed these early cases again in the second half of 2004.

According to Dutch standards, we obtained planar totalbody and SPECT images 24 h after intravenous administration of 200 MBq indium-111-octreotide (Octreoscan; Mallinckrodt, Petten, Netherlands; radiation dose 10 mSv) [22], using standard methods (Siemens Multispect 2 gamma camera, medium-energy collimator, 10 min spotviews, 64 projections of 30 s). If interfering bowel activity was seen, images were recorded again at 48 h.[23] We withheld laxatives only if patients presented with diarrhoea. All patients were allowed to continue their treatment.

SRS scans were interpreted by dedicated specialists as part of routine care and independently reread by a nuclear medicine physician (PLJ), who was masked to the results of other imaging examinations and to the extension of tumour spread in the study patients.

CT (4–16 slice, Siemens Somatom Sensation, Siemens Medical Systems, Erlangen, Germany; radiation dose 8–20 mSv)24 was done with oral contrast and intravenous contrast enhancement (Visipaque 270, 120 mL, 2·5 mL/s). The reconstruction interval was 3–8 mm. All patients underwent CT of the entire abdomen and pelvis. The CT imaging area was extended to include the chest in 26 patients, and the neck and chest in three patients because of clinical suspicion of tumours in those regions. CT scans were interpreted by dedicated specialists as part of routine care. At the time of image fusion, results were reviewed again by the investigators, and for discrepancies, consensus was reached after multidisciplinary discussion.

As a composite reference standard for the presence of tumour lesions, we used all available cytological, histological, follow-up, and imaging findings, because cytological or histological verification of every lesion is not feasible and not justifiable ethically in all patients because of the tumour load in many of these patients. If possible, new fi

ndings on PET were verifi ed by other investigations other than CT and PET–CT fusion. These were: MRI (n=8), bone scintigraphy (n=9), planar radiographs (n=13), sonography (n=4), surgery (n=10), or biopsy (n=5). These investigations included verification of lesions in body regions that were outside the CT field. However, in many cases, the number of new and previously unknown lesions on PET imaging was high, which led to the analysis of every individual localisation.

After images had been interpreted, CT and 18F-DOPA PET images were fused automatically by use of threedimensional fusion software (Siemens Leonardo workstation) with manual fine adjustments. Experienced physicians compared the fusion images with the results of visual matching for the accuracy of lesion localisation.

As markers for serotonin metabolism, we measured serotonin concentrations in platelets and urinary 5-hydroxyindole acetic acid (5-HIAA) in a 24-h urine sample (upper reference limits 5·4 nmol/109 platelets and 3·8 mmol/mol creatinine, respectively). As markers of catecholamine metabolism, we measured urinary concentrations of metanephrine, normetanephrine, and 3-methoxytyramine in a 24-h urine collection (upper reference limits 99, 260, and 197 µmol/mol creatinine, respectively).[14,25] Sampling procedures and analytical methods were done as previously described.[24–30] We measured serum concentrations of chromogranin A by use of a radioimmunoassay (Cga-React, Cis Bio International, Marcoule, France) as a marker for tumour volume (reference interval 20.0–100.0 mg/L).

Statistical analysis

Analysis was done at three levels. At the first level, individual patients were analysed. Image studies were regarded as positive if a patient had at least one lesion. The second level of analysis addressed body regions—head and neck, mediastinum, lungs, liver, abdomen and pelvis, bone, and soft tissue of the extremities. A region was regarded as positive, if at least one lesion was detected in that region. The third level analysed the individual lesions that were counted for all imaging methods. If the number of lesions in one region (eg,liver) was more than ten, the number of lesions was truncated at ten lesions for that region to avoid bias.

SRS is a whole-body procedure, whereas CT covers only the most relevant parts of the body. To eliminate possible bias towards whole-body imaging methods, we only analysed regions for which all three imaging methods were available.

Sensitivities were calculated with the composite reference standard and were compared with paired observations and McNemar's test. Patient-based sensitivity was calculated as the proportion of patients with at least one lesion detected. Regional sensitivity was calculated by dividing the number of patients with a positive region (detected with that particular method) by the total number of patients in whom that region was positive by any imaging method. We calculated lesion-based sensitivity by dividing the number of

lesions detected with a particular method by the total number of lesions detected by any method. Pitman's test for paired data was used to compare the number of lesions per region. Wilcoxon's test was used to compare the number of patients with five or fewer positive body regions detected by PET and by combined SRS and CT. For correlations, Spearman's *r* test was calculated. Significance level was 0.05, twosided. We did statistical analysis by using the SPSS package version 12.0.

Role of the funding source

The sponsor of the study had no role in study design, data collection, data analysis, data interpretation, or writing of the report. The corresponding author had full access to all the data in the study and had final responsibility for the decision to submit for publication.

RESULTS

Between October, 2003, and February, 2006, we asked 68 consecutive patients to participate in the study (figure 1); however, three declined PET scanning, and we could not obtain all required information for 12, because of various logistical reasons (eg, no biochemistry or pathology findings, no SRS). Sensitivity was calculated in the remaining 53 patients assessed, of whom 25 were newly diagnosed with carcinoid disease (table 1). The median time between PET and CT was 59 days (range 1–191) and between PET and SRS was 47 days (1–206). Mean values for these intervals were 25 days (SD 57) and 42 days (75), respectively. In retrospect, the interval was short compared with disease progression in all patients. One patient developed a carcinoid crisis after intravenous administration of 18F-DOPA, which was treated success fully.[31]

^{18}F-DOPA PET produced high-quality tomographical images that were easily interpretable (figure 2). More patients had positive lesions detected by ^{18}F-DOPA PET than by SRS or by combined SRS and CT (table 2; ^{18}F-DOPA PET *vs* combined SRS and CT, p=0.45). Four patients were recorded as negative on SRS, seven on CT, and two on combined SRS and CT (both of whom were shown to have tumours when assessed 6 months later with SRS).

Table 3 shows region-based and lesion-based sensitivities. Of 326 regions that were assessable, 122 (37%) were judged as positive for tumour. ^{18}F-DOPA PET detected 117 of these positive regions (sensitivity 95%), whereas SRS only detected 80 (sensitivity 66%; table 3). When data from SRS and CT were combined, sensitivity
reached 79% but was substantially lower than that for ^{18}F-DOPA PET (^{18}F-DOPA PET *vs* combined SRS and CT, p=0.0001).

687 lesions were regarded as positive for tumour (table 3). ^{18}F-DOPA PET detected 658 lesions (sensitivity 96%), and SRS detected 315 (sensitivity 46%). Combined SRS and

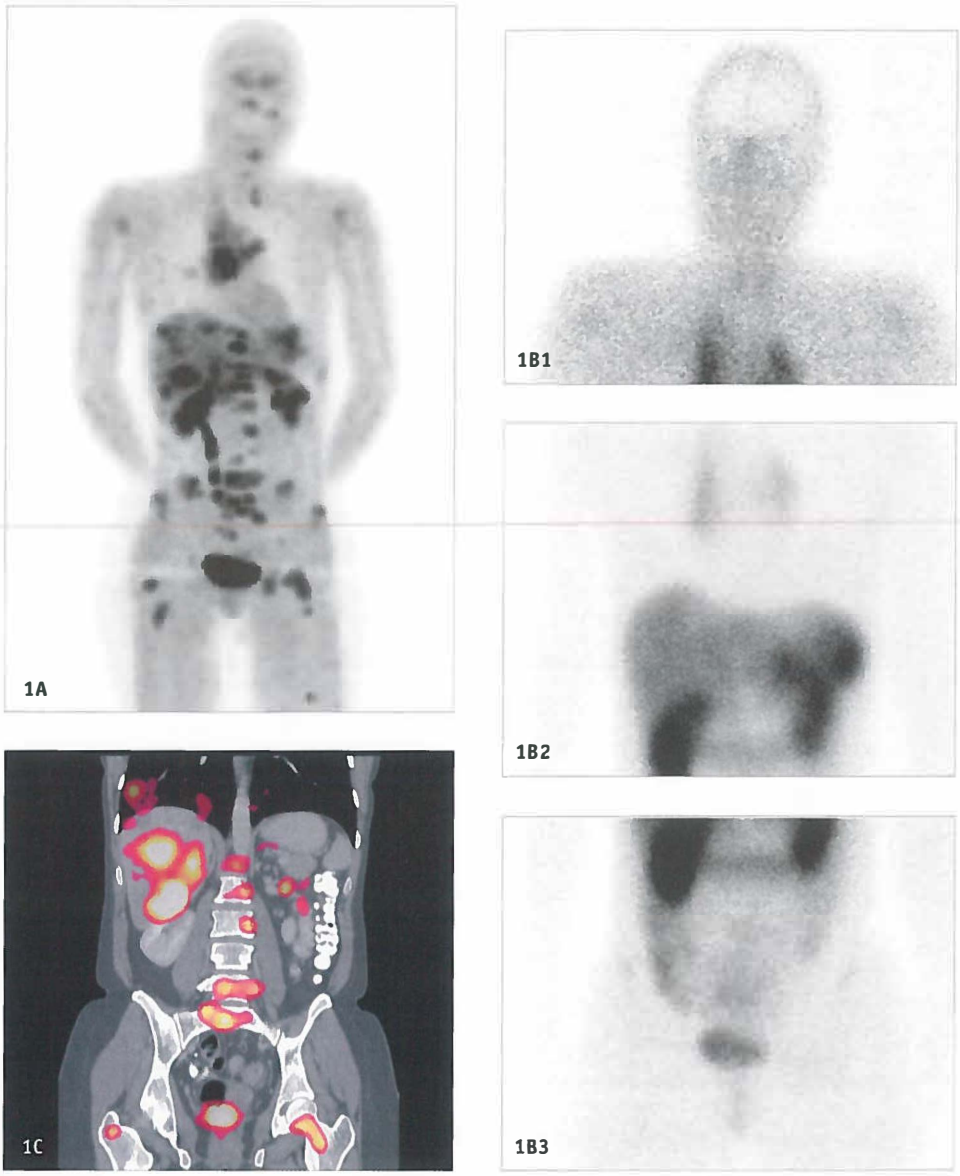

Figure 1. Patient with carcinoid disease with bone, mediastinal, liver and abdominal metastases.
Panel A shows a 18F-DOPA PET image. Red arrows indicate areas with physiological 18F-DOPA uptake (striatum, kidneys, ureter, bladder) whereas all other black spots are tumour lesions. Panel B shows the planar somatostatin receptor scintigraphic images, arrowheads indicate mediastinal tumour lesions. Panel C shows a CT-PET fusion image, all coloured areas denote tumour lesions. In this patient both planar and SPECT somatostatin receptor scintigraphy missed most lesions found with 18F-DOPA PET imaging. The abdominal and femoral lesions were not observed on CT

Table 1. Characteristics of the 53 patients included

Characteristics	Value
Sex (no of patients) Male/Female	25/28
Median age in years (Range)	59 (35-77)
New patients vs patients with known disease (no of patients)	25/28
Histological vs biochemical diagnosis	52/1
Primary localization of carcinoid tumour	
Lung	5
Duodenum/ Jejunum/ Ileum	3/ 3/ 25
Colon	1
Unknown	16
Patients with carcinoid syndrome	21
Treatment during scan	
Somatostatin analogues (n)	15
Somatostatin analogues + interferon (n)	1
Biochemical parameters (elevated in n patients/total number of patients)	
Platelet serotonin	42/51
Urinary 5-hydroxyindolacetic acid	35/51
Urinary metanephrine	5/48
Urinary normetanephrine	7/48
Urinary 3-methoxytyramine	16/48
Serum chromogranin A	21/31

Table 2. Patient based analysis

Imaging modality	Number patients with positive lesions	Sensitivity	Average number of lesions per patient
^{18}F-DOPA PET	53	100%	12·4
SRS alone	49	92·5%	6·4
CT alone	46	86·8%	8·1
SRS + CT	51	96·2%	8·8

CT detected 450 lesions (sensitivity 65%; ^{18}F-DOPA PET *vs* combined SRS and CT, p<0.0001). Most positive lesions were found in the liver and abdominopelvic regions. ^{18}F-DOPA PET showed more lesions in these two regions than did combined SRS and CT (liver, 348 *vs* 261, p<0.0001; abdomen/pelvis, 203 *vs* 135, p<0.0001, respectively).

^{18}F-DOPA PET detected a mean of 2.2 (SD 0.93) positive regions per patient, versus 1.8 (0.81) detected by combined SRS and CT (p=0.0007). Based on our reference standard and follow-up, we could not record any false-positive lesions. The median number of lesions per patient was 12 for ^{18}F-DOPA PET and ten for combined SRS and CT (table 2). A mean of

Table 3. Sensitivities of imaging modalities in patients with carcinoid tumours.

	PET Sensitivity (95%CI)	SRS Sensitivity (95%CI)	CT Sensitivity (95%CI)	SRS+CT Sensitivity (95%CI)	Number of positive regions or lesions
Region based analysis					
Mediastinal*	92(74-99)	69(38-91)	15(1-46)	69(38-91)	13
Lung*	60(13-96)	80(27-99)	40(40-87)	80(27-99)	5
Liver	98(88-100)	77(62-89)	75(60-87)	89(75-96)	44
Pancreas	100(26-100)	0(0-74)	67(7-100)	67(7-100)	3
Abdomen / pelvis	97(86-100)	72(55-85)	62(44-77)	87(72-96)	39
Bone	92(63-100)	31(1-62)	46(19-75)	54(25-81)	13
Extremities	100(45-100)	20(0-73)	20(0-73)	20(0-73)	5
Total	**95**(90-98)**	**66(57-74)**	**57(48-66)**	**79(70-86)**	**122**
Lesion based analysis					
Mediastinal *	95(82-100)	41(25-58)	8(1-21)	44(28-60)	39
Lung*	55(23-84)	53(16-77)	36(10-70)	64(30-90)	11
Liver	97** (95-94)	53(48-59)	66(61-71)	73(68-78)	360
Pancreas	100(26-100)	0(0-74)	67(7-100)	67(7-100)	3
Abdomen / pelvis	96** (93-98)	41(35-48)	49(42-56)	64(57-71)	208
Bone	97(88-100)	31(20-44)	41(29-54)	48(35-61)	61
Extremities	100(45-100)	20(0-73)	20(0-73)	20(0-73)	5
Total	**96**(95-98)**	**46(43-50)**	**54(51-58)**	**65(62-69)**	**687**

In the head and neck region no lesions were found with either imaging modality. Therefore, this region has been omitted from this table. *Only regions in the field of view of all modalities were compared. ** p<0.001 for the comparison of ^{18}F-DOPA PET with the combination SRS and CT.

13.5 lesions (SD 7.9) per patient were found overall (^{18}F-DOPA PET, 12.4 [7.4]; SRS, 6.2 [5.6]; combined SRS and CT, 8.8 [6.4]; ^{18}F-DOPA PET *vs* combined SRS and CT, p<0.0001). Thus, ^{18}F-DOPA PET detects an additional tumourpositive region in one of three patients, and detects four additional lesions per patient.

Urinary 5-HIAA excretion correlated with the number of tumour lesions detected by ^{18}F-DOPA PET (r=0.41, p=0.003), by CT (r=0.40, p=0.003), and by combined SRS and CT (r=0.38, p=0.006). Platelet serotonin concentrations correlated only with the number of tumour lesions detected by ^{18}F-DOPA PET (r=0.45, p=0.001). We recorded no correlation between the total number of tumours detected by any imaging method and concentrations of serum chromogranin A, urinary metanephrine, normetanephrine, or 3-methoxytyramine.

DISCUSSION

We showed improved diagnostic sensitivity of ^{18}F-DOPA PET in staging and identifi cation of carcinoid tumours, compared with currently applied, standard whole-body imaging with SRS. Compared with the combination of SRS with CT, ^{18}F-DOPA PET PET detected substantially more individual tumour lesions, more affected body regions, and more lesions per region. The improved lesion detection of carcinoid tumours with ^{18}F-DOPA PET provides a better understanding of the true extent of tumour spread in patients.

The precise mechanisms that determine the uptake of ^{18}F-DOPA in neuroendocrine tissues are not yet fully elucidated. The increased demand for aminoacids, precursors in the overactive secretory pathways in neuroendocrine tumours,[14] probably induces high uptake of this aminoacid tracer in tumours by upregulation of transmembrane aminoacid transporters. However, intracellular mechanisms, such as the highly active aminoacid decarboxylase enzyme that is specifically active in neuroendocrine tumours, probably contribute to tracer uptake.[11,13] Overactivity of the catecholamine pathway could induce uptake of the catecholamine precursor tracer ^{18}F-DOPA, but ^{18}F-DOPA uptake was also present in the absence of increased urinary catecholamine metabolite secretion.

Only two small studies[6,17] have been reported on ^{18}F-DOPA PET scanning in patients with carcinoid tumours. Hoegerle and colleagues[6] did a lesion-based analysis (n=17) and found that ^{18}F-DOPA PET was more sensitive than SRS, CT, and MRI in detecting primary tumours and lymph-node metastases.[6] However, the performance of 18F-DOPA PET for the detection of organ metastases was similar to that of SRS and worse than that of CT and MRI combined. Our improved results might be due to the use of oral carbidopa pretreatment, which increases the concentration and availability of ^{18}F-DOPA, thereby improving lesion detectability.[32] Hoegerle and co-workers[6] also used either CT or MRI, and studied fewer patients than we did. Becherer and colleagues[17] studied 23 patients, in whom 18 carcinoid

tumours had been detected. ^{18}F-DOPA PET yielded high sensitivities in a regionbased analysis similar to that used in our study. However, they detected fewer lesions in the lung (one of five patients who had lung tumours) than that seen in our study (three of five patients with lung tumours), although the numbers for this region were low in both studies. In the Becherer study,[17] CT was the gold standard, and only lesions visible on ^{18}F-DOPA PET were regarded as false-positive.

A notable alternative for the imaging of neuroendocrine tumours is the use of a direct precursor for the serotonin pathway, ^{11}C-5-hydroxytryptophan (^{11}C-5-HTP). This tracer has been investigated in 42 patients with various neuroendocrine tumours, after pretreatment with carbidopa.[33] ^{11}C-5-HTP PET detected carcinoid tumours in 13 of these patients, which was similar to our results with ^{18}F-DOPA. General applicability was limited by the difficult tracer synthesis of ^{11}C-5-HTP and the short halflife of a ^{11}C-based tracer of 20 min (half-life of an ^{18}F-based tracer is 110 min). Other developments include the search for new radiolabelled somatostatin analogues for improved SRS SPECT imaging and SRS PET imaging.[34–36]

A perfect gold standard is difficult to establish in any diagnostic accuracy study. In our study, new diagnostic methods might have been much better than current standard methods and might detect many unknown lesions that can never all be verified by cytological or histological analysis. Where possible, new findings were verified but we also assumed that when several lesions were verified by one technique, other lesions with identical and unequivocal uptake of this same tracer in the same patient could also be regarded as true tumours. The composite reference standard depended to some extent on the ^{18}F-DOPA PET results, and also on the CT and SRS results. Thus, our sensitivity values should be interpreted with caution.

In view of the many new lesions detected by ^{18}F-DOPA PET and the fact that cytological and histological verification has a risk of bleeding complications in these highly vascularised lesions, we did not consider the undertaking of ten biopsies in one patient as feasible.

Enhanced detection of lesions with ^{18}F-DOPA PET can lead to improvements in patients' care. In particular, the imaging method's excellent detection properties for liver, bone, and abdominal lesions could lead to alterations in surgery, medical treatment, and radiotherapy plans. Neuroendocrine tumours are currently classified by the WHO framework, which is based on morphological, clinical, and functional aspects of the tumour and its metastases. Treatment options depend on the tumour mass, functional activity, and growth behaviour of these tumours.[37,38] ^{18}F-DOPA PET could add important information on tumour localisations and prognosis and be used to aid research in the response to new molecular-targeted drugs, possibly even replacing SRS. However, we did not aim to record how use of this technique could change management, since we included patients with at

least one histologically confirmed lesion or with known extensive disease. Furthermore, image interpreters need to develop experience with the technique before being completely accurate. With the excellent sensitivity of ^{18}F-DOPA PET recorded in patients with proven tumours, future studies are under way to measure the technique's detection capability in patients suspected of having a neuroendocrine tumour.

In summary, ^{18}F-DOPA PET significantly improves the detection of carcinoid tumours and their metastases compared with conventional techniques, and detects an additional tumour-positive region in one of three patients, and a mean of four additional lesions per patient. This technique might also contribute greatly to the staging of these patients. With the rapidly expanding availability of PET and increasing commercial production and distribution of radiotracers, the availability of tracers such as ^{18}F-DOPA will probably also increase. Furthermore, treatment of these patients is often centralised in well-equipped hospitals. Although ^{18}F-DOPA PET is almost sufficient for staging, addition of CT improves the localisation of lesions, which is relevant to guide surgical and radiotherapeutical procedures. The new trend of combined PET–CT scanning could therefore become a one-stop procedure in the staging of carcinoid tumours.

ACKNOWLEDGMENTS

Our work was supported by grant 2003-2936 from the Dutch Cancer Society. We thank dr W W de Herder, Erasmus MC, Rotterdam, The Netherlands, for valuable advice.

Authors contributions

K P Koopmans participated in the patient recruitment, PET scanning, data collection, data analysis and writing of the report. E G E de Vries participated in the design of the study, patient recruitment, data analysis and writing of the report. I P Kema participated in the design of the study, biochemical analysis, data analysis and writing of the report. P H Elsinga participated in the design of the study, data analysis and writing of the report. O C Neels participated in the data analysis and writing of the report. W J Sluiter participated in the statistical analysis and writing of the report. A N A van der Horst-Schrivers participated in the patient recruitment, data analysis and writing of the report. P L Jager (corresponding author) participated in the design of the study, patient recruitment, data analysis, interpretation of PET data and writing of the report.

REFERENCES

1. Pearse AG. The APUD cell concept and its implications in pathology. Pathol Annu 1974; 9: 27–41.
2. Moertel CG, Lefkopoulo M, Lipsitz S, Hahn RG, Klaassen D. Streptozocin-doxorubicin, streptozocin-fluorouracil or chlorozotocin in the treatment of advanced islet-cell carcinoma. N Engl J Med 1992; 326: 519–23.
3. Oberg K, Kvols L, Caplin M et al. Consensus report on the use of somatostatin analogs for the management of neuroendocrine tumors of the gastroenteropancreatic system. Ann Oncol 2004; 15: 966–73.
4. Plockinger U, Rindi G, Arnold R et al. Guidelines for the diagnosis and treatment of neuroendocrine gastrointestinal tumours. A consensus statement on behalf of the European Neuroendocrine Tumour Society (ENETS). Neuroendocrinology 2004; 80: 394–424.
5. Modlin IM, Kidd M, Latich I, Zikusoka MN, Shapiro MD. Current status of gastrointestinal carcinoids. Gastroenterology 2005; 128: 1717–51.
6. Hoegerle S, Altehoefer C, Ghanem N et al. Whole-body 18F dopa PET for detection of gastrointestinal carcinoid tumors. Radiology 2001; 220: 373–80.
7. Kaltsas G, Rockall A, Papadogias D, Reznek R, Grossman AB. Recent advances in radiological and radionuclide imaging and therapy of neuroendocrine tumours. Eur J Endocrinol 2004; 151: 15–27.
8. Kumbasar B, Kamel IR, Tekes A, Eng J, Fishman EK, Wahl RL. Imaging of neuroendocrine tumors: accuracy of helical CT versus SRS. Abdom Imaging 2004; 29: 696–702.
9. Fahey FH, Harkness BA, Keyes JW, Jr., Madsen MT, Battisti C, Zito V. Sensitivity, resolution and image quality with a multi-head SPECT camera. J Nucl Med 1992; 33: 1859–63.
10. de Herder WW, Hofland LJ, van der Lely AJ, Lamberts SW. Somatostatin receptors in gastroenteropancreatic neuroendocrine tumours. Endocr Relat Cancer 2003; 10: 451–8.
11. Meijer WG, Copray SC, Hollema H et al. Catecholamine-synthesizing enzymes in carcinoid tumors and pheochromocytomas. Clin Chem 2003; 49: 586–93.
12. Pearse AG. The APUD cell concept and its implications in pathology. Pathol Annu 1974; 9: 27–41.
13. Gilbert JA, Bates LA, Ames MM. Elevated aromatic-L-amino acid decarboxylase in human carcinoid tumors. Biochem Pharmacol 1995; 50: 845–50.
14. Kema IP, de Vries EG, Slooff MJ, Biesma B, Muskiet FA. Serotonin, catecholamines, histamine, and their metabolites in urine, platelets, and tumor tissue of patients with carcinoid tumors. Clin Chem 1994; 40: 86–95.
15. Feldman JM, Moore JO. Biogenic amines in carcinoid tumors. Biog Amines 1989; 6: 247–52.
16. Ahlstrom H, Eriksson B, Bergstrom M, Bjurling P, Langstrom B, Oberg K. Pancreatic neuroendocrine tumors: diagnosis with PET. Radiology 1995; 195: 333–7.
17. Becherer A, Szabo M, Karanikas G et al. Imaging of advanced neuroendocrine tumors with (18)F-FDOPA PET. J Nucl Med 2004; 45: 1161–7.
18. Vries EFJ, Luurtsema G, Brussermann M, Elsinga PJ, Vaalburg W. Fully automated synthesis module for the hiegh yield one-pot preparation of 6-[18F]-fluoro-L-DOPA. Appl Radiat Isot 1999; 51: 389–419.
19. Brown WD, Oakes TR, DeJesus OT et al. Fluorine-18-fluoro-L-DOPA dosimetry with carbidopa pretreatment. J Nucl Med 1998; 39: 1884–91.
20. Bergstrom M, Lu L, Eriksson B et al. Modulation of organ uptake of 11C-labelled 5-hydroxytryptophan. Biog Amines 1996; 12: 477–85.
21. Ishikawa T, Dhawan V, Chaly T et al. Fluorodopa positron emission tomography with an inhibitor of catechol-O-methyltransferase: effect of the plasma 3-O-methyldopa fraction on data analysis. J Cereb Blood Flow Metab 1996; 16: 854–63.
22. International Commission on Radiological Protection. ICRP Publication 80: Radiation dose to patients from radiopharmaceuticals, 80 Annals of the ICRP Volume 28/3. Elsevier; 2000.

23. Balon HR, Goldsmith SJ, Siegel BA et al. Procedure guideline for somatostatin receptor scintigraphy with (111)In-pentetreotide. J Nucl Med 2001; 42: 1134–8.
24. International Commission on Radiological Protection. ICRP Publication 87: Managing Patient Dose in Computed Tomography. Annals of the ICRP Volume 30/4, ICRP Online. Elsevier; 2001.
25. Eisenhofer G, Kopin IJ, Goldstein DS. Catecholamine metabolism: a contemporary view with implications for physiology and medicine. Pharmacol Rev 2004; 56: 331–49.
26. Kema IP, Schellings AM, Hoppenbrouwers CJ, Rutgers HM, de Vries EG, Muskiet FA. High performance liquid chromatographic profiling of tryptophan and related indoles in body fluids and tissues of carcinoid patients. Clin Chim Acta 1993; 221: 143–58.
27. Willemsen JJ, Ross HA, Wolthers BG, Sweep CG, Kema IP. Evaluation of specific high-performance liquid-chromatographic determinations of urinary metanephrine and normetanephrine by comparison with isotope dilution mass spectrometry. Ann Clin Biochem 2001; 38: 722–30.
28. Kema IP, Meiborg G, Nagel GT, Stob GJ, Muskiet FA. Isotope dilution ammonia chemical ionization mass fragmentographic analusis of urinary 30-methylated catecholamine metabolites. Rapid sample clean-up by derivatization and extraction of lyophilic samples. J Chromatogr Biomed Appl 1993; 671: 181–9.
29. Kema IP, Meijer WG, Meiborg G, Ooms B, Willemse PH, de Vries EG. Profiling of tryptophan-related plasma indoles in patients with carcinoid tumors by automated, on-line, solid-phase extraction and HPLC with fluorescence detection. Clin Chem 2001; 47: 1811–20.
30. Mulder EJ, Oosterloo-Duinkerken A, Anderson GM, de Vries EG, Minderaa RB, Kema IP. Automated on-line solid-phase extraction coupled with HPLC for measurement of 5-hydroxyindole-3-acetic acid in urine. Clin Chem 2005; 51: 1698–703.
31. Koopmans KP, Brouwers AH, De Hooge MN et al. Carcinoid crisis after injection of 6-18F-fluorodihydroxyphenylalanine in a patient with metastatic carcinoid. J Nucl Med 2005; 46: 1240–3.
32. Orlefors H, Sundin A, Lu L et al. Carbidopa pretreatment improves image interpretation and visualisation of carcinoid tumours with (11)C-5-hydroxytryptophan positron emission tomography. Eur J Nucl Med Mol Imaging 2006; 33: 60–5.
33. Orlefors H, Sundin A, Garske U et al. Whole-body (11)C-5-hydroxytryptophan positron emission tomography as a universal imaging technique for neuroendocrine tumors: comparison with somatostatin receptor scintigraphy and computed tomography. J Clin Endocrinol Metab 2005; 90: 3392–400.
34. Hubalewska-Dydejczyk A, Fross-Baron K, Mikolajczak R, Maecke HR, Huszno B, PachD, Sowa-Staszczak A, Janota B, Szybinski P, Kulig J. (99m)Tc-EDDA/HYNIC-octreotate scintigraphy, an efficient method for the detection and staging of carcinoid tumours: results of 3 years' experience Eur J Nucl Med Mol Imaging 2006; May 24; [Epub ahead of print]
35. Hofmann M, Maecke H, Borner R, Weckesser E, Schoffski P, Oei L, Schumacher J, Henze M, Heppeler A, Meyer J, Knapp H. Biokinetics and imaging with the somatostatin receptor PET radioligand (68)Ga-DOTATOC: preliminary data. Eur J Nucl Med. 2001; 28:1751–7.36.
36. Seemann MD, Meisetschlaeger G, Gaa J, Rummeny EJ. Assessment of the extent of metastases of gastrointestinal carcinoid tumors using whole-body PET, CT, MRI, PET/CT and PET/MRI. Eur J Med Res. 2006;11: 58–65
37. Solcia E, Kloppel G, Sobin LH, eds. Histological typing of endocrine tumours, 2nd edn, Heidelberg: WHO, 2000.
38. Modlin IM, Kidd M, Latich I, et al. Current status of gastrointestinal carcinoids. Gastroenterology 2005; 128:1717-51

Chapter four

Carcinoid Crisis after Injection of 18F-DOPA in a Patient with Metastatic Carcinoid

Klaas P. Koopmans, MD[1]; Adrienne H. Brouwers, MD, PhD[1]; Marjolijn N. De Hooge[2], Anouk N. Van der Horst- Schrivers, MD[3]; Ido P. Kema PhD[4]; Bruce H. Wolffenbuttel, MD, PhD[5]; Elisabeth G. De Vries, MD, PhD[3]; and Pieter L. Jager, MD, PhD[1].

[1]Departments of Nuclear Medicine and PET center; [2]Nuclear Medicine and Pharmacy; [3]Medical Oncology; [4]Clinical Chemistry and [5]Endocrinology, University Medical Center Groningen, The Netherlands.

J Nucl Med 2005; 46: 1240–3

ABSTRACT

A carcinoid crisis is a severe complication of the carcinoid syndrome that can arise in patients with advanced metastatic neuroendocrine tumors. It can be initiated by stress, catecholamines and tumor manipulation. In this report we present a case in which an injection with the catecholamine tracer ^{18}F-DOPA, used for PET imaging, induced a carcinoid crisis. Octreotide can be used for treatment and should be available. Tracer injection should be slow.

Key words:18F-DOPA; carcinoid syndrome; carcinoid crisis; neuroendocrine tumors

INTRODUCTION

The carcinoid syndrome can occur in patients with a metastasized midgut carcinoid. This syndrome is characterized by episodes of flushing, diarrhea, abdominal pain and wheezing.[1-3] A carcinoid crisis is a serious complication of the carcinoid syndrome. A crisis is characterised by a sudden onset of different symptoms at once which can consist of prolonged cutaneous flushing, severe dyspnea, peripheral cyanosis, tachycardia and sometimes hemodynamic instability, which can be fatal.[4-6]

In recent years, PET scanning using 6-[^{18}F]-fluoro-dihydroxy-phenylalanine (^{18}F-DOPA) has emerged as a new and accurate modality to image neuroendocrine tumors.[7,8] ^{18}F-DOPA is an amino acid, but also an important precursor in catecholamine metabolism. In this paper, we report a case in which the rapid intravenous administration of a bolus of ^{18}F-DOPA, used for a PET imaging study, initiated a carcinoid crisis.

CASE REPORT

A 61 year old woman with extensive liver metastases from a carcinoid tumor was referred to our PET center for a ^{18}F-DOPA PET scan. She participated in a diagnostic research project that was approved by the local institutional review board, and had given informed consent. One and a half year earlier she was diagnosed with carcinoid disease and elevated 5-hydroxy indol acetic acid (5-HIAA) excretion based on a primary tumor in the ileum and extensive liver metastases. To alleviate symptoms of diarrhea she received 20 mg slow-release octreotide intramuscularly every 4 weeks. Despite this treatment she still experienced episodes of diarrhea and flushing at the time of referral for the PET scan. During the last two visits to the outpatient clinic her blood pressure was 190/100 mmHg. In the last month her urine 5-hydroxy indol acetic acid (5-HIAA) level had slightly risen from 102 to 124 mmol/mmol creatinine. Since 8 years she had type 2 diabetes for which she received glibenclamide.

Conform our scan protocol she received 150 mg carbidopa orally after 6 hours of

fasting. One hour later a bolus of 160 MBq ^{18}F-DOPA with a specific activity of 6 GBq/mmol was administered intravenously in a few seconds. Total injected volume was 8 ml consisting of 5.63 mg ^{18}F-DOPA and 6 ml NaCl 0.9%. Radiosynthesis of ^{18}F-DOPA had been performed according to the method described by De Vries *et al.* and was no different from previous syntheses.[9] Approximately 3 minutes after injection she complained about a strange feeling in the abdomen, extending to her chest, shortness of breath, and nausea, but no itching. This was followed by severe vomiting. Physical examination revealed facial flushing with facial edema, peripheral cyanosis and thoracic erythema. Her blood pressure was 185/90 mmHg, with a regular heart rate of 72/min. Her ECG was normal. Blood glucose was 8.6 mmol/l. She was given 2 mg of the antihistamine clemastine (Tavegil ®, Novartis, Switzerland) intravenously. Approximately 10 minutes after this injection her vomiting had stopped and her other complaints slowly diminished in the next 30 minutes. She felt herself fit to be scanned and one hour after injection of FDOPA the scan procedure was started(Fig. 1). When the scan was finished, blood and urine samples were collected to evaluate for histamine, catecholamine and serotonin metabolites. These data could be compared with measurements that had been performed in the morning before the PET scan. Finally she went home in a good condition, approximately 2 hours after the injection.

Two weeks later she told us that she had experienced similar, but less severe, episodes (without vomiting and peripheral cyanosis) spontaneously before. Based on these symptoms and an increase in urinary 5-HIAAs her octreotide slow-release dose was increased from 20 mg to 30 mg monthly.

Figure 1. Anterior projection image from a ^{18}F-DOPA PET scan showing extensive liver metastases and a supraclavicular lesion. Note physiological uptake in the striatum, kidneys and bladder.

DISCUSSION

Initially we ascribed the symptoms of this patient to an anaphylactic reaction caused by the injection of ^{18F}-DOPA. We treated her as such by giving an antihistamine. However, based on additional clinical and biochemical information it appears that this incident was a carcinoid crisis induced by the injection of ^{18}F-DOPA.

Laboratory parameters are important to determine the nature of such incidents. During anaphylaxis mast cells and basophils degranulate upon activation by cross-linking of mast cell-bound IgE with antigen or complement components. Products released during this degranulation include histamine, prostaglandins, leukotrienes, platelet activating factor and tryptase. Supportive for a diagnosis of anaphylaxis are increased serum tryptase levels and increased urine N-methyl-histamine, a histamine metabolite, that remains elevated for several hours.[10,11] In our patient tryptase and urine N-methyl-histamine were within normal range (Table 1), which virtually excludes an anafylactic reaction as the cause for the incident. A carcinoid crisis is the result of a massive release of serotonin and other products, such as histamine, kallikreins [12] or catecholamines.[13] Especially levels of serotonin and its metabolites (5-HIAA) are elevated and remain so for several hours.[14-16] In our patient, urine 5-HIAA had doubled within a few hours. In addition, serum tryptophan was lowered by 50% (Table 1).[17] From these values it can be concluded that there has been a period of massive serotonin production and release which together with her symptoms and history, is diagnostic for a carcinoid crisis. The low tryptophan level, the first precursor in the serotonin pathway, confirms the increased activity of this pathway.

Various causes for the carcinoid crisis have been reported. Besides mechanical stimulation of the tumor and triggering by catecholamines (especially noradrenalin), a carcinoid crisis can also be triggered by stress, hypercapnia, hypothermia, hypotension, hypertension, initiation of chemotherapy or drugs that cause release of histamine.[5,12,15,18-20] In our case the rapid injection with the catecholamine tracer ^{18F}-DOPA triggered the release of serotonin by the tumor cells, thus initiating the carcinoid crisis.

Possible mechanisms for the initiation of a carcinoid crisis by ^{18}F-DOPA can be local conversion in tumor tissue of ^{18}F-DOPA to noradrenaline, induced by the enzymes aromatic acid decarboxylase (AADC) and dopamine beta-hydroxylase (DBH). These enzymes, especially AADC, can be abundantly present in carcinoids and remain active even in the presence of carbidopa.[21,22] Noradrenaline could then stimulate the tumor cells to release serotonin. This mechanism seems most likely, because the amount of the injected tracer is relatively high (5.6 mg), due to the low specific activity. Another mechanism might be local irritation by ^{18F}-DOPA in the vessel walls of the adrenal gland. The adrenergic system would then release noradrenalin which in turn stimulates the tumor cells to release serotonin. Also for ^{123}I-MIBG it has been proposed that rapid uptake of ^{123}I-MIBG in chromaffin granules, either in the normal adrenal gland, or in tumor tissue, might cause rapid noradrenalin secretion. Every neuroendocrine tumor which produces and stores serotonin and catecholamines in secretory granules could react with massive outpouring

Table 1. Blood and urine measurements before and after scan procedure.

	Reference values	Unit	Before*	After †	1 month later‡
Plasma					
noradrenalin	< 4.31	nmol/l		3.34	
adrenalin	< 0.22	nmol/l		0.11	
dopamine	§	nmol/l		0.11	
serotonin	2.8-5.4	nmol/10^9 thrombocytes	26	27	21
tryptophan	40 - 70	µmol/l	45.1	25.7	26.4
5-HIAA	§	nmol/l	3939.0	3407.0	3502.0
tryptase	< 11.4	µg/l		4.72	
Urine					
creatinine	7.1 – 13.5	mmol/l	6.6	3.9	6.4
5-HIAA	0.8-3.8	mmol/mol creatinine	124.2	247.3	101.1
noradrenalin	< 30	µmol/ mol creatinine		17	
adrenalin	< 10	µmol/ mol creatinine		2.1	
dopamine	< 300	µmol/ mol creatinine		41	
POHPAA	10.0 - 20.0	mmol/ mol creatinine		–	–
HVA	1.1 - 5.5	mmol/ mol creatinine		4.1	3.7
VA	5.0 - 15.0	mmol/ mol creatinine		1.3	11.0
MOPEG	0.4 - 1.5	mmol/ mol creatinine		1.1	0.8
VMA	0.5 - 2.5	mmol/mol creatinine		2.2	1.4
DOPAC	< 2.0	mmol/ mol creatinine		0.5	0.8
Metanephrine	33.0 - 99.0	mmol/ mol creatinine		96	91
Normetanephrine	64.0 - 260.0	µmol/ mol creatinine		181	221
3-MT	45.0 - 197.0	µmol/ mol creatinine		444	519
M-histamine	< 150	µmol/ mol creatinine		52	50
MIMA	0.9 - 1.9	mmol/mol creatinine		2.1	
serotonin	0 - 66	µmol/ mol creatinine	274	271	294

* Blood and urine samples routinely taken 5 hours before 18F-DOPA injection.
† Blood and urine samples taken directly after PET scanning, 2.5 hours after 18F-DOPA injection.
‡ One month after the 18F-DOPA PET scan blood and urine samples were taken to obtain an individual baseline reference.
§ In the normal subject not detectable.
Abbreviations: POHPAA, p-hydroxyphenylacetic acid; HVA: homovanillic acid; VA, vanillic acid, MOPEG, 3-methyl-4-hydroxyphenylethylene glycol; VMA, vanillylmandelic acid; DOPAC, 3,4-dihydroxyphenylacetic acid; 3-MT, 3-methoxytyramine; M-histamine, 1-methyl-histamine; MIMA, methyl-imidazol-acetic acid

of hormones, thus initiating the carcinoid crisis. However, patients most at risk are probably the patients with pre-existing carcinoid syndrome and the existence of extensive liver metastasesor the existence of metastases in another part of the body where the venous blood flow directly enters the systemic circulation. There are currently no risk-factors known that can indicate which

of these patients develop a carcinoid crisis.[1]

The difference between a carcinoid crisis and a severe episode of the carcinoid syndrome can be difficult to make and there is a gradual transition. However, the hallmark of a carcinoid crisis is the sudden (violent) onset of different symptoms at once. Our patient developed much more severe and diverse symptoms shortly after injection of ^{18}F-DOPA than the symptoms she usually experienced during an episode of her carcinoid syndrome. Also her biochemical findings suggest that she had gone through an episode with massive release of serotonin. Therefore it seems more likely that our patient experienced a carcinoid crisis instead of a severe episode of her carcinoid syndrome.

Considering the severity of a carcinoid crisis, preventive measures should be taken and nuclear medicine workers must be aware of this risk and its treatment. This becomes more relevant since the application of ^{18}F-DOPA PET seems more and more valuable for patient care. A preventive measure could be to administer ^{18}F-DOPA slowly instead of a bolus. By avoiding rapidly building peak first-pass concentrations, slow injection can most likely prevent a rapid secretion of noradrenalin by tumor cells. This strategy is similar to the advise given for the administration of ^{123}I-MIBG by the manufacturer. Treatment of a carcinoid crisis should consist of blocking the release of the mediators from tumor tissue by giving somatostatin analogs, such as octreotide.[20,23] In the acute situation 100-500 µg octreotide can be safely administered intravenously.[6] Ketanserin has been used successfully in patients with a carcinoid crisis to block the actions of mediators. It is a selective antagonist of the 5-HT_2 receptor, alpha-1-adrenoreceptor, H_1-histamine receptor and it decreases the central sympathetic outflow.[23] Ketanserin can be given as a 10 mg intravenous bolus injection. To treat hypotension, catecholamines should never be used, as they may stimulate the tumor to release even more serotonin.

CONCLUSION

We present a case of a patient with a carcinoid tumor with extensive liver metastases who developed a carcinoid crisis upon injection with ^{18F}-DOPA. As a carcinoid crisis can be fatal, PET centers using ^{18F}-DOPA for imaging patients with biochemically active and metastasized carcinoid disease should be aware of this rare syndrome. The tracer must be administered slowly and intravenous somatostatin analogs and perhaps also ketanserin should be at hand to treat this condition.

ACKNOWLEDGMENTS

This work was supported by grant 2003-2936 from the Dutch Cancer Society.

REFERENCES

1. Soga J, Yakuwa Y, Osaka M. Carcinoid syndrome: a statistical evaluation of 748 reported cases. J Exp Clin Cancer Res. 1999; 18(2):133-141.
2. Philippe J. APUDomas: acute complications and their medical management. Baillieres Clin Endocrinol Metab. 1992; 6(1):217-228.
3. Van der Horst-Schrivers AN, Wymenga AN, Links TP, Willemse PH, Kema IP, de Vries EG. Complications of midgut carcinoid tumors and carcinoid syndrome. Neuroendocrinology. 2004; 80 Suppl 1:28-32.
4. Bissonnette RT, Gibney RG, Berry BR, Buckley AR. Fatal carcinoid crisis after percutaneous fine-needle biopsy of hepatic metastasis: case report and literature review. Radiology. 1990; 174(3 Pt 1):751-752.
5. Janssen M, Salm EF, Breburda CS, van Woerkens LJ, de Herder WW, Zwaan C et al. Carcinoid crisis during transesophageal echocardiography. Intensive Care Med. 2000; 26(2):254.
6. Kvols LK. Therapeutic considerations for the malignant carcinoid syndrome. 1989; 28(3):433-438.
7. Hoegerle S, Altehoefer C, Ghanem N, Koehler G, Waller CF, Scheruebl H et al. Whole-body 18F dopa PET for detection of gastrointestinal carcinoid tumors. Radiology. 2001; 220(2):373-380.
8. Becherer A, Szabo M, Karanikas G, Wunderbaldinger P, Angelberger P, Raderer M et al. Imaging of Advanced Neuroendocrine Tumors with (18)F-FDOPA PET. J Nucl Med. 2004; 45(7):1161-1167.
9. Vries E.F.J., Luurtsema G., Brussermann M., Elsinga P.J., Vaalburg W. Fully automated synthesis module for the hiegh yield one-pot preparation of 6-[18F]-fluoro-L-DOPA. Appl Radiat Isot. 1999; 51:389-419.
10. Yocum MW, Khan DA. Assessment of patients who have experienced anaphylaxis: a 3-year survey. Mayo Clin Proc. 1994; 69(1):16-23.
11. Bochner BS, Lichtenstein LM. Anaphylaxis. N Engl J Med. 1991; 324(25):1785-1790.
12. Vaughan DJ, Brunner MD. Anesthesia for patients with carcinoid syndrome. Int Anesthesiol Clin. 1997; 35(4):129-142.
13. Matuchansky C, Launay JM. Serotonin, catecholamines, and spontaneous midgut carcinoid flush: plasma studies from flushing and nonflushing sites. Gastroenterology. 1995; 108(3):743-751.
14. Kharrat HA, Taubin H. Carcinoid crisis induced by external manipulation of liver metastasis. J Clin Gastroenterol. 2003; 36(1):87-88.
15. Karmy-Jones R, Vallieres E. Carcinoid crisis after biopsy of a bronchial carcinoid. Ann Thorac Surg. 1993; 56(6):1403-1405.
16. Balestrero LM, Beaver CR, Rigas JR. Hypertensive crisis following meperidine administration and chemoembolization of a carcinoid tumor. Arch Intern Med. 2000; 160(15):2394-2395.
17. Kema IP, de Vries EG, Muskiet FA. Clinical chemistry of serotonin and metabolites. J Chromatogr B Biomed Sci Appl. 2000; 747(1-2):33-48.
18. Ozgen A, Demirkazik FB, Arat A, Arat AR. Carcinoid crisis provoked by mammographic compression of metastatic carcinoid tumour of the breast. Clin Radiol. 2001; 56(3):250-251.
19. Mehta AC, Rafanan AL, Bulkley R, Walsh M, DeBoer GE. Coronary spasm and cardiac arrest from carcinoid crisis during laser bronchoscopy. Chest. 1999; 115(2):598-600.
20. Kvols LK, Martin JK, Marsh HM, Moertel CG. Rapid reversal of carcinoid crisis with a somatostatin analogue. N Engl J Med. 1985; 313(19):1229-1230.
21. Gilbert JA, Bates LA, Ames MM. Elevated aromatic-L-amino acid decarboxylase in human carcinoid tumors. Biochem Pharmacol. 1995; 50(6):845-850.
22. Meijer WG, Copray SC, Hollema H, Kema IP, Zwart N, Mantingh-Otter I et al. Catecholamine-synthesizing enzymes in carcinoid tumors and pheochromocytomas. Clin Chem. 2003; 49(4):586-593.
23. Hughes EW, Hodkinson BP. Carcinoid syndrome: the combined use of ketanserin and octreotide in the management of an acute crisis during anaesthesia. Anaesth Intensive Care. 1989; 17(3):367-370.

Chapter five

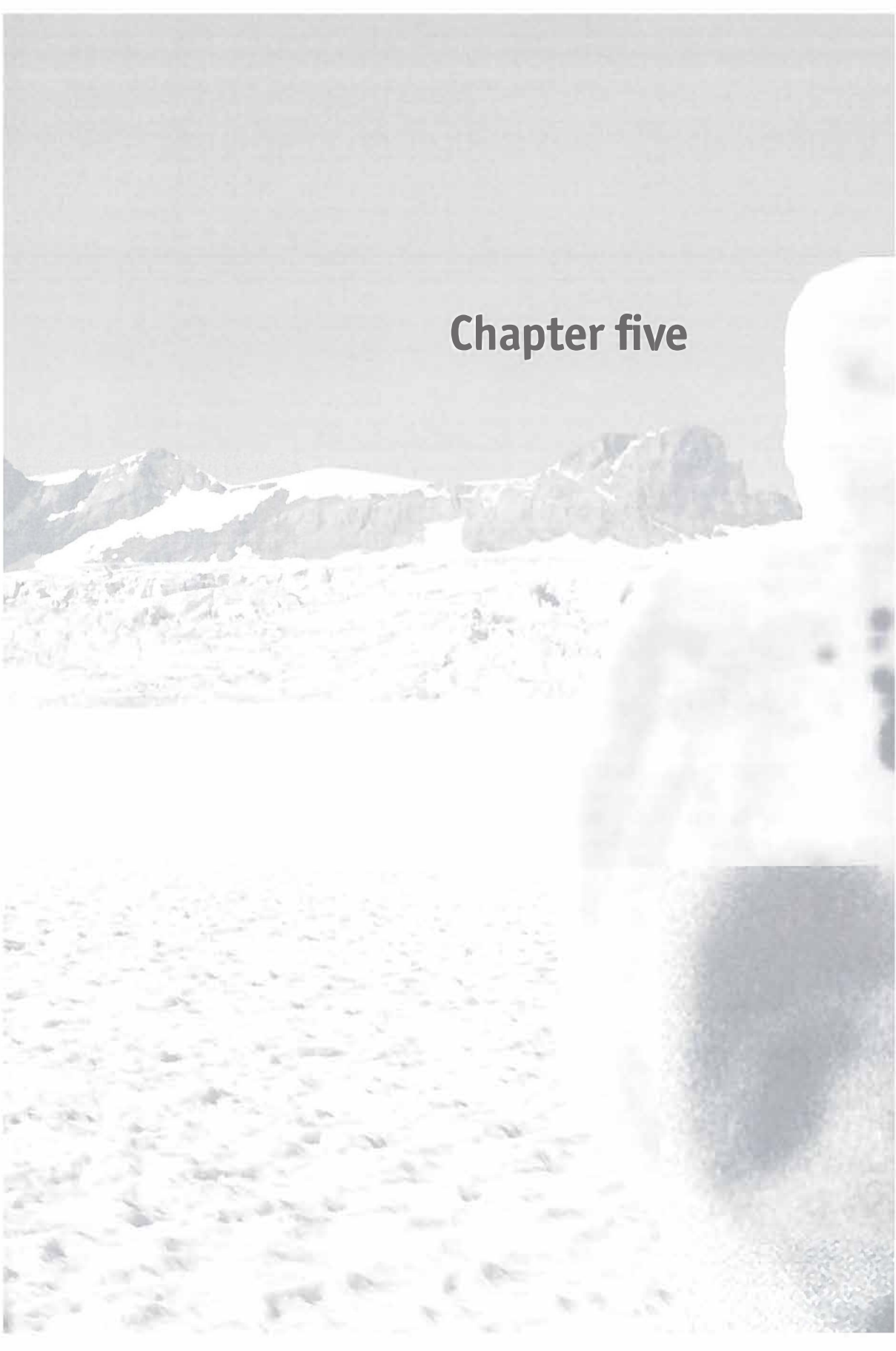

Improved staging of patients with carcinoid and islet cell tumours with ^{18}F-dihydroxy-phenyl-alanine (^{18}F-DOPA) and ^{11}C-5-Hydroxy-tryptophan (^{11}C-5-HTP) positron emission tomography

Klaas P Koopmans, Oliver C Neels, Ido P Kema, Philip H Elsinga, Wim J Sluiter, Koen Vanghillewe, Adrienne H Brouwers, Elisabeth GE de Vries, Pieter L Jager.

Departments of Nuclear Medicine and Molecular Imaging (KPK, OCN, PHE, AHB, PLJ), Medical Oncology (EGEV), Pathology and Laboratory Medicine (IPK) and Endocrinology (WJS). University Medical Centre Groningen and University of Groningen, Groningen, The Netherlands.
Department of Radiology (KV), Martini Hospital Groningen, The Netherlands

In Print

SUMMARY

Background To evaluate and compare diagnostic sensitivity of PET scanning in carcinoid and islet cell tumour patients with a serotonin and a catecholamine precursor as tracers.

Methods Carcinoid (n=24) or pancreatic islet cell tumour (n=23) patients with at least one lesion on conventional imaging including somatostatin receptor scintigraphy (SRS) and CT scan underwent ^{11}C-5-hydroxytryptophan (^{11}C-5-HTP) PET and 6-[F-18]fluoro-L-dihydroxy-phenylalanin (^{18}F-DOPA) PET. PET findings were compared with a composite reference standard derived from all available imaging, clinical and cytological/histological information.

Findings In carcinoid tumour patients per patient analysis showed sensitivities for ^{11}C-5-HTP PET, ^{18}F-DOPA PET, SRS and CT of 100, 96, 86, 96 % respectively and in islet cell tumours of 100, 89, 78, 87%. In carcinoid patients per-lesion analysis revealed sensitivities for ^{11}C-5-HTP PET, ^{11}C-5-HTP PET/CT, ^{18}F-DOPA PET, ^{18}F-DOPA PET/CT, SRS, SRS/CT and CT alone of respectively 78, 89, 87, 98, 49, 73 and 63% and in islet cell tumours of 67, 96, 41, 80, 46, 77 and 68%. In all carcinoid patients ^{18}F-DOPA PET and ^{11}C-5-HTP PET detected more lesions than SRS ($p < 0 \cdot 001$). ^{11}C-5-HTP PET was superior to ^{18}F-DOPA PET in islet cell tumours ($p < 0 \cdot 0001$). In all cases CT improved the sensitivity of the nuclear scans.

Interpretation ^{18}F-DOPA PET/CT is the optimal imaging modality for staging in carcinoid patients and ^{11}C-5-HTP PET/CT in islet cell tumour patients.

INTRODUCTION

Carcinoid tumours and pancreatic islet cell tumours are relatively indolent tumours. They belong to the group of neuroendocrine tumours that arise from neuroendocrine cells. These tumours can produce and secrete a large variety of products because of their intrinsic ability to take up, accumulate and decarboxylate amine precursors.[1] Treatment options for these tumours include curative or debulking surgery, systemic treatment treatment with somatostatin analogues, interferon and chemotherapy.[2]

To assess individual treatment options, accurate knowledge of tumour localisation, biochemical activity and rate of progression is essential. The initial work-up for patients with carcinoid and islet cell tumours consists of morphological imaging methods such as CT, combined with functional whole body imaging using somatostatin receptor scintigraphy (SRS).[3,4] However, on CT and MR imaging of the abdomen it can be difficult to correctly distinguish tumours and mesenterial metastases from intestinal structures. In addition, CT and MR lesions cannot always be perfectly characterized as being malignant, especially in the pancreas, as frequently benign lesions or cysts may have rather similar or a mixed appearance.[5-7]

Apart from the advantage of covering the whole body in a single investigation, functional imaging methods also allow characterization of lesions on CT or MR. SRS is often

used for this purpose. However, it may produce false negative findings, due to variable affinity and expression levels of somatostatin receptors or small size of lesions because of the limited resolution of the gammacamera and single photon emission tomography (SPECT) methods.[8,9]

Recently, two positron emission tomography (PET) tracers have emerged as potential functional imaging modalities in neuroendocrine tumours. In combination with the high resolution of PET this may lead to a clinically relevant improvement in detection, characterization and staging of these tumours. The first new tracer method is ^{18}F-DOPA PET, employing the catecholamine precursor 6-[F-18]fluoro-L-dihydroxyphenylalanin (^{18}F-DOPA)[5,6,10] whose uptake is based on the property of neuroendocrine tumours to take up amine precursors.[1,11] For the detection of carcinoid disease, its superiority over presently used modalities has been shown, but this advantage is less clear for islet cell tumours.[5,6] The second metabolic PET tracer ^{11}C-5-hydroxytryptophan (^{11}C-5-HTP) is a direct precursor for the serotonin pathway and therefore a potentially sensitive universal method for neuroendocrine tumour detection. However, availability and experience with ^{11}C-5-HTP is limited due to its complex production.[12-14] Currently, there are no head-to-head studies available in which ^{18}F-DOPA is compared to ^{11}C-5-HTP PET in their ability to detect neuroendocrine tumours. Therefore, the aim of this study was to evaluate the diagnostic sensitivity of ^{11}C-5-HTP in comparison with ^{18}F-DOPA PET in a large population of patients with a carcinoid or islet cell tumour.

METHODS

Patients

Patients eligible for this prospective single-centre diagnostic accuracy study were: new patients referred to our centre with a carcinoid or pancreatic islet cell tumour, based on clinical, histological and/ or biochemical findings and at least one abnormal lesion detected on CT, MRI, sonography or SRS, and patients known to have a histopathologically proven neuroendocrine tumour, who had a clinical indication for (re)staging and who had at least one abnormal lesion on conventional imaging studies. We excluded patients under 18 years of age, pregnant patients and those with an additional non-neuroendocrine tumour. Each consecutive patient underwent ^{11}C-5-HTP PET, ^{18}F-DOPA PET, SRS, CT of the abdomen and also the chest, when indicated, within a short interval, and in random order. Biochemical analysis for relevant tumour markers in blood and urine was performed. All patients were allowed to continue their medication.

The local medical ethics committee approved the study and all patients gave written informed consent.

PROCEDURES

^{11}C-5-HTP PET and ^{18}F-DOPA PET

For the reduction of tracer decarboxylation and subsequent renal clearance all patients received 2 mg/kg carbidopa orally as pre-treatment 1 h prior to the ^{11}C-5-HTP and ^{18}F-DOPA injection to increase tracer uptake in tumour cells.[16,17] ^{11}C-5-HTP was produced using a multi-enzymatic synthesis of enantiomerically pure ^{11}C-5-HTP on a Zymark robotic system.[13,15] Patients fasted for 2 h before the examination. Whole body 2D-PET images were acquired 10 min after the intravenous (IV) administration of ^{11}C-5-HTP (200 $\pm$ 50 MBq, with an estimated mean radiation dose of 0·67 mSv) on a Siemens ECAT HR+ positron camera (Siemens, Knoxville, TN, USA) with attenuation correction (7-10 bed positions of 5 min emission and 3 min transmission scan).

^{18}F-DOPA was produced as described earlier.[17] Patients fasted for 6 h before the examination. Whole body 2D-PET images were acquired as described for ^{11}C-5-HTP PET 60 min after the IV administration of ^{18}F-DOPA (180 $\pm$ 50 MBq, with mean radiation dose of 4 mSv[18]).

Two nuclear medicine physicians (KPK, PLJ) blinded for the results of other imaging examinations and clinical information interpreted the sets of ^{11}C-HTP and ^{18}F-DOPA PET images independently. Discrepant cases were reviewed in a multidisciplinary team and a consensus was reached. Only lesions with an unequivocal visibility clearly above normal activity in that body region were considered abnormal.

Somatostatin receptor scintigraphy

According to Dutch standards, 24 h after IV administration of 200 MBq ^{111}In-octreotide (Octreoscan; Mallinckrodt, Petten, The Netherlands – with an estimated mean radiation dose of 10 mSv[19]), planar total-body and SPECT images were obtained using standard methods. (Siemens Multispect 2 gammacamera, medium energy collimator, 10 min spotviews, 64 projections of 30 s). If interfering bowel activity was observed, 48 h images were recorded.[20]

SRS scans were interpreted by dedicated specialists as part of routine patient care and subsequently independently reread by a nuclear medicine physician (PLJ) blinded for the results of other imaging examinations and clinical information.

CT

CT (4-16 slice, Siemens Somatom Sensation, Siemens Medical Systems, Erlangen, Germany – with an estimated mean radiation dose of 8-20 mSv[21]) was performed using oral contrast and IV contrast (Visipaque 270, 120 mL, 2·5 mL/s) enhancement. The reconstruction interval was 0·75-5 mm. All patients underwent an abdominal CT, 42 patients also a chest CT. CT scans were interpreted as part of routine patient care and were reread by an experienced radiologist

(KV) blinded for the clinical information. In discrepant cases consensus was reached after multidisciplinary discussion.

Composite Reference standard

As a composite reference standard for presence of tumour lesions, all available cytological, histological, follow-up findings and all imaging findings were used. This is considered the optimal gold standard, as cytological or histological verification of every lesion is not feasible and not justifiable in these patients.[5]

Whenever possible, new findings on PET were verified with additional investigations.

Biochemical analysis

As markers for serotonin metabolism we measured serotonin levels in platelets and urinary 5-hydroxy indol acetic acid (5-HIAA) in a 24 h urine collection (upper reference limits 5·4 nmol /10^9 platelets and 3·8 mmol/mol creatinine, respectively).[22-25] Serum chromogranin A was determined using a radioimmunoassay (Cga-React, Cis Bio International, Gif-sur-Yvette, France) as a marker for general neuroendocrine tumour activity (reference interval 20-100 mg/L).

Data and statistical analysis

The STARD checklist was used during design and writing of this report.[26] Based on earlier studies, ^{18}F-DOPA PET and ^{11}C-5-HTP PET are both accurate techniques for staging of neuroendocrine tumours, but results may differ in subgroups.[5,6,14] Therefore we aimed to study approximately 25 carcinoid and 25 islet cell tumour patients to make a statistically meaningful comparison between both diagnostic methods. We wanted to be able to document an increase in sensitivity from 65% (average value, for islet cell tumour patients for conventional imaging) to 90% with ^{11}C-5-HTP PET, using McNemar's test for comparison with 80% power and 5% two-sided significance levels. Analyses were performed at the level of individual patients and individual lesions. When the number of lesions in one organ (e.g. liver) was higher than 10, the number of lesions was truncated at 10 for that region to avoid bias.

PET and SRS are whole body modalities, while CT only covers the most relevant parts of the body. In order to eliminate bias towards total body imaging methods, only body areas for which all four imaging modalities were available have been evaluated.

Sensitivities were calculated using the composite reference standard, and were compared using paired observations and McNemar's test. Patient based sensitivity was calculated as number of patients with a positive test (at least one lesion detected) by total number of patients. Per lesion sensitivity of a modality was calculated by dividing the number of positive

lesions detected with that modality by the total number of positive lesions. Significance level was ·05, two-sided. The statistical tests were carried out using the SPSS package version 12·0.

Role of the funding source

The funding source the Dutch Cancer Society played no role in the conduct of the study, the collection and interpretation of the data, or in the drafting of the report. All authors had full access to all the data of the study and agreed to submit the final manuscript for submission.

RESULTS

Patients

Between February 2005 and February 2007, 50 consecutive patients were recruited, of which 3 patients declined one or more of the imaging procedures leaving full data of 24 patients with a carcinoid tumour and 23 patients with an islet cell tumour for analysis, as presented in the flow diagram (figure 1). Patient characteristics are presented in table 1. All carcinoid patients and 39% of islet cell tumour patients had biochemical proof of increased serotonin metabolism. CT, SRS, ^{11}C-5-HTP PET, ^{18}F-DOPA PET were carried out within a median of 55 days. In 29 patients both PET scans were performed on the same day. The mean interval between both PET scans was 18 days. Newly detected lesions were confirmed with MRI (n=2), bone scintigraphy (n=2), planar X-ray (n=3) and sonography (n=3), surgery (n=3) or biopsy (n=1). Results in a representive patient are shown in figure 2.

Patient based analysis

Based on our selection criteria, all patients were considered positive for tumour. In a per patient analysis in carcinoid tumour patients, ^{11}C-5-HTP PET detected one or more tumour lesions in all 24 patients (sensitivity 100%, table 2), whereas ^{18}F-DOPA PET and CT detected one or more tumour lesions in 23 of 24 patients (sensitivity 96%) and SRS detected one or more tumour lesions in 18 of 21 patients (sensitivity 86%).

In a per patient analysis in patients with islet cell tumours, ^{11}C-5-HTP detected one or more tumour lesions in 23 of a total of 23 patients (sensitivity 100%) CT detected one or more tumour lesions in 20 of 23 patients (sensitivity 87%), SRS in 14 of 19 patients (sensitivity 78%) and ^{18}F-DOPA PET 16 of 23 patients (sensitivity 89). However, there were no statistically significant differences.

Lesion based analysis.

In patients with a carcinoid tumour, 371 tumour lesions were detected based on the composite

reference standard (table 3). The largest number of lesions was present in liver and abdomen (75% of all). ^{18}F-DOPA PET and ^{11}C-5-HTP PET had the highest sensitivity for the detection of these lesions compared to the other imaging modalities. The smallest lesion size that could be detected with ^{18}F-DOPA PET and ^{11}C-5-HTP PET was approximately 5 mm, as measured and confirmed on the PET-CT fused images. Overall ^{18}F-DOPA PET found most lesions, followed by ^{11}C-5-HTP PET. However, this difference was not statistically significant. ^{18}F-DOPA PET and ^{11}C-5-HTP PET were both significantly better in detecting tumour lesions than SRS (^{18}F-DOPA PET: p= 0·001 for ^{11}C-5-HTP PET: p=0·008). The combination ^{18}F-DOPA PET with CT had the highest sensitivity for detection of carcinoid lesions (98%), as CT detected lesions missed by nuclear medicine techniques, and vice versa. Therefore, combining nuclear medicine techniques with CT yielded more lesions. When SRS would have been left out, not a single lesion would have been missed.

In patients with islet cell tumours, a total of 294 tumour lesions were detected. Most lesions (71%) were found in the liver and abdomen. In these patients ^{11}C-5-HTP PET and CT performed equally well, and were both better than the other imaging modalities, although

Table 1. Patient characteristics.

Characteristics			Value
Sex (n of patients) Male/Female			29/18
Median age in years (range)			56 (18-79)
New patients vs patients with known disease (no patients)			11/36
Patients with abdominal carcinoid (n patients)			24
		Patients with carcinoid syndrome	12
	Treatment during scan		
		Somatostatin analogues (n)	17
		Somatostatin analogues + interferon (n)	2
Patients with islet cell tumours (n patients)			23
	Treatment during scan		
		Somatostatin analogues (n)	4
		Somatostatin analogues + interferon (n)	1
		Chemotherapy	1
		Radiotherapy on bone metastases	1

The results for the patient based analysis are presented with the number of tumour positive patients, patient based sensitivity with 95%CI and the mean and median number of lesions per patient.

Table 2. Patient based analysis.

Imaging modality	Number of patients with positive lesions	Sensitivity (95%CI)	Mean and median number of lesions per patient (range)
Carcinoid tumour (n=24)			
CT	23	96% (78 -100)	7·5; 9·7 (0 – 30)
SRS	18	86% (62 – 95)	5·5; 6·9 (0 – 30)
^{18}F -DOPA PET	23	96% (73 – 100)	11·0; 13·4 (0 – 33)
^{11}C-5-HTP PET	24	100% (85 – 100)	10·0; 12·1 (0 – 33)
Islet cell tumour (n=23)			
CT	20	87% (66 – 97)	7·0; 8·7 (0 – 41)
SRS	14	78% (56 – 97)	1·0; 5·1 (0 – 40)
^{18}F-DOPA PET	16	89% (66 – 97)	1.0; 5.2 (0 – 40)
^{11}C-5-HTP PET	23	100% (84 – 100)	3·0; 8·7 (1 – 40)

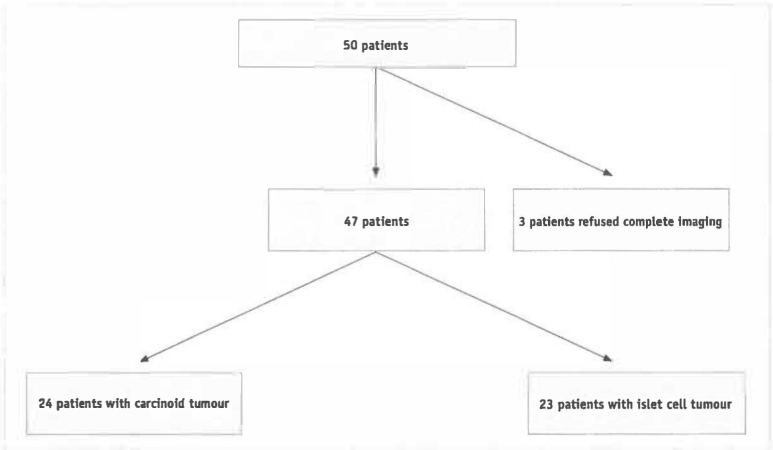

Figure 1. In this flow diagram a schematically view of the recruited patients is given.

not statistically significant. Both SRS and ^{18}F-DOPA PET had a relatively poor performance for islet cell tumour detection. Again, combining SRS and PET with CT led to an increased number of detected islet cell tumour lesions and therefore increased sensitivity (table 3) The combination of ^{11}C-5-HTP PET with CT had the highest sensitivity. When SRS would have been left out, only 8% of all lesions would have been missed. These PET negative lesions were found in two patients.

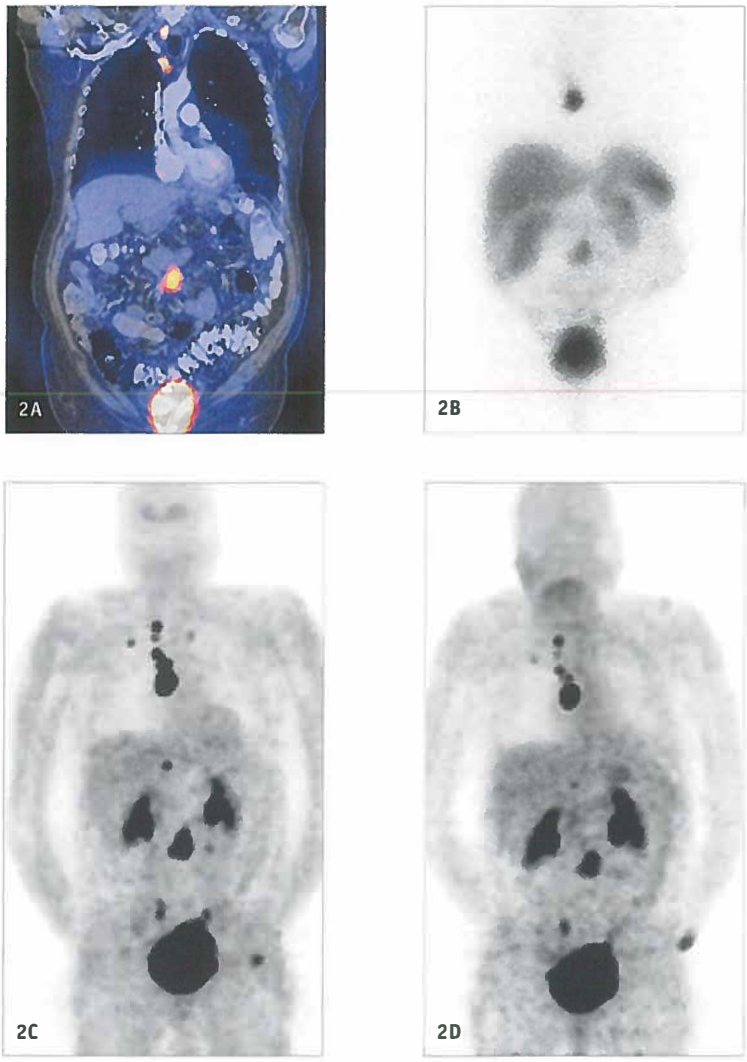

Figure 2. Fused ^{18}F-DOPA – PET CT scan (A), SRS (B), ^{18}F-DOPA PET (C) and ^{11}C-5-HTP PET (D) of a 80 year old male patient with metastatic carcinoid tumour.

The CT scan shows a mesenterial mass and two smaller lesions in the upper mediastinum. On SRS (both planar and SPECT, not shown here) only the larger mediastinal mass, the large mesenterial mass and a small lesion on the left cranial side of the urinary bladder could be found. Both ^{18}F-DOPA PET and ^{11}C-5-HTP PET showed a number of smaller lesions in the upper mediastinum and upper lobes of both right and left lung, with ^{18}F-DOPA yielding the best contrast. Note that the small lung lesions show less ^{11}C-5-HTP uptake than ^{18}F -DOPA uptake.

There was no statistical relationship between elevation of biochemical parameters and imaging results of ^{18}F-DOPA PET, ^{11}C-5-HTP PET, SRS, or CT.

DISCUSSION

This study demonstrates that both ^{11}C-5-HTP PET and ^{18}F-DOPA PET have excellent sensitivity to detect carcinoid and islet cell tumours lesions. ^{11}C-5-HTP PET was the only imaging method, which was able to detect tumour lesions in all carcinoid and islet cell tumour patients. In carcinoid patients ^{18}F-DOPA PET was the best modality as it detected more lesions compared to all other modalities including ^{11}C-5-HTP PET, CT and SRS. In islet cells tumours ^{11}C-5-HTP PET detected more tumour positive patients and lesions than ^{18}F-DOPA PET and SRS (figure 3). Adding CT to both PET techniques resulted in a slight further improvement in sensitivity (table 3). Therefore ^{18}F-DOPA PET-CT is considered the optimal technique for staging of patients with carcinoid tumours, and ^{11}C-5-HTP PET-CT for islet cell tumour patients. In patients with carcinoid tumours, SRS scanning can be omitted without missing any lesions.

For islet cell tumours, this is less clear-cut. ^{11}C-5-HTP PET combined with CT gives the best tumour detection for most patients. However, in a minority, namely 8% of patients, SRS performs equal or better then metabolic PET imaging methods. Therefore, in patients with islet cell tumours SRS remains of additional value.

Overactivity of the serotonin and most likely also the catecholamine pathway appears to be the key factor that determines the intracellular tracer concentration. Increased activity of transmembrane amino acid transporters results in high entry of both tracers in cells. In the tumoral cytoplasm ^{11}C-5-HTP and ^{18}F-DOPA PET are metabolized via the abundantly present enzyme aromatic amino acid decarboxylase (AADC) to hormonal products which can be stored in pathway specific secretory vesicles. In contrast to islet cell tumors,most patients with carcinoid tumours the serotonin pathway is highly active. In these cells, the storage capability for the ^{11}C-5-HTP metabolites is relatively saturated by endogeneous serotonin. The ^{11}C-5-HTP metabolites are therefore rapidly degraded via mono amino oxidase activity and subsequently excreted from the cell. This may explain the superior diagnostic performance for ^{18}F-DOPA PET in carcinoid and ^{11}C-5-HTP in islet cell tumors.[27]

The intracellular tracer concentration is directly related to the probability of visualisation using the PET scanner. These high tracer concentrations allow the detection of smaller lesions, up to 5 mm in diameter.

In both patient groups CT detected additional lesions and was therefore complementary to the PET techniques. The combination of ^{11}C-5-HTP PET with CT proved to be the best method to detect islet cell tumour lesions, whereas the combination ^{18}F-DOPA PET with CT detected most tumour lesions in patients with carcinoid disease. Both PET combinations performed better then the combination of SRS with CT in both tumour types. Although difficult to quantify, another advantage of combining CT with ^{11}C-5-HTP or ^{18}F-DOPA

PET is the ability to characterise neuroendocrine origin of lesions of lesions found on CT.

Both PET methods allow better staging and estimation of the total body tumour load. The addition of ^{11}C-5-HTP PET to CT in islet cell tumour patients clearly helps to provide a better understanding of the number of lesions and their distribution. This will support treatment decisions. In addition, better estimation of the total body tumour load and the detection of metastases in unknown regions may refine clinical management. Finally, the recent development of combined PET-CT scanning gives superior diagnostic information in a single session, largely obviates the need for SRS, and reduces the burden of multiple diagnostic tests.

Table 3. Lesion based analysis.

	CT	SRS	SRS + CT	^{18}F -DOPA PET	^{18}F -DOPA PET + CT	^{11}C-5-HTP PET	HTP PET + CT	
	Sensitivity (95%CI)	Sensitivity (95%CI)	Sensitivity (95%CI)	Sensitivity (95%CI)	Sensitivity (95%CI)	Sensitivity (95%CI)	Sensitivity (95%CI)	Number of positive regions
Carcinoid tumours								
Head and neck	46% (19-75)	31% (87-62)	69% (38-91)	85% (54-99)	92% (63-100)	85% (54-99)	92% (63-100)	13
Mediastinal*	**75% (53-90)**	25% (10-47)	91% (67-98)	58% (36-78)	100% (84-100)	54% (32-75)	54% (32-75)	24
Lung*	60% (34-84)	50% (21-74)	90% (59-99)	40% (16-68)	73% (44-93)	13% (1-41)	73% (44-93)	15
Liver	67% (59-74)	62% (54-70)*	78% (71-85)	93% (88-96)	100% (98-100)	84% (78-90)	91% (86-95)	158
Pancreas	50% (0-100)	0% (0-88)	50% (0-100)	50% (0-100)	100% (12-100)	50% (0-100)	100% (12-100)	2
Abdomen / pelvis	68% (59-76)	50% (41-59)	83% (75-89)	87% (79-92)	99% (95-100)	81% (73-87)	95% (89-98)	122
Bone	28% (14-45)	69% (52-84)	69% (52-84)	100% (89-100)	100% (89-100)	92% (77-98)	92% (77-98)	36
Extremities	0	100	100	0	0	0	0	1
Total	**63% (58-68)**	**49% (44-54)§**	**73% (68-78)**	**87% (84-91)**	**98% (96-99)**	**78% (74-83)**	**89% (86-92)**	**371**
Islet cell tumours								
Head and neck	0% (0-63)	100% (36-100)	100% (36-100)	25% (0-82)	25% (0-82)	50% (5-95)	50% (5-94)	4
Mediastinal *	**61% (40-79)**	37% (18-56)	63% (40-79)	43% (24-63)	68% (47-84)	79% (59-92)	93% (76-99)	28
Lung*	0	0	0	0	0	0	0	0
Liver	77% (69-84)	57% (48-65)	85% (78-91)	39% (31-48)	86% (79-92)	67% (59-75)	96% (91-99)	132
Pancreas	50% (26-74)	50% (26-74)	86% (58-97)	56% (30-79)	83% (58-97)	79% (52-94)	94% (72-100)	18
Abdomen / pelvis	80% (6-89)	31% (20-42)	81% (69-89)	29% (19-41)	83% (72-91)	50% (38-62)	100% (95-100)	76
Bone	32% (17-51)	46% (27-62)	46% (27-62)	68% (49-83)	68% (49-83)	97% (84-100)	97% (84-100)	34
Extremities	50% (0-100)	0% (0-89)	0% (0-89)	50% (0-100)	100% (12-100)	50% (0-100)	50% (0-100)	2
Total	**68% (63-74)**	**46% (40-52)**	**77% (72-82)**	**41% (36-47)**	**80% (75-85)**	**67% (62-73)**	**96% (93-98)**	**294**

Table 3. The sensitivities for the combination SRS with CT, 18F-DOPA PET with CT and 11C-5-HTP PET with CT are shown. To illustrate the additional value of combining these scans with each other, the results for the combination of nuclear imaging methods with CT are shown. * p = 0 ·007 for the comparison of SRS with 18F -DOPA PET; § p=0·001 for the comparison of SRS with 18F-DOPA PET and p=0·008 for the comparison of SRS with 11C-5-HTP PET.

All other published data regarding ^{11}C-5-HTP are from the group of Uppsala, Sweden. They studied 42 patients with a mixture of neuroendocrine and non-endocrine tumour patients. They concluded that ^{11}C-5-HTP PET was superior to SRS and CT for neuroendocrine tumour lesions and could be regarded as a universal imaging agent for these tumours.[13] No head to head comparison of ^{18}F-DOPA and ^{11}C-5-HTP versus CT and SRS was performed. Recent data also point to the utility of ^{18}F-DOPA PET in assessing pancreatic lesions in infants and adults with hyperinsulinism.[28]

In our study in both patient groups ^{11}C-5-HTP PET was far superior to SRS and in islet cell tumour patients ^{11}C-5-HTP PET performed even better than ^{18}F-DOPA PET. Therefore, ^{11}C-5-HTP PET could indeed be seen as a universal imaging agent for carcinoid and islet cell tumours. However, the synthesis of ^{11}C-5-HTP PET is complex. For efficient use of available resources and time it seems logical to use ^{18}F-DOPA PET for all patients with non-islet cell tumours and ^{11}C-5-HTP PET only for those with a proven or a suspected islet cell tumour. As PET is now in general performed in combination with CT, this even further improves the lesion detection and characterization properties of both PET scans and provides anatomical information all in a single and rapid session.

ACKNOWLEDGEMENTS

Supported by grant 2003-2936 from the Dutch Cancer Society.

Contributors: KP Koopmans participated in patient recruitment, PET scanning, data collection, data analysis, and writing of the report. OC Neels participated in the design of the study, tracer production, data analysis and writing of the report. IP Kema participated in the design of the study, biochemical analysis, data analysis, and writing of the report. PH Elsinga participated in the design of the study, data analysis,
and writing of the report. WJ Sluiter participated in the statistical analysis and writing of the report. K Vanghillewe participated in the data analysis, interpretation of radiologic data and writing of the report. AH Brouwers participated in the design of the study, data analysis and writing of the report. EGE de Vries participated in the design of the study, patient recruitment, data analysis, and writing of the report. PL Jager participated in the design of the study, patient recruitment, data analysis, interpretation of PET data, and writing of the report.

Conflict of interest statement

All authors declare that they have no conflict of interest.

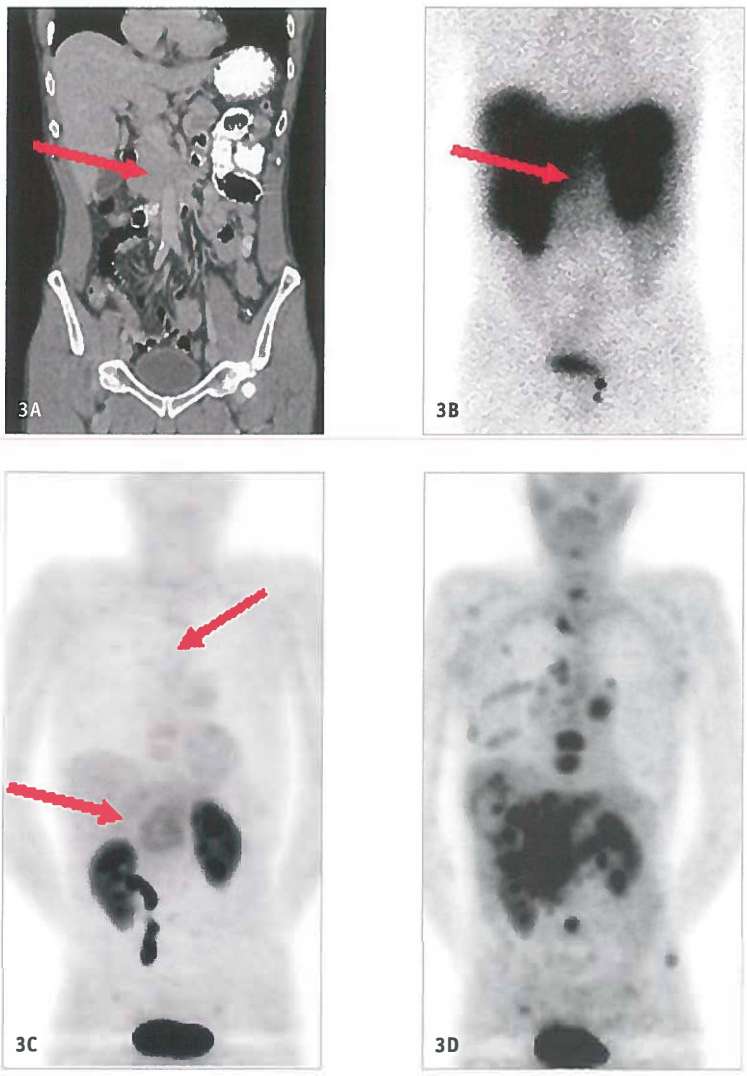

Figure 3. CT scan (A), SRS (B), ^{18}F-DOPA PET (C) and ^{11}C-5-HTP PET (D) of a 54 year old male patient with metastatic islet cell tumour.

The CT scan shows a large mass in the pancreatic head region (arrow), SRS shows equivocal (arrow) and ^{18}F-DOPA PET shows low uptake in the pancreatic region and minor uptake in the upper chest and in two thoracic vertebrae. ^{11}C-5-HTP PET, however, shows numerous bone, liver and abdominal lesions, including the pancreatic region with much higher contrast.

REFERENCES

1. Pearse AG. The APUD cell concept and its implications in pathology. *Pathol Annu* 1974;**9**:27–41.
2. Moertel CG, Lefkopoulo M, Lipsitz S, et al. Streptozocin-doxorubicin, streptozocin-fluorouracil or chlorozotocin in the treatment of advanced islet-cell carcinoma. *N Engl J Med* 1992;**326**:519–23.
3. Modlin IM, Kidd M, Latich I, et al. Current status of gastrointestinal carcinoids. *Gastroenterology* 2005; **128**:1717–51.
4. Plockinger U, Rindi G, Arnold R, et al. Guidelines for the diagnosis and treatment of neuroendocrine gastrointestinal tumours. A consensus statement on behalf of the European Neuroendocrine Tumour Society (ENETS). *Neuroendocrinology* 2004; **80**:394–424.
5. Koopmans KP, de Vries EG, Kema IP, et al. Staging of carcinoid tumours with 18F-DOPA PET: a prospective, diagnostic accuracy study. *Lancet Oncol* 2006; **7**:728–34.
6. Hoegerle S, Altehoefer C, Ghanem N, et al. Whole-body 18F dopa PET for detection of gastrointestinal carcinoid tumours. *Radiology* 2001; **220**:373–80.
7. Kumbasar B, Kamel IR, Tekes A, et al. Imaging of neuroendocrine tumours: accuracy of helical CT versus SRS. *Abdom Imaging* 2004; **29**:696–702.
8. De Herder WW, Hofland LJ, van der Lely AJ, et al: Somatostatin receptors in gastroenteropancreatic neuroendocrine tumours. *Endocr Relat Cancer* 2003; **10**:451–58.
9. Fahey FH, Harkness BA, Keyes JW, Jr., et al. Sensitivity, resolution and image quality with a multihead SPECT camera. *J Nucl Med* 1992; **33**:1859–63.
10. Becherer A, Szabo M, Karanikas G, et al. Imaging of advanced neuroendocrine tumours with (18)F-FDOPA PET. *J Nucl Med* 2004; **45**:1161–67,
11. Meijer WG, Copray SC, Hollema H, et al. Catecholamine-synthesizing enzymes in carcinoid tumours and pheochromocytomas. *Clin Chem* 2003; **49**:586–93.
12. Bjurling P, Watanabe Y, Tokushige M, et al. Synthesis of b-11C-labelled L-tryptophan and 5-hydroxy-L-tryptophan using a multi-enzymatic reaction route. J *Chem Soc* 1981; 1331–34.
13. Orlefors H, Sundin A, Garske U, et al. Whole-body (11)C-5-hydroxytryptophan positron emission tomography as a universal imaging technique for neuroendocrine tumours: comparison with somatostatin receptor scintigraphy and computed tomography. *J Clin Endocrinol Metab* 2005; **90**:3392–400.
14. Neels OC, Jager PL, Koopmans KP, et al. Development of a reliable remote-controlled synthesis of ß-[^{11C}]-5-hydroxy-*L*-tryptophan on a Zymark robotic system. *J Labelled Comp Radiopharm* 2006; **49**:889–95.
15. Bergstrom M, Lu L, Eriksson B, et al. Modulation of organ uptake of 11C-labelled 5-hydroxytryptophan. *Biog Amines* 1996; **12**:477–85.
16. Orlefors H, Sundin A, Lu L, et al. Carbidopa pretreatment improves image interpretation and visualisation of carcinoid tumours with (11)C-5-hydroxytryptophan positron emission tomography. *Eur J Nucl Med Mol Imaging* 2005; **33**:60–65.
17. Vries EFJ, Luurtsema G, Brussermann M, et al. Fully automated synthesis module for the high yield one-pot preparation of 6-[18F]-fluoro-L-DOPA. *Appl Radiat Isot* 1999; **51**:389-419.
18. Brown WD, Oakes TR, DeJesus OT, et al. Fluorine-18-fluoro-L-DOPA dosimetry with carbidopa pretreatment. *J Nucl Med* 1998; **39**:1884–91.
19. International Commission on Radiological Protection: ICRP publication 80: radiation dose to patients from radiopharmaceuticals. Pergamom, Oxford: Elsevier, 2000.

20. Balon HR, Goldsmith SJ, Siegel BA, et al. Procedure guideline for somatostatin receptor scintigraphy with (111)In-pentetreotide. *J Nucl Med* 2001; **42:**1134–38.
21. International Commission on Radiological Protection: ICRP Publication 87: Managing patient dose in computed tomography. ICRP Online. Elsevier, 2001. http://www.icrp.org
22. Kema IP, Schellings AM, Hoppenbrouwers CJ, et al. High performance liquid chromatographic profiling of tryptophan and related indoles in body fluids and tissues of carcinoid patients. *Clin Chim Acta* 1993; **221**:143–58.
23. Kema IP, Meiborg G, Nagel GT, et al. Isotope dilution ammonia chemical ionization mass fragmentographic analysis of urinary 3O-methylated catecholamine metabolites. Rapid sample clean-up by derivatization and extraction of lyophilic samples. *J Chromatogr Biomed Appl* 1993; **671**:181–89.
24. Kema IP, Meijer WG, Meiborg G, et al. Profiling of tryptophan-related plasma indoles in patients with carcinoid tumours by automated, on-line, solid-phase extraction and HPLC with fluorescence detection. *Clin Chem* 2001; **47**:1811–20.
25. Willemsen JJ, Ross HA, Wolthers BG, et al. Evaluation of specific high-performance liquid-chromatographic determinations of urinary metanephrine and normetanephrine by comparison with isotope dilution mass spectrometry. *Ann Clin Biochem* 2001;**38**:722–30.
26. Bossuyt PM, Reitsma JB, Bruns DE, et al. Towards complete and accurate reporting of studies of diagnostic accuracy: the STARD initiative. Standards for reporting of diagnostic accuracy. *Clin Chem* 2003; **49**:1–6.
27. Smith CC. Evidence for separate serotonin and catecholamine compartments in human platelets. *Biochim Biophys Acta* 1996; **1291**: 1–4.
28. Mohnike K, Blankenstein O, Christesen HT, et al. Proposal for a standardized protocol for 18F-DOPA-PET (PET/CT) in congenital hyperinsulinism. *Horm Res* 2006; **66**:40–42.

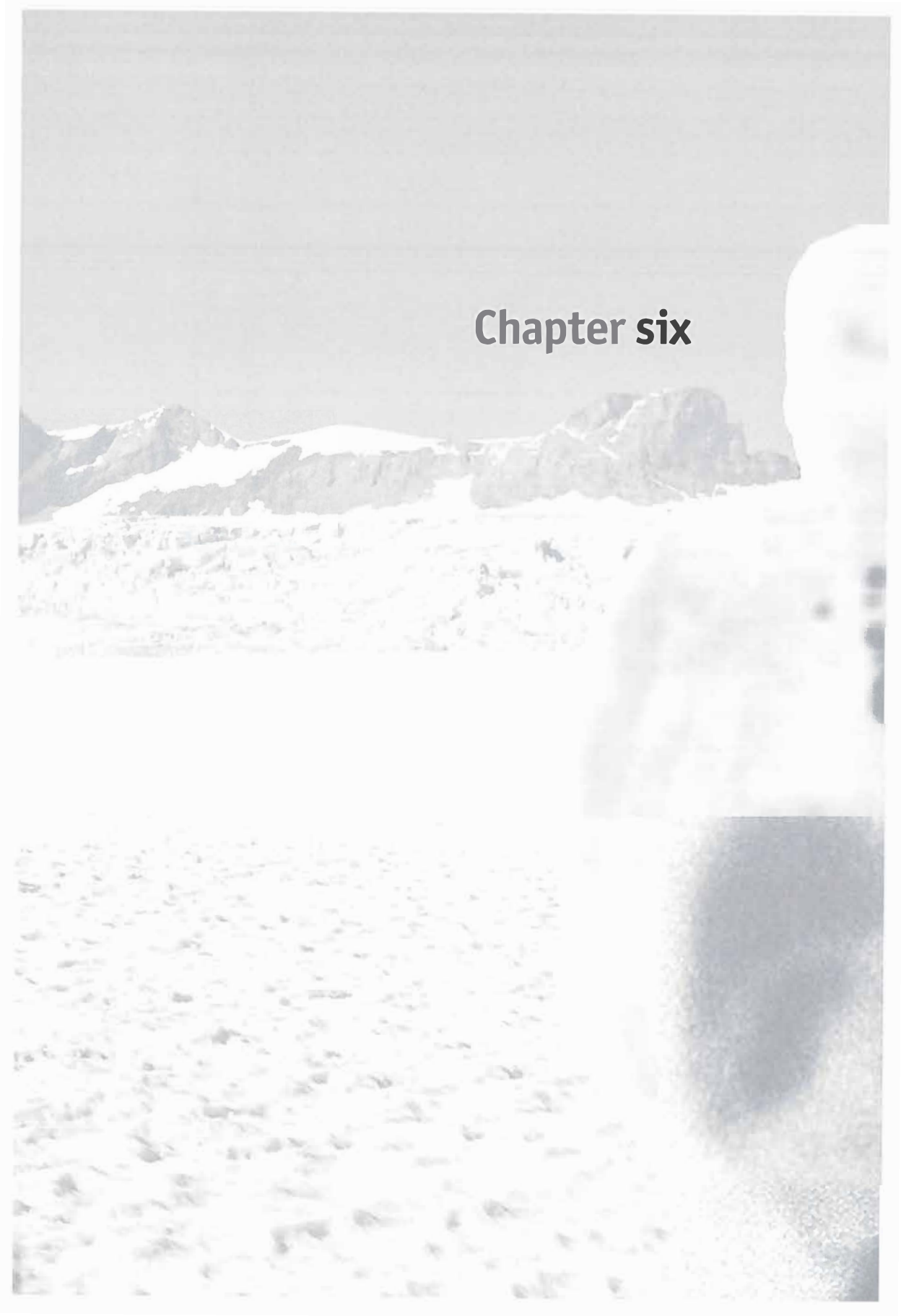

Chapter six

^{18}F-dihydroxyphenylalanine positron emission tomography in patients with biochemical evidence of medullary thyroid cancer: relation with tumor differentiation

K.P. Koopmans[1], J.W.B. de Groot[2], J. Th. M. Plukker[3], E.G.E. de Vries[4], I.P. Kema[5], W.J. Sluiter[2] P.L. Jager[1], T.P. Links[2]

[1]Departments of Nuclear Medicine and Molecular Imaging, [2]Endocrinology, [3]Surgical Oncology, [4]Medical Oncology and [5]Pathology and Laboratory Medicine.

University Medical Center Groningen, Groningen, The Netherlands

In Print

ABSTRACT

Introduction Curative treatment for recurrent medullary thyroid cancer (MTC), diagnosed by rising serum calcitonin is surgery, but tumor localization is difficult. Therefore the value of ^{18}F-dihydroxyphenylanaline positron emission tomography (^{18}F-DOPA PET), ^{18}F-deoxyglucose PET (^{18}FDG PET), ^{99m}Tc-V-di-mercapto-sulphuricacid (DMSA) scintigraphy and MRI and/or CT was studied.

Methods 21 patients with biochemical recurrent/residual MTC underwent ^{18}F-DOPA PET, ^{18}FDG PET, DMSA scintigraphy and MRI or CT. Patient- and lesion based sensitivities were calculated using a composite reference consisting of all imaging modalities.

Results In 76% of all patients with MTC one or more imaging modalities was positive for MTC lesions. In 6 out of 8 patients with a calcitonin level < 500 ng/L imaging results were negative. In 15 patients with positive imaging results, ^{18}F-DOPA PET detected 13 (sensitivity 62%, with 4.6 lesions per patient [lpp]). Morphologic imaging (n=19) was positive in 7 (sensitivity 37%, 4.7 lpp), DMSA (n=18) in 5 (sensitivity 28%, 1.1 lpp) and ^{18}FDG PET (n=17) in 4 (sensitivity 24%, 1.6 lpp). In a lesion based analysis ^{18}F-DOPA PET detected 95 of 134 lesions (sensitivity 71%), morphologic imaging 80 of 126 (sensitivity 64%), DMSA 20 of 108 (sensitivity 19%) and ^{18}FDG PET 48 of 102 (sensitivity 30%). In 2 of 3 patients with a calcitonin/CEA doubling time of ≤12 months ^{18}FDG PET performed better than ^{18}FDOPA PET, in the third patient ^{18}FDG PET was not performed.

Conclusion MTC lesions are best detectable when serum calcitonin was >500 ng/L. Then, ^{18}F-DOPA PET is superior to ^{18}FDG PET, DMSA-V and morphologic imaging. With short calcitonin doubling times (≤ 12 months), ^{18}FDG PET may be superior.

INTRODUCTION

Medullary thyroid carcinoma (MTC) originates from the parafollicular C-cells of the thyroid. It accounts for 3% to 10% of all thyroid malignancies. [1] Because C-cells produce calcitonin, this hormone serves as a reliable tumor marker for MTC. Another frequently used marker is carcino-embryonic antigen (CEA).[1,2] Calcitonin doubling time can be helpful in the judgment of the clinical course [3,4] although the transition to progressive disease with overt metastases is often unpredictable.

Thus far, surgery consisting of a total thyroidectomy and extensive lymph node dissection is the only effective curative treatment [5-7] in primary MTC. However, after clinical curative surgery, biochemical cure rates vary from 34% to 44%. Again, the only curative treatment option in these patients with residual or recurrent disease after initial treatment is re-operation. But, surgery can only be successful when the surgeon is accurately informed about the location of local and distant metastases and usually only when residual

or recurrent MTC is confined to the neck.

Therefore it is important to identify the source of the increased calcitonine as early as possible. However, the source of calcitonin production is hard to identify with conventional medical imaging and therefore distant metastases cannot be reliably ruled out. ^{18}F-fluoro-2-deoxy-D-glucose positron emission tomography (^{18}F-FDG PET) and ^{99m}Tc(V)dimer captosuccinic acid scintigraphy (DMSA) have reasonable sensitivity for the detection of MTC metastases. However, in about half of the patients persistent MTC cannot be detected with any morphological (computed tomography [CT] or magnetic resonance imaging [MRI]) or functional imaging (^{18}F-FDG PET, DMSA or ^{111}In-octreotide scintigraphy).[4,9-10]

Apart from the problematic restaging, another clinical problem is the unpredictable clinical course in patients with persistent disease. Although the overall survival of patients with biochemical detectable disease is relative long, the transition to progressive disease is often unpredictable.[3] Early detection of such an accelerated phase might lead to better treatment, and for this purpose serum calcitonin doubling time has proven to be valuable.[3,4]

^{18}F-dihydroxyphenylanaline (^{18}F-DOPA) PET is a new functional nuclear medicine procedure that enables metabolic imaging of MTC. This approach is based on the increased activity of large amino acid transporter (LAT) systems in neuroendocrine tumors such as MTC.[11] The first reports of the use of ^{18}F-DOPA PET in patients with MTC are promising, but included only a very small number of patients.[12,13] The aim of the present study was to assess the value ^{18}F-DOPA PET in patients with elevated calcitonin and CEA levels in comparison with the results with ^{18}F-FDG PET, DMSA and morphological imaging (CT and/or MRI). The secondary aim was to evaluate whether there was a relation between the level and the course of tumor markers and imaging results.

METHODS

Patients

Patients who had histologically proven MTC and elevated serum calcitonin levels after initial surgical treatment were eligible for this prospective single center study. They were included between January 2003 and March 2007. The local medical ethics committee approved the study and all patients gave written informed consent.

Imaging protocol

According to our protocol, all patients with recurrent or residual MTC, diagnosed by elevated serum calcitonin and/or CEA and/or chromogranin A levels, underwent ^{18}F-DOPA PET, DMSA scintigraphy, ^{18}F-FDG PET scanning and morphologic imaging with CT or MRI.

DMSA and ^{18}F-FDG PET were not performed when such scans had been made repeatedly with negative results in the previous two years. The regions of metastasis or recurrence were divided into five areas: regional, lung, liver abdomen and bone.

^{18}F-FDG PET, DMSA scintigraphy and morphological imaging were performed as described previously.[9] These scans were interpreted by dedicated specialists as part of routine patient care and subsequently independently reread.

^{18}F-DOPA PET

^{18}F-DOPA was locally produced as described earlier. [14] Patients fasted for 6 hours before the examination and were allowed to continue all medication. Whole body 2D- PET images were acquired 60 minutes after the intravenous administration of ^{18}F-DOPA (180 $\pm$ 50 MBq), on a Siemens ECAT HR+ positron camera (Siemens, Knoxville, TN) with attenuation correction (7–10 bed positions of 5 minutes emission and 3 minutes transmission scan, total scanning time approximately 60 minutes). For the reduction of tracer decarboxylation and subsequent renal clearance all patients received 2 mg/kg carbidopa orally as pre-treatment 1 hour prior to the ^{18}F-DOPA injection to increase tracer uptake in tumor cells. [15-17]

Two nuclear medicine physicians interpreted the ^{18}F-DOPA PET images independently. These readers were unaware of calcitonin, CEA, and chromogranin A levels and the results of other imaging examinations. Only lesions in each body region with an unequivocal visibility clearly above normal activity, known from patients and regions without tumors, were considered abnormal.

Composite reference standard

As a composite reference standard for the presence of tumor lesions all available cytological, histological, follow-up findings and all imaging findings were used. [18] In these patients, cytological or histological verification of every lesion is neither feasible nor justifiable. Histological confirmation of disease would be the ideal verification of tumor activity, but for obvious reasons surgery or biopsy of all lesions on the combined imaging methods is not feasible. Whenever possible, new findings were verified with additional other investigations, such as ^{111}In-octreotide scintigraphy (n=3), meta-iodobenzylguanidine (MIBG) (n=3), bone scintigraphy (n=1) and surgical findings (n=5).

Biochemical analysis

As markers for tumor activity we measured serum calcitonin levels (reference values 0.3-12 ng/L) by enzyme-linked immunosorbent assay (Sangui Biotech Inc., Santa Ana, CA) and plasma CEA levels (reference values 0.5-5.0 µg/L), which were measured by chemilumnescent microparticle immunoassay (Abbott Laboratories, Abbott Park, IL). Serum chromogranin A was determined using a radioimmunoassay (Cga-React, Cis Bio International,

Gif-sur-Yvette, France) as a marker for tumor volume (reference values 20.0-100.0 mg/L). The formula log2 x dT/(logB – logA) was used to estimate the calcitonin and the CEA doubling time. In this formula, A is the initial and B is the following calcitonin or CEA concentration. dT is the time difference between the measurements of A and B in months.[19]

Data and statistical analysis

Because all patients presented with elevated serum calcitonin levels, any imaging study not showing a clear abnormality was classified as false-negative in the patient based analysis. In addition, region and lesion-based sensitivities were calculated using the composite reference standard described above, and were compared using paired observations and McNemar's test. Patient-based sensitivity was calculated as the number of patients with a positive test (at least one lesion detected) by the total number of patients in whom the test was performed. Regional sensitivity was calculated by dividing the number of regions positive for tumor detected by that modality by the total number of tumor positive regions (composite reference), and the lesion based sensitivity by dividing the number of detected lesions by the total number of lesions (composite reference). For the patient based analysis, McNemar's test was used to compare ^{18}F-DOPA PET findings with those from ^{18}F-FDG PET, ^{99m}Tc(V)DMSA and morphological imaging. To compare the number of patients with 0, 1, 2, 3 or more positive regions between ^{18}F-DOPA PET and the other imaging modalities, Pitman's test was used. These tests were not corrected for multiple testing. For the comparison of number of lesions per region, Wilcoxon's test was used. The Chi^2 test was used to to compare proportions of abnormal biochemical markers in positive and negative imaging. Significance level was 0.05, two sided. Confidence intervals are mentioned in the tables. The statistical tests were carried out using the SPSS package 12.0.

RESULTS

Twenty-one consecutive patients (10 men and 11 women) were included. Twelve patients had sporadic MTC, 8 had multiple endocrine neoplasia (MEN) syndrome type 2A and 1 had MEN 2B. All diagnostic imaging examinations of the same patient were completed within a 9-month interval, which was always relatively short in comparison with the rate of disease progression, They were performed at least 4 months after any therapy. ^{18}F-FDG PET was obtained in 18 patients, DMSA scintigraphy in 19 patients, and MRI or CT of the neck and mediastinum in 18 patients. In the other patients such scans had been made repetitively in the previous two years with negative results. All these patients underwent the imaging procedures after initial total thyroidectomy with central compartment dissection and additional neck dissection on indication. Laparoscopy for detection of minimal, capsular liver diseas was not part of the standard dissemination strategy. Median age was 52 years

Table 1. Patient characteristics of the study population.

Patient no	Age (years) / Sex	Type MTC	CgA (mg/L)	Calcitonin (ng/L)	Calcitonin doubling Time (months)	CEA µg/L	CEA doubling time (months)	CT/ MR	DMSA	FDG PET	F-DOPA PET	Imaging performance / histological confirmation
1	71/m	spor	58	418	53	5.2	143	neg	neg	neg	neg	-
2	**56/v (†)**	**MEN 2a**	**32**	**10500**	**8**	**414.8**	**9**	**li5; os2**	**neg**	**he1; li2;os2**	**li2;os2**	-
3	66/m	spor	37	825	13	7.3	247	neg	neg	neg	ab1	++
4	71/m	spor	466	120000	24	2209.5	29	li8; os10	neg	neg	li10;os2	+
5	68/v	MEN 2a	200	27190	91	1459.5	151	li10; os5	ne3; th1; li4;os1	neg	he1; ne3; th1; li10; os1	+
6	48/m	MEN 2b	147	1080	61	32.5	103	neg	neg	neg	ne1	+/Y
7	56/m	MEN 2a	35	48	43	1.4	268	n/p	neg	neg	neg	-
8	27/v	MEN 2a	23	73	29	1.2	77	neg	os2	ne1	neg	--
9	52/m	spor	77	173	34	14	-46	neg	neg	neg	neg	-
10	43/v	MEN 2a	28	86	76	1.1	-40	neg	neg	neg	ab1	+
11	59/v	spor	56	1596	-22	30.3	56	he1; ne2	n/p	n/p	he1; ne2	-
12	**57/m (†)**	**spor**	**910**	**109000**	8	**647.1**	**15**	**he1; ne1; th10; li5**	**n/p**	**n/p**	**he1; ne2; th10; li8**	**+/Y**
13	**48/v**	MEN 2a	82	112	-43	0.5	232	n/p	neg	neg	neg	-
14	78/m	MEN 2a	147	2812	**27**	3.4	-108	ne1; th5	ne1	n/p	ne1; th3; li1	+/Y
15	34/v	spor	26	4600	29	9.8	-42	neg	n/p	n/p	ne1	+/Y
16	72/v	MEN 2a	120	19350	68	194.3	-98	neg	neg	neg	ne1; th1; li10	++
17	45/m	spor	284	1049	108	29.5	50	neg	h1	neg	neg	--
18	**65/v (†)**	**spor**	**55**	**1160**	**4**	**41.9**	7	**he1; ne3; os10**	**neg**	**ne4; th6; li7; os1**	**he1; ne3; th1; li5; os1**	**+**
19	58/v	spor	1090	24	23	0.6	22	neg	neg	neg	neg	-
20	26/v	spor	35	261	n/a	0.9	-24	neg	neg	neg	neg	-
21	79/m	spor	144	1758	13	664.8	12	n/p	ne2; ab1	ne1; th3; li1; ab2	**ne1**; th2; li1; **ab3**	-

Patients marked bold are patients with a short calcitonin doubling time. (†) Patients who died due to their disease. Spor, sporadic medullary thyroid cancer; MEN, multiple endocrine neoplasia; CgA; Chromogranin A, reference level <100 ug/L; Calcitonin reference level < 12 ng/L; CEA: carcino-embryogenic antigen, reference level < 5 ug/L; n/p, not performed. Imaging regions: he, head; ne, neck; th, thorax; li, liver; ab, abdomen; os, ossal. The number behind the region denotes the number of lesions for that region. Imaging performance: - = no added value to conventional, + = more lesions detected, ++ = ^{18}FDOPA PET only positive imaging modality. -- ^{18}FDOPA PET inferior. Y: imaging results have been cytologically confirmed.

Table 2. Patient based analysis.

Imaging modality (performed in n patients)	Number of patients with positive lesions	Sensitivity (95% CI)	Mean number of lesions per patient (range)
CT/MR (18)	7	39% (17-65)	4.7 (0-18)
DMSA (18)	5	28% (9-54)	1.1 (0-13)
^{18}FDG PET (17)	4	24% (6-50)	1.6 (0-18)
^{18}F-DOPA PET (21)	13	62% (38-82)	4.6 (0-21)

Based on the inclusion criteria, all patients were considered positive for tumor. Sensitivities for the patient based analysis were calculated using the total number of patients scanned per imaging modality as reference.

(range 19-75). Clinical characteristics of the individual patients are listed in table1.

Imaging results

Patient based analysis

^{18}F-DOPA PET produced high quality tomographic images that were easily interpretable (Figure 1). In 6 patients (29%) no lesions could be detected with either of the imaging methods used, and these were therefore classified as false-negative. Table 2 summarizes the imaging results per patient. Although morphologic imaging methods were able to detect a slightly larger number of tumor lesions per positive patient (patient based sensitivity 39%, 4.7 lesions per patient [lpp]), ^{18}F-DOPA PET was able to detect 13 tumor positive patients (patient based sensitivity 62%, 4.6 lpp). DMSA and ^{18}F-FDG PET performed considerably less. DMSA detected five and ^{18}F-FDG PET detected four tumor positive patients (sensitivity of 26% for DMSA vs 22% for ^{18}F-FDGPET , 1.1 lpp vs 1.6 lpp). DMSA and ^{18}F-FDG PET were both positive in one patient, but detected different lesions. However, due to the small number of patients, no statistical significant difference in the patient based analysis could be reached between the described imaging methods. In four patients surgery was performed as a result of ^{18}F-DOPA PET findings. In these patients the lesions detected with ^{18}F-DOPA PET were resected and proven tumor positive with pathologic analysis.

Region based analysis

Table 3 describes the region-based analysis. Of the 126 regions evaluated, 37 (29%) were considered positive for tumor. ^{18}F-DOPA PET detected 33 of these positive regions (sensitivity 89%), whereas morphological imaging detected 17 positive regions (sensitivity 52%), DMSA scintigraphy 9 positive regions (sensitivity 33%) and ^{18}F-FDG PET 12 (sensitivity 48%).

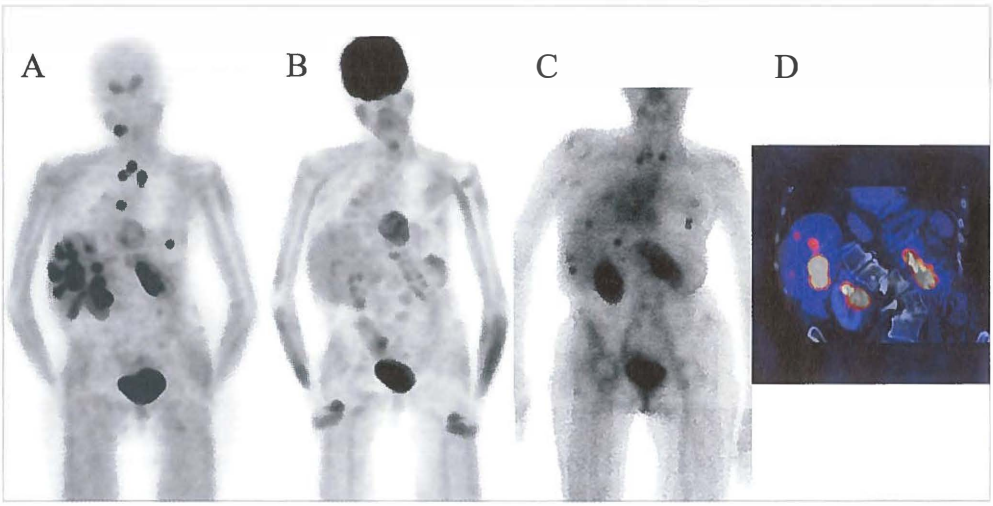

Figure 1. Patient 5: 68 year old female patient with a MEN 2a related metastasized recurrent medullary thyroid cancer.
Her calcitonin doubling time was 91 months (calcitonin 27,190 ng/Ll) and her CEA doubling time 151 months (CEA 1,460 µg/L). ^{18}F-DOPA PET (figure 1A) showed the largest number of lesions, located in the neck, upper mediastinum, left thorax, live rand skeleton. ^{18}FDG PET (Figure 1B) only showed physiological uptake, but no tumor lesions. DMSA (Figure 1C) showed lesions in the upper mediastinum, left thorax, liver and skeleton, although with a much smaller number of lesions. In Figure 1D an ^{18}F-DOPA PET – CT fusion slice is presented, showing liver lesions.

Lesion based analysis

A total of 134 lesions were considered positive for tumor based on the composite reference standard. ^{18}F-DOPA PET detected 95 of 134 (sensitivity 71%) lesions. The sensitivity of ^{18}F-DOPA PET was higher than that of morphologic imaging in which both were performed (p=0.019). Morphologic imaging detected 80 of 126 lesions (sensitivity 64%). DMSA and FDG were inferior to ^{18}F-DOPA PET, as DMSA detected only 20 of 108 (sensitivity 19%, p=0.031 for the paired comparison of ^{18}F-DOPA PET with DMSA) and ^{18}F-FDG PET only 48 of 102 (sensitivity 30%, p=0.123 for the paired comparison of ^{18}F-DOPA PET with ^{18}F-FDG PET)(Table 3). Most lesions were present in the liver and bone (liver 41, bone 27). ^{18}F-DOPA PET showed more lesions in the liver region (47 for ^{18}F-DOPA PET, vs 28 for CT/MRI), however, morphologic imaging methods were able to detect more bone lesions (27 for CT/MRI vs 8 for ^{18}F-DOPA PET). The combination of CT/MRI, DMSA and ^{18}F-FDG PET results in a total of 90 lesions (sensitivity 71%), which is still slightly less than the number of lesions detected by ^{18}F-DOPA PET alone.

Table 3. Region and lesion based analysis.

	CT/MRI (sens%, 95% CI)	**DMSA** (sens%, 95% CI)	**^{18}FDG PET** (sens%, 95% CI)	**^{18}F-DOPA PET** (sens%, 95% CI)
Region analysis, positive regions				
Head	3 (50%, 10-90%)	2 (50%, 5-95%)	0 (0%, 0-63%)	4 (66%, 1-89%)
Neck	4 (44%, 5-79%)	3 (50%, 0-93%)	4 (67%, 21-97%)	8 (80%, 43-98%)
Thorax	2 (44%, 4-87%)	0 (0%, 0-63%)	2 (67%, 3-78%0	6 (100%, 52-100%)
Liver	4 (57%, 27-100%)	1 (17%, 0-66%)	3 (60%, 13-96%)	8 (100%, 61-100%)
Abdomen	0 (0%, 0-88%)	1 (33%, 0-93%)	1 (33%, 0-93%)	3 (100%, 26-100%)
Bone	4 (100%, 31-100%)	2 (50%, 5-95%)	2 (50%, 5-95%)	4 (100%, 37-100%)
Total	**17 (52%, 33-69%)**	**9 (33%, 16-54%)**	**12 (48%, 28-69%)**	**33 (89%, 74-97%)**
Lesion analysis, positive lesions				
Head	3 (38%, 8-76%)	4 (67%, 24-92%)	0 (0%, 0-38%)	4 (50%, 15-85%)
Neck	7 (47%, 19-70%)	6 (55%, 24-76%)	7 (70%, 41-89%)	13 (814%, 54-96%)
Thorax	15 (65%, 44-83%)	0 (0%, 0-14%)	9 (82%, 60-94%)	18 (69%, 48-86%)
Liver	28 (55%, 39-68%)	4 (9%, 2-19%)	10 (23%, 12-37%)	47 (90%, 84-99%)
Abdomen	0 (0%, 0-55%)	1 (20%, 0-73%)	2 (40%, 4-89%)	5 (100%, 45-100%)
Bone	27 (100%, 86-100%)	5 (19%, 6-38%)	3 (11%, 2-29%)	8 (30%, 14-50%)
Total	**80 (64%, 55-72%)**	**20 (19%, 12-26%)**	**31 (30%, 23-39%)**	**95 (71%, 62-78%)**

Number of positive regions and lesions per modality are given with sensitivity (%) and 95% confidence interval. Sensitivities were calculated using the composite reference data limited to the patients scanned with the involved imaging modality.

Comparison of imaging with calcitonin

All patients had elevated serum calcitonin levels (median 1,064 ng/L; range, 24–120,000 ng/L). Using an arbitrary calcitonin threshold of 500 ng/L (*4*), 12 of the 13 patients with serum calcitonin levels higher than 500 ng/L had positive ^{18}F-DOPA PET scans (p=0.002 for the comparison of positive of scan results versus calcitonin > 50 ng/L). Of the 8 patients with a serum calcitonin level below 500 ng/L, 6 had negative imaging results. One patient (patient 10) showed a lesion lateral of the right side of the urinary bladderlesion which was only present on ^{18}F-DOPA PET. This patient had normal CEA levels and the median calcitonin doubling time was 27 months (range 4–108 months).

After combining a calcitonin level of >500 ng/L with calcitonin doubling time >12 months as classification of biochemically active but slowly progressive MTC, we evaluated 10 patients. ^{18}F-DOPA PET was positive in 9 patients. In 7 of these 10 patients ^{18}F-DOPA PET detected more lesions than the other imaging modalities, in 3 patients ^{18}F-DOPA PET detected the same lesions as the other imaging modalities and in patient 21 (with doubling time just over 12 months) ^{18}F-DOPA PET revealed an additional abdominal lesion that did not show up on all other imaging modalities but failed to identify a thoracic lesion which was identified by ^{18}F-FDG PET. In contrast, ^{18}F-FDG PET was negative in 6 of 7 patients with a calcitonin level of >500 ng/L and a calcitonin doubling time > 12 months. In one patient (patient 21) ^{18}F-FDG PET detected an additional thoracic lesion but failed to identify one abdominal lesion which was detected by ^{18}F-DOPA PET. Two patients, #4 and #5, were exceptional: they had very high CgA and Calcitonin levels, but a long doubling time for both. ^{18}F-FDG PET was, in contrary to ^{18}F-DOPA PET and CT, negative in these two patients. These doubling times and the clinical behaviour suggest a slow growing tumor with a low glucose need in these patients.

A calcitonin level of >500 ng/L and a calcitonin doubling time < 12 months as characterization of biochemically active and a rapidly progressing tumor was present 3 patients. These 3 patients (#2, #12 and #18) have died since entering the study. Patients #2 and #18 had more ^{18}F-FDG PET positive lesions then ^{18}F-DOPA PET positive lesions. Unfortunately, due to progressive disease, patient #12 did not undergo a ^{18}F-FDG PET scan. These findings suggest better tumoral ^{18}F-FDG than ^{18}F-DOPA uptake in this subgroup with rapidly growing tumors.

Comparison of imaging with CEA

CEA levels (median 11.9 µg/L; range 0.5-2209.5 µg/L) were elevated in 14 patients (68%). In these patients, ^{18}F-DOPA PET was positive in 11 patients (two sided p= 0.0176 for the comparison of positive ^{18}F-DOPA PET results and elevated CEA), CT/MR in 6 patients (two sided p= 0.064 for the comparison of positive CT/MR results and elevated CEA), DMSA in 3 patients and ^{18}F-FDG PET in 3 patients. In 2 patients with elevated CEA (#1 and #15), imaging yielded no positive scan results. Of the 7 patients with normal CEA, 1 patient (#14) had numerous lesions (and an elevated calcitonin) and 1 patient (# 10) showed 1 tumor positive lesion on ^{18}F-DOPA PET imaging. CEA doubling time was generally in agreement with calcitonin doubling time.

Clinical outcome

The 3 patients(#2, #12 and #18) that died since entering the study were characterized by a short calcitonin (<12 months) and CEA doubling time (<15 months). From our imaging results, these patients had extensively metastasised disease.

In 4 patients surgery was performed based on ^{18}F-DOPA PET findings. Prior to surgery, ^{18}F-DOPA PET images were fused with MR images for optimal anatomic localization. ^{18}F-DOPA PET findings were histopathologically confirmed in 4 cases. In all patients calcitonin and CEA levels dropped after surgery but did not return to within normal range. However, in 3 of these patients these markers are rising again and in 1 of these 3 patients the calcitonin doubling time is now < 12 months.

DISCUSSION

Our results show that ^{18}F-DOPA PET improves staging in patients with biochemical suspected relapse or residual MTC. ^{18}F-DOPA PET detects more tumor positive regions and lesions then CT/MRI, DMSA and ^{18}F-FDG PET separately. Even when the results of CT/MRI, DMSA and ^{18}F-FDG PET are pooled, ^{18}F-DOPA PET detects a slightly larger number of lesions. In addition this study shows that chances of obtaining a positive ^{18}F-DOPA PET and a negative ^{18}F-FDG PET are higher in those with a more indolent course of disease, while FDG is more frequently positive as well when clinical course is more aggressive, reflected by a rapid tumor marker increase. In addition, our data indicate that morphological imaging methods sometimes are complementary to the other imaging methods used in our study.

Two small studies, a retrospective study of Beuthien-Baumann [20] and a prospective study of Hoegerle [12], suggested a role for ^{18}F-DOPA PET in MTCs. In both studies only a lesion-based analysis was performed. Whereas Beuthien-Baumann et al. only had written results of morphological imaging at their disposal [19], Hoegerle et al. were able to use morphological data for their analysis [13]. Both studies have used biochemical data, but did not use these to establish a measure for biologic tumor behavior tumor progression.

In our study calcitonin and CEA doubling times improved our understanding of the conflicting results of FDG and ^{18}F-DOPA PET that are sometimes encountered. It seems that shorter calcitonin and CEA doubling times are associated with increased tumoral glucose metabolism and a decreased tumoral ^{18}F-DOPA metabolism (figure 2). This is in line with findings in other aggressive (dedifferentiated?) neuroendocrine tumors, such as small cell lung cancer and metastatic paraganglioma from patients with a SDHB gene mutation, in which FDG PET has a very high sensitivity for the detection of tumor lesions, whereas more 'specialized' tracers, such as ^{18}F-DOPA and ^{18}F-dopamine only show marginally tumoral uptake.[21,22] It is important to distinguish between local disease recurrence, which may be surgically curable, and systemic disease, in which case the aim is palliation . Therefore, it is important to adequately stage patients with MTC. ^{18}F-DOPA PET can provide a better understanding of tumor load, local as well a systemic disease and can support the clinical decision in these patients with often slowly progressive tumors. For the control of

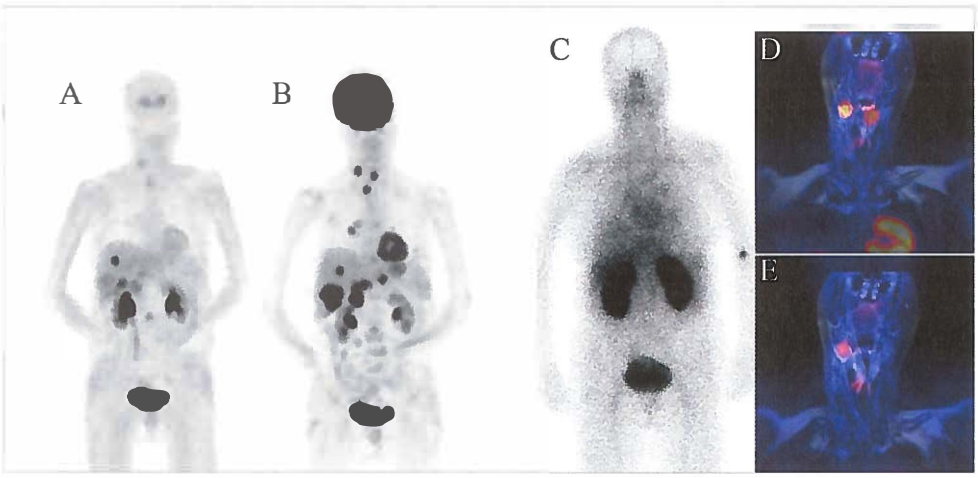

Figure 2 Patient 18: 65 year old female patient with sporadic medullary thyroid cancer.
Her calcitonin doubling time was 4 months (calcitonin 1160 ng/L) and her CEA doubling time 7 months (CEA 41.9 µg/L). In Figure 2A a ^{18}F-DOPA PET projection image is presented, showing lesions with vague uptake in the skull, neck, liver and spine, but also lesions with intense uptake. The ^{18}FDG PET (Figure 2B) showed many more lesions with intense uptake in the neck, mediastinum, liver and spine. The DMSA scan (Figure 2C) showed no lesions at all. In Figure 2D1 a ^{18}FDG PET – MR fusion slice is presented, showing 3 lesions in the neck. However, on the ^{18}F-DOPA PET – MR fusion (figure 2D2), only 2 lesions show vague uptake. The different lesional uptake within one patient illustrates most likely different degrees of tumor dedifferentiation within one patient.

local recurrent disease clearance of lymph node metastases by systematic dissection may provide local control in the neck and mediastinum [5,6,7,23,24] and may prevent tracheal and esophageal invasion because of tumor infiltration.[25,26] Local recurrent disease indisputably requires systematic lymph node dissection.[6,7,27] There is still controversy on the treatment of metastasized disease. After apparent curative surgery for primary tumors, patients with persistent hypercalcitoninemia may have a 10-year survival of around 65%. [3,28]. However, for local disease control, dissection of the central and both lateral lymph node compartments of the neck may still have a role, but more accurate knowledge of both the number and localization of the metastases can be helpful in the decision whether or not to perform surgery. When only one distant lymph node compartment (either the contralateral side of the neck or the mediastinum) is involved, there is 10% chance of cure. [29]

Defining the gold standard for imaging studies in which new tracers may yield better results than the commonly used imaging methods is a difficult problem. Therefore, we choose to use a gold standard consisting of the combined data from all imaging modalities together.[18] Since patients with MTC have a good life expectancy and undergo regular imaging to assess possible tumor growth, it was ethically not justifiable to try to verify all newly detected lesions. However, in four patients who did undergo surgery as a consequence

of positive ^{18}F-DOPA PET findings, the detected lesions were resected and histologically confirmed to be tumor positive.

Combining multiple imaging modalities yields the best results for the detection of recurrent MTC. Morphologic imaging is important for accurate anatomic localization of MTC lesions. In our study, we did not have combined PET-CT available, and therefore we performed software based rigid fusion of conventional imaging methods with PET to achieve a more accurate localization. Also in this study CT/MRI had excellent lesion visualisation properties, and often demonstrated lesions less evident on PET and vice versa. In addition, combined PET-CT decreased reader uncertainties in deciding whether a lesion is real or not in this study, although it is difficult to catch that effect in numbers. Combined PET-CT will offer the best of both worlds and may become the diagnostic imaging procedure of choice in MTC (one-stop shop).

Establishing a perfect gold standard is difficult in every diagnostic accuracy study. As in our case, newer diagnostic methods can be far better than current standard methods and detect many unknown lesions, that can never all be verified using cytological or histological analysis. Whenever possible we verified new findings, but also used common sense, and assumed that, when several lesions were verified, other lesions with identical and unequivocal uptake of this specific tracer in the same patient could also be regarded as true tumour lesions. Some dependency of PET results and our composite reference standard is present in this study. However, this dependency is also present for CT and SRS. Still, our sensitivity values should be regarded with some caution.[18, 30]

There is an ongoing search for new tracers for MTC, as the problem of increased tumor marker and negative imaging is felt in many centers. Even in this study with extensive diagnostic tests 5/21 (24%) of the patients remained negative on all performed tests. For not all imaging modalities were available in the patients the value of FDG PET in progressive disease has been underexposed, so more data about difference in FDOPA and FDG PET uptake are necessary to proven the value in progressive MTC patients.

New approaches such as gastrin receptor scintigraphy are promising owing to the high expression of the cholecystokinin 2 receptor in MTCs.[31,32] However, due to the variation in biologic behaviour of MTC, the future will learn what the best imaging approach for these tumors will be. Very likely individual tailoring with different imaging methods based on biologic behavior will be necessary for optimal staging of MTC in patients

In conclusion, ^{18}F-DOPA PET is superior to ^{18}F-FDG PET and DMSA scintigraphy in staging of MTC and probably the best non-invasive staging method yet available. A decrease in serum calcitonin doubling time and a shift from ^{18}F-DOPA PET positivity to more ^{18}F-FDG PET indicates aggressive tumor behavior and may support the choice for systemic therapy.

REFERENCES

1. Kebebew E, Ituarte PH, Siperstein AE, Duh QY, Clark OH. Medullary thyroid carcinoma: clinical characteristics, treatment, prognostic factors, and a comparison of staging systems. *Cancer.* 2000;88:1139-1148.
2. Orlandi F, Caraci P, Mussa A et al. Treatment of medullary thyroid carcinoma: an update. *Endocr Relat Cancer.* 2001;8:135-147.
3. de Groot JW, Plukker JT, Wolffenbuttel BH et al. Determinants of life expectancy in medullary thyroid cancer: age does not matter. *Clin Endocrinol.* 2006;65:729-736.
4. Ong SC, Schoder H, Patel SG et al. Diagnostic accuracy of 18F-FDG PET in restaging patients with medullary thyroid carcinoma and elevated calcitonin levels. *J Nucl Med.* 2007;48:501-507.
5. Moley JF, DeBenedetti MK. Patterns of nodal metastases in palpable medullary thyroid carcinoma: recommendations for extent of node dissection. *Ann Surg.* 1999;229:880-887.
6. Scollo C, Baudin E, Travagli JP et al. Rationale for central and bilateral lymph node dissection in sporadic and hereditary medullary thyroid cancer. *J Clin Endocrinol Metab.* 2003;88:2070-2075.
7. de Groot JW, Links TP, Sluiter WJ et al. Locoregional control in patients with palpable medullary thyroid cancer: results of standardized compartment-oriented surgery. *Head Neck.* 2007;29:857-863.
8. Cohen EG, Shaha AR, Rinaldo A, Devaney KO, Ferlito A. Medullary thyroid carcinoma. *Acta Otolaryngol.* 2004;124:544-557.
9. de Groot JW, Links TP, Jager PL, Kahraman T, Plukker JT. Impact of 18F-fluoro-2-deoxy-D-glucose positron emission tomography (FDG-PET) in patients with biochemical evidence of recurrent or residual medullary thyroid cancer. *Ann Surg Oncol.* 2004;11:786-794.
10. Khan N, Oriuchi N, Higuchi T, Endo K. Review of fluorine-18-2-fluoro-2-deoxy-D-glucose positron emission tomography (FDG-PET) in the follow-up of medullary and anaplastic thyroid carcinomas. *Cancer Control.* 2005;12:254-260.
11. Uchino H, Kanai Y, Kim DK et al. Transport of amino acid-related compounds mediated by L-type amino acid transporter 1 (LAT1): insights into the mechanisms of substrate recognition. *Mol Pharmacol.* 2002;61:729-737.
12. Hoegerle S, Altehoefer C, Ghanem N et al. 18F-DOPA positron emission tomography for tumour detection in patients with medullary thyroid carcinoma and elevated calcitonin levels. *Eur J Nucl Med.* 2001;28:64-71.
13. Gourgiotis L, Sarlis NJ, Reynolds JC et al. Localization of medullary thyroid carcinoma metastasis in a multiple endocrine neoplasia type 2A patient by 6-[18F]-fluorodopamine positron emission tomography. *J Clin Endocrinol Metab.* 2003;88:637-641.
14. de Vries EF, Luurtsema G, Brussermann M, Elsinga PJ, Vaalburg W. Fully automated synthesis module for the high yield one-pot preparation of 6-[18F]-fluoro-L-DOPA. *Appl Radiat Isot.* 1999;51:389-419.
15. Brown WD, Oakes TR, DeJesus OT et al. Fluorine-18-fluoro-L-DOPA dosimetry with carbidopa pretreatment. *J Nucl Med.* 1998;39:1884-1891.
16. Ishikawa T, Dhawan V, Chaly T et al. Fluorodopa positron emission tomography with an inhibitor of catechol-O-methyltransferase: effect of the plasma 3-O-methyldopa fraction on data analysis. *J Cereb Blood Flow Metab.* 1996;16:854-863.
17. Orlefors H, Sundin A, Lu L et al. Carbidopa pretreatment improves image interpretation and visualisation of carcinoid tumours with 11C-5-hydroxytryptophan positron emission tomography.

Eur J Nucl Med Mol Imaging. 2006;33:60-65.

18. Koopmans KP, de Vries EG, Kema IP et al. Staging of carcinoid tumours with 18F-DOPA PET: a prospective, diagnostic accuracy study. *Lancet Oncol*.. 2006;7:728-734.
19. Miyauchi A, Onishi T, Morimoto S et al. Relation of doubling time of plasma calcitonin levels to prognosis and recurrence of medullary thyroid carcinoma. *Ann Surg*. 1984;199:461-466.
20. Beuthien-Baumann B, Strumpf A, Zessin J, Bredow J, Kotzerke J. Diagnostic impact of PET with (18)F-FDG, (18)F-DOPA and 3-O-methyl-6-[(18)F]fluoro-DOPA in recurrent or metastatic medullary thyroid carcinoma. *Eur J Nucl Med Mol Imaging*. 2007; DOI 10.1007/s00259-007-0425-2
21. Jacob T, Grahek D, Younsi N et al. Positron emission tomography with [(18)F]FDOPA and [(18)F]FDG in the imaging of small cell lung carcinoma: preliminary results. *Eur J Nucl Med Mol Imaging*. 2003;30:1266-1269.
22. Timmers HJ, Kozupa A, Chen CC et al. Superiority of fluorodeoxyglucose positron emission tomography to other functional imaging techniques in the evaluation of metastatic SDHB-associated pheochromocytoma and paraganglioma. *J Clin Oncol*. 2007;25:2262-2269.
23. Gimm O, Ukkat J, Dralle H. Determinative factors of biochemical cure after primary and reoperative surgery for sporadic medullary thyroid carcinoma. *World J Surg*. 1998;22:562-567.
24. Machens A, Holzhausen HJ, Dralle H. Prediction of mediastinal lymph node metastasis in medullary thyroid carcinoma. *Br J Surg*. 2004;91:709-712.
25. Kebebew E, Kikuchi S, Duh QY, Clark OH. Long-term results of reoperation and localizing studies in patients with persistent or recurrent medullary thyroid cancer. *Arch Surg*. 2000;135:895-901.
26. Machens A, Hinze R, Lautenschlager C, Thomusch O, Dralle H. Thyroid carcinoma invading the cervicovisceral axis: routes of invasion and clinical implications. *Surgery*. 2001;129:23-28.
27. Moley JF, DeBenedetti MK. Patterns of nodal metastases in palpable medullary thyroid carcinoma: recommendations for extent of node dissection. *Ann Surg*. 1999;229:880-887.
28. Bergholm U, Bergstrom R, Ekbom A. Long-term follow-up of patients with medullary carcinoma of the thyroid. *Cancer*. 1997;79:132-138.
29. Machens A, Holzhausen HJ, Dralle H. Contralateral cervical and mediastinal lymph node metastasis in medullary thyroid cancer: systemic disease? *Surgery*. 2006;139:28-32.
30. Behr TM, Jenner N, Radetzky S et al. Targeting of cholecystokinin-B/gastrin receptors in vivo: preclinical and initial clinical evaluation of the diagnostic and therapeutic potential of radiolabelled gastrin. *Eur J Nucl Med*. 1998;25:424-430.
31. Gotthardt M, Behe MP, Beuter D et al. Improved tumour detection by gastrin receptor scintigraphy in patients with metastasised medullary thyroid carcinoma. *Eur J Nucl Med Mol Imaging*. 2006;33:1273-1279.

Chapter seven

Somatostatin receptor scintigraphy is superior to meta-iodo-benzylguanidine scintigraphy imaging in head and neck paragangliomas: a prospective, diagnostic accuracy study

Klaas P. Koopmans[1], Pieter L. Jager[1], Ido P. Kema[2], Michiel N.Kerstens[3], Frans W. Albers[4], Robin P.F. Dullaart[3]

Departments of Nuclear Medicine and Molecular Imaging[1], Clinical Chemistry[2],
Endocrinology[3] and Ear Nose and Throat Diseases[4], University Medical Center Groningen, University of Groningen, The Netherlands.

ABSTRACT

Aim of this study is to evaluate the value of somatostatin receptor scintigraphy (SRS), I-meta-iodo-benzylguainidine scintigraphy (MIBG) and morphologic imaging (CT or MRI) for the detection of head and neck paragangliomas.

Methods

Patients underwent CT and/or MRI, SRS and MIBG imaging. A composite reference standard was used, consisting of clinical and histological data and CT/MRI, with which all imaging modalities were compared. Urinary metanephrine and normetanephrine measurements were also obtained.

Results

Twenty nine consecutive patients (F:17; M:12) with suspected head and neck paraganglioma were included. Both morphologic and SRS imaging were positive in 27 patients (sensitivity of 93%, 95% CI 77-98%), MIBG only in 13 patients (44%, 95% CI 23-61%) ($p < 0.001$ compared to SRS). On a lesion-based analysis, morphologic imaging detected 31 lesions (sensitivity 82%, 95% CI 65-92%), SRS 34 (89%, 95% CI 75-97%) and MIBG 15 lesions (42%, 95% CI 26-59%). SRS was superior to MIBG ($p=0.001$). SRS detected an unknown carcinoid tumor in 2 patients; MIBG detected an additional adrenal pheochromocytoma in 1 patient. Elevated urinary metanephrine and/or normetanephrines excretion was found in 6 patients. The number of lesions on SRS and MIBG correlated with abnormal metanephrine and/or normetanephrine excretion ($p=0.005$ and $p=0.02$, respectively).

Conclusions

SRS is superior to MIBG, but equal to morphologic imaging for the detection of head and neck paraganglioma. SRS is of clinical significance for a better characterization of head and neck paraganglioma and can detect additional neuroendocrine tumors. MIBG imaging is useful when a concomitant (adrenal) pheochromocytoma is suspected.

INTRODUCTION

Paragangliomas are rare tumors that stem from cells of the diffuse neuroendocrine system in the paraganglia of the parasympathetic nervous system. Paragangliomas constitute approximately 0.6% of the head and neck tumors. [1] Usually these tumors of the head and neck are located in close association with the parasympathetic nervous system along the cranial nerves and the arterial vasculature and can be present from the skull base to the aortic arch. [2] Approximately 90% of paragangliomas are benign. Furthermore paragangliomas

can arise in multiple locations in patients with succinate dehydrogenase subunit B, C or D germline mutations (SDHB, SDHC and SDHD).[3-5] In most cases conventional imaging methods, such as computed tomography (CT) and magnetic resonance imaging (MRI), combined with arteriography can confirm the diagnosis of a paraganglioma. Nevertheless, radiological data may not be sufficient to characterize lesions. Not all tumors are accessible for biopsy due to the risk of neurologic complications and the highly vascularized nature of paragangliomas.[6] Thus, other techniques may be helpful to confirm a diagnosis of a paraganglioma and to disclose multifocality of paragangliomas.

Given the overexpression of somatostatin receptors in paragangliomas, as in most other neuroendocrine tumors, somatostatin receptor scintigraphy (SRS) can be used for visualization of these tumors.[7] In addition, these tumors have the basic capacity to take up and decarboxylize amino acid precursors.[8] In approximately 30% of all paragangliomas, the catecholamine pathway is active.[9] In this catecholamine pathway the amino acid phenylalanine is metabolized to dopamine, adrenalin and noradrenalin. As a noradrenalin analogue, metaiodobenzylguanidine (MIBG), which is most commonly labeled with either ^{123}I or ^{131}I is a radiopharmaceutical that is taken up by the noradrenalin transporter. The combination of active catecholamine pathway and the presence of uptake mechanisms for catecholamine metabolites enables the use of MIBG for visualizing paragangliomas.[10]

The diagnostic yield of SRS and MIBG for the visualization of head and neck paragangliomas has been determined in several studies, but a direct comparison has been made in only few patients.[11-15] The present study was initiated to evaluate the diagnostic sensitivities of SRS, MIBG scintigraphy and CT or MRI in a group of consecutive patients with head and neck paragangliomas, and to compare these imaging results with a composite reference standard, consisting of clinical findings, histological data and morphologic imaging results. The secondary aim of this study was to assess if there is a relation between catecholamine production of paragangliomas and tracer uptake, which could lead to better selection of patients for optimal imaging protocols.

Patients and methods

Patients seen at the outpatient endocrinology clinic between January 1993 and January 2007 were included in this study. All patients included were referred from the department of ear, nose and throat diseases because of a strong suspicion of a head and neck paraganglioma based on complaints, localization and radiographic appearance of the tumor or had a histopathologically proven head and neck paraganglioma with a clinical indication for restaging. We excluded patients younger than 18 years and those who were pregnant. Every patient underwent SRS, MIBG and CT/MRI scanning of the head and neck region, and biochemical analysis. Imaging methods were undertaken in random order.

SRS imaging

Twenty-four hours after administration of 200 MBq ^{111}In-octreotide (Octreoscan, Mallinckrodt, Petten, The Netherlands) planar total body scans (4 spotviews of 10 min in a 128 matrix and side views of the head and neck) were obtained using a large-field-of-view double headed gamma camera (MULTISPECT 2, Siemens Inc, Hoffman Estates, IL) with a medium energy all purpose collimator. System resolution was 12 mm FWHM at 10 cm distance. Both 173 and 247 keV photopeaks of ^{111}In were used (15% windows for each). In addition, in some patients single photon emission computed tomography (SPECT) acquisition and processing was performed by taking 64 projections (2x 32; 5.6˚ / step of 30 seconds duration each in a 128 x 128 matrix format. Total scan procedure took ~60 min. Transaxial tomograms were reconstructed without prefiltering with a Butterworth cutoff filter frequency of 0.35. When necessary because of interfering bowel activity, additional 48 hour images were recorded. This scanning protocol was performed conform Dutch guidelines.

MIBG imaging

Fifteen min after administration of 10 drops Lugol's solution (to prevent thyroid uptake of possibly formed free ^{123}Iodine) 200 MBq ^{123}I-MIBG was administered. Twenty four hours later, planar total body scans (4 spotviews of 10 min in a 256 matrix) were acquired using the same gamma camera as for the SRS scan. A medium energy all purpose collimator was used and the 158 KeV photopeak was registered using a 15% window. In addition, SPECT acquisition was done using the same specifications as described in the section SRS imaging. Transaxial tomograms were reconstructed without prefiltering with a Butterworth cutoff filter frequency of 0.2 – 0.4 and attenuation correction was a Chang's attenuation coefficient of 0.11 cm^{-1}. Due to the interval of at least one week between the scans, no interference between the tracers should be expected. This scanning protocol was performed conform Dutch guidelines.

CT scan

CT (1-16 slice, Siemens Medical Systems, Erlangen, Germany) was performed before and during intravenous contrast enhancement using 3-10 mm slice thickness increments. Patients underwent a CT scan always covering the head and neck area and if there was suspicion of lesions elsewhere, the involved body region was also covered. These CT scans were interpreted by dedicated specialists as part of routine patient care. At the time of data analysis, the investigators again reviewed results and in discrepant cases consensus was reached after multidisciplinary discussion.

MRI

MRI was carried with a 1.5 T scanner (Vision, Siemens, Erlangen, Germany). The imaging protocol included standard spin-echo T1-weighted (TR/TE = 700/14 ms), proton-density and T2-weighted scans (TR/TE/TE2 = 2500/20/90 ms) A spin echo technique was used to obtain 5 mm contiguous 3-dimensional sections of the abdomen. T1-weighted images (TR/TE=600/15 ms) and T2-weighted images (TR/TE= 2000/15-90 ms) were obtained. T1-weighted images were also acquired after the intravenous administration of gadolinium - DTPA (0.2 ml/kg of weight body, Magnevist, Schering, Berlin, Germany).

Image interpretation

As this study ran for a considerable period, improvements in diagnostic equipment came up for all modalities during the course of the study. Basic detection principles did not change and in general the equipment was always relatively modern for the time period used. Therefore, this potential bias was assumed to be small. All SRS and MIBG scans were read twice. The first assessment was directly after the image reconstruction as part of patient care and the second interpretation was done at the time of data analysis, blinded for other imaging and biochemical information. For both tracers the number and location of lesions were scored. In addition, for each lesion an uptake score was established grading uptake intensity: 0: no uptake, 1: uptake lesion equals background uptake, 2: uptake lesion > background uptake, 3: uptake lesion >> background uptake. Background was defined as uptake in normal neck musculature. In this way a semi-quantitative uptake score was established grading the amount of whole body tumor uptake for both tracers.

Composite reference

As a composite reference standard for the presence of tumor lesions, morphologic imaging data, clinical findings and histological data were use. Cytological confirmation was neither feasible nor justifiable for all lesions in these patients. In case of additional findings on SRS or MIBG imaging, these were verified with CT, MRI, ^{18}F-DOPA PET, bone scintigraphy, surgery, biopsy or follow-up whenever possible.

Biochemical measurements

In each patient 3 24 hour urine collections were obtained to document metanephrine and normetanephrine excretion. Biochemical results were classified as abnormal when the average value of these 3 measurements was elevated. Metanephrine levels of > 99 µmol/mol creatinine and metanephrine levels of >260 µmol/mol creatinine were considered abnormal. Biochemical analysis was performed using methods described earlier.[16-18]

Data and statistical analysis

Analysis was performed at two levels. At the first level individual patients were analyzed. Image studies were considered positive when at least one lesion in a patient was considered positive. The second level was the level of the individual lesions that were counted for all imaging modalities.

Sensitivities were calculated using the composite reference standard described above, and were compared using paired observations and McNemar's test. Patient based sensitivity was calculated as the number of patients with a positive test (at least one lesion detected) divided by the total number of patients. For the comparison of number of lesions per region, Wilcoxon's rank test was used. For correlations between biochemical parameters and scan results, Spearman's correlation coefficient (Rs) was calculated. A two-sided p-value < 0.05 was considered significant. The statistical tests were carried out using the SPSS package version 12.0.

RESULTS

Patients

29 consecutive patients (F:M 17:12) participated in this study (table 1). The median time between SRS and MIBG scintigraphy was 7 days and the median time between SRS/MIBG and CT or MR was 78 days. In all patients conventional imaging was performed with either CT of the head and neck region (14 patients) or MRI of the head and neck region (15 patients).

Patient-based analysis

All 29 patients were considered positive for paragangliomas based on the composite reference standard and histological data (table 2). Morphological imaging as well as SRS correctly identified 27 of 29 patients (sensitivity 93%, 95 CI 77 - 98%), whereas MIBG correctly identified 13 patients (sensitivity 44%, 95 CI 23-61%). In our study group, SRS detected a significant larger number of tumor positive patients than MIBG ($p< 0.001$). We found that SRS uptake was more intense than MIBG uptake in 7 patients, equal to MIBG uptake in 3 patients and less intense than MIBG uptake in 2 patients.

Lesion-based analysis

A total of 38 lesions were identified using the composite reference standard. Morphologic imaging detected 31 of these lesions (sensitivity 82%, 95% CI 65-92%) with an average of 1.07 lesions per patient (lpp), SRS detected 34 (sensitivity 89%, 95 CI 75-98, 1.17 lpp) and MIBG detected 15 lesions correctly (sensitivity 42%, 95% CI 26-59% and 0.52 lpp). SRS detected more lesions than MIBG ($p=0.0001$, an example is shown in Figure 1). In 6 patients $>$ 1 lesion was present in the head and neck region (table 1).

TABLE 1. Patient characteristics.

ID	Age / sex	Tumor type	SRS lesions	MIBG lesions	CT/MR	Blood pressure	Elevated urinary catecholamine metabolites	Confirmation/ treatment
1	47/f	Glomus caroticum L	Neck L	Neck L	0	normal		follow-up
2	55/m	Glomus vagale L	Jaw L	Jaw L	Jaw L	hypertension		surgery
3	40/f	Glomus caroticum R+L, pheochromocytoma Left SDHD mutation	Jaw R+L	Left adrenal gland	Jaw R+L	hypertension	N	surgery
4	33/m	Glomus tympanicum R	Ear R	0	Ear R	normal		surgery
5	54/f	Glomus tympanicum L	0	0	Skull base L	hypertension		surgery
6	51/m	Glomus temporale L	Ear L	0	Ear L	hypertension		surgery
7	71/m	Glomus caroticum L	Jaw R	Jaw R	Jaw R	normal		surgery
8	39/f	Glomus tympanicum L	Ear L	0	Ear L	normal	M	surgery
9	57/f	Glomus temporale L	Ear L	0	Ear L	normal		surgery
10	52/m	Glomus caroticum L	Neck L	0	Neck L	hypertension		embolisation
11	71/f	Glomus temporale L	Ear L	Ear L	Ear L	normal		follow-up
12	94/f	Glomus tympanicum R	Ear R	0	Ear R	normal		follow-up
13	65/f	Glomus tympanicum R Carcinoid R lung	Ear R, lung hilus R	0	Ear R	normal		follow-up, surgery
14	70/f	Glomus jugularis L+R, caroticum L	Neck R+L, mastoid R	Neck R+L	Neck R+L, mastoid R	hypertension		Follow up, histology
15	68/m	Glomus temporale R	Mastoid R	Mastoid R	Mastoid R	normal	M	follow-up
16	80/f	Glomus tympanicum R	Ear R	0	Ear R	normal		surgery
17	75/f	Glomus temporale L	Skull base, neck R+L	Skull base, neck R+L	Skull base	hypertension	M	follow-up
18	71/m	Glomus temporale L	Ear L	0	Ear L	normal	M	follow-up
19	33/m	Glomus jugularis L	Skull base L	0	Skull base L	hypertension		surgery
20	47/f	Glomus jugularis R	Skull base R	0	Skull base R	hypertension		surgery
21	55/m	Glomus vagale L	Skull base L	0	Skull base L	normal		surgery
22	68/m	Glomus vagale L	Skull base L	Skull base L	Skull base L	normal		surgery
23	61/m	Glomus jugularis R	Ear R	Ear R	Ear R	normal		follow-up
24	53/m	Glomus caroticum L	Neck L	Neck L	Neck L	hypertension		embolisation
25	63/f	Glomus jugularis L	Ear L	0	Ear L	normal		follow-up
26	65/f	Glomus caroticum L+R Abdominal carcinoid	Neck L Abdomen R	Neck L Abdomen R	Neck L+R	normal		surgery
27	64/f	Glomus caroticum R	Jaw R	Jaw R	Jaw R	normal		follow-up
28	71/f	Glomus caroticum R	Jaw R	0	Jaw R	normal		follow-up
29	65/m	Glomus tympanicum R	0	0	Ear R	normal		follow-up

F: female; m: male. Blood pressure: hypertension is defined as systolic blood pressure >140 mm Hg and/or diastolic blood pressure > 90 mm Hg. Biochemistry: M, metanephrine; N, normetanephrine.

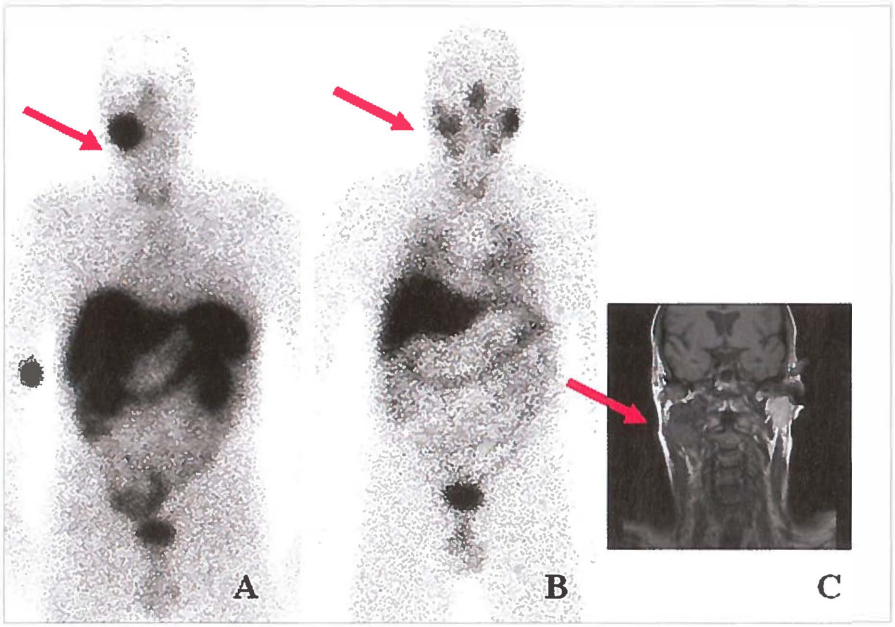

Figure 1. MIBG negative paraganglioma.
In panel A the SRS image is shown with pathologic uptake in the right jaw, whereas in panel B, this lesion was not seen on the MIBG scan. In panel C a MRI coronal slice is shown for the lesion in the right jaw.

TABLE 2. Patient and region based analysis of patients with paraganglioma

	CT/MRI	SRS	MIBG
Patient based analysis			
N positive patients	27*	27*	13
Sensitivity (95% CI)	93% (77-98)	93% (77-98)	44% (23-61)
Mean number of lesions (range)	1.07 (0 - 3)	1.17 (0 - 3)	0.52 (0 - 3)
Lesion based analysis			
N positive lesions	31**	34**	15
Sensitivity (95% CI)	82% (65-92)	89% (75-97)	42% (26-59)

In this table sensitivities for head and neck paraganglioma of CT, SRS and MIBG, are presented based on a patient and lesion based analysis in 29 tumor positive patients. * SRS and CT were significantly better than MIBG ($p<0.001$). ** SRS and CT were better than MIBG ($p=0.001$).

Secondary tumors and discrepant cases

In 3 patients (10%), previously unknown neuroendocrine tumors were found outside the head and neck region. In 1 patient, SRS showed a lung carcinoid (patient 13) and in another patient (patient 26) SRS detected a carcinoid lesion in the abdomen (Figure 2). These tumors did not show MIBG uptake. However, MIBG scintigraphy led to the detection of a left sided adrenal pheochromocytoma, which was not detected on the SRS scan (patient 3). This patient was found to have a SDHD gene mutation.

Biochemical results

Four patients had elevated urinary metanephrine excretion, whereas one patient (the case with adrenal pheochromocytoma) had elevated urinary normetanephrine excretion (table 1). On a lesion-based analysis, elevated urinary meta- and/or normetanephrine excretion was correlated with the number of SRS lesions (Rs=0.51, p= 0.005) and the number of MIBG lesions (Rs=0.47, p=0.02). These relationships were not significant on a patient-based analysis. The correlation between the presence of hypertension and abnormal urinary metanephrine and/or normetanephrine excretion was not significant.

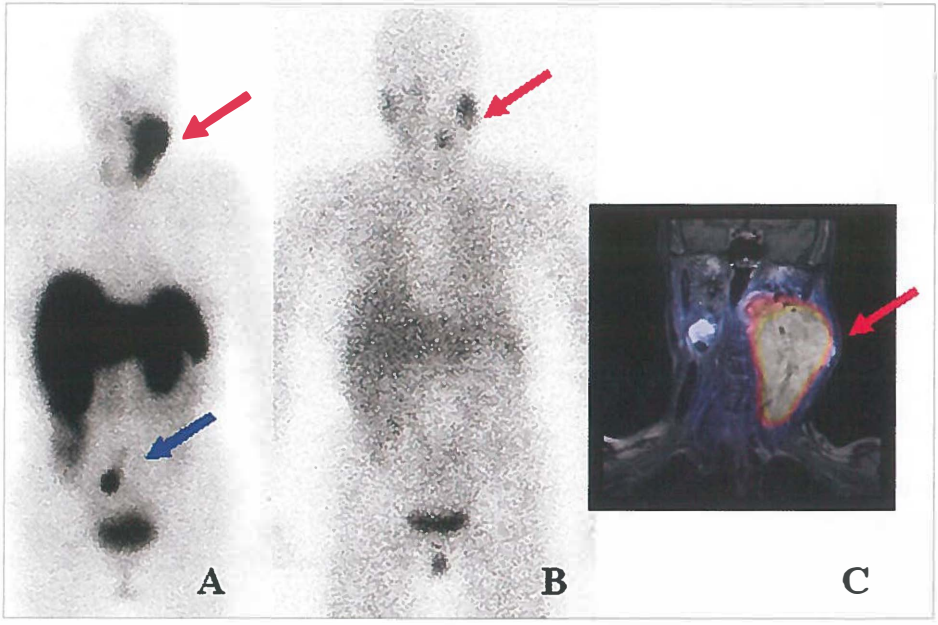

Figure 2. unexpected abdominal carcinoid lesion.
Panel A shows the SRS image with a lesion in the left neck (red arrow) and a lesion in the abdomen (blue arrow). Panel B: although visible on the MIBG scan, the neck lesion appears much smaller on the MIBG scan (red arrow) and the abdominal lesion showed no MIBG uptake. In panel C a SRS and MRI fusion image is shown for the neck lesion.

DISCUSSION

In our cohort of 29 consecutive patients with head and neck paraganglioma, it is evident that SRS is superior in the detection of head and neck paragangliomas compared to MIBG imaging. SRS performed equally well as morphologic imaging methods for detection of head and neck paraganglioma on a patient-based analysis, and detected some additional lesions in the head and neck region compared to CT/MRI. Thus, SRS imaging is likely to contribute to optimal lesion characterization in this patient category. Furthermore, in view of the low yield of MIBG imaging, we suggest that this scan should not be routinely used in the evaluation of head and neck paraganglioma.

The main difference between the present report and previous studies concerning the performance characteristics of SRS and MIBG imaging is that most other studies also included paragangliomas outside the head and neck region.[19-21] Nonetheless, our present results are in line with these other studies. Muros et. al showed that in a study with 8 patients, that SRS had a sensitivity of 100% versus 56% for MIBG[22]. In retrospective study from Erickson et al. [23] the clinical records of 236 benign paraganglioma patients, including those with tumors outside the head and neck region, were evaluated. In 25 of these patients, in whom MIBG imaging was performed, it was found that this technique was able to detect only 62% of the paragangliomas, but no comparison could be made with SRS. In a study in 34 patients, Kwekkeboom et al.[24] showed that SRS has high sensitivity of 94% for the detection of paragangliomas. Importantly, that study showed that the use of whole body imaging revealed additional paraganglioma lesions in 9 patients.

A potentially important clinical finding of our study is that SRS demonstrated to previously unknown carcinoid tumors. To our knowledge co-incidence of head and neck paraganglioma with carcinoid tumors have not been reported earlier. However, the only co-existing adrenal pheochromocytoma in the present series was discovered with MIBG but not with SRS imaging. This finding agrees with a report that showed adrenal pheochromocytoma in 7 of 40 patients with either an SDHD mutation or a positive family history for head and neck paragangliomas.[25] Thus, there remains an indication to perform MIBG imaging in case of clinical suspicion of (adrenal) pheochromocytoma.

In our study, 5 of 29 subjects (17 %), including the patient with adrenal pheochromocytoma, had elevated urinary metanephrine and/or normetaneophrine excretion. In comparison, in the retrospective analysis of 236 benign paragangliomas, excess catecholamine production was found in 31 % of tested subjects.[26] In our study, there was only a modest correlation of abnormal catecholamine production, as documented by elevated urinary metanephrines and/or normetanephrine excretion, with SRS as well as with MIBG results on a lesion-based analysis. However, since urinary catecholamine measurements can be easily obtained, we propose the perform MIBG in addition to SRS imaging in those patients with clinically or biochemically suspected (adrenal) pheochromocytoma.

Recently, other imaging techniques have been employed to detect neuroendocrine tumors. Preliminary data have shown a high yield of ^{18}F-DOPA PET imaging in carcinoid tumors.[27] Thus far, ^{18}F-DOPA has been used in only small groups of patients with paraganglioma, but the results are promising.[28,29] Although ^{18}F-DOPA PET was able to find more paraganglioma lesions than MRI and MIBG no direct comparison with SRS imaging has been made thus far. Moreover, it can be expected that the performance of ^{18}F-DOPA PET in patients with SDH gene mutations will be less optimal due to their proneness to dedifferentiation. In such cases, the use of ^{18}F-DOPA PET or FDG PET imaging may be useful.[30,31]

Finally, although we did not present follow-up data with repeated nuclear imaging studies, it seems reasonable to assume that SRS is of merit to detect residual and/or recurrent paraganglioma after initial treatment, and that ^{177}Lu-DOTA-TYR3-octreotate may be useful to treat residual disease in selected.[32]

In conclusion, we found a very high sensitivity of SRS imaging for the detection of paragangliomas in the head and neck region. Although SRS has an equal sensitivity as morphologic imaging methods for paragangliomas, it has two major advantages. First, SRS is able to characterize lesions as being of a neuroendocrine origin. Second, this nuclear imaging technique has the advantage of being a whole body imaging technique, which can, as shown in this study, lead to the detection of additional neuroendocrine lesions.

ACKNOWLEDGEMENTS

The research of K.P. Koopmans, MD, is financially supported by grant 2003-2936 from the Dutch Cancer Foundation.

REFERENCES

1 Lee JH, Barich F, Karnell LH et al. National Cancer Data Base report on malignant paragangliomas of the head and neck. *Cancer.* 2002;94:730-737.

2 Baysal BE, Willett-Brozick JE, Lawrence EC et al. Prevalence of SDHB, SDHC, and SDHD germline mutations in clinic patients with head and neck paragangliomas. *J Med Genet.* 2002;39:178-183.

3 Baysal BE, Willett-Brozick JE, Lawrence EC et al. Prevalence of SDHB, SDHC, and SDHD germline mutations in clinic patients with head and neck paragangliomas. *J Med Genet.* 2002;39:178-183.

4 Timmers HJ, Kozupa A, Chen CC et al. Superiority of fluorodeoxyglucose positron emission tomography to other functional imaging techniques in the evaluation of metastatic SDHB-associated pheochromocytoma and paraganglioma. *J Clin Oncol.* 2007;25:2262-2269.

5 McCaffrey TV, Myssiorek D, Marrinan M. Head and neck paragangliomas: physiology and biochemistry. *Otolaryngol Clin North Am.* 2001;34:837-44, v.

6 Duet M, Sauvaget E, Petelle B et al. Clinical impact of somatostatin receptor scintigraphy in the management of paragangliomas of the head and neck. *J Nucl Med.* 2003;44:1767-1774.

7 Muros MA, Llamas-Elvira JM, Rodriguez A et al. 111In-pentetreotide scintigraphy is superior to 123I-MIBG scintigraphy in the diagnosis and location of chemodectoma. *Nucl Med Commun.* 1998;19:735-742.

8 Pearse AG. The APUD cell concept and its implications in pathology. *Pathol Annu.* 1974;9:27-41.

9 Erickson D, Kudva YC, Ebersold MJ et al. Benign paragangliomas: clinical presentation and treatment outcomes in 236 patients. *J Clin Endocrinol Metab.* 2001;86:5210-5216.

10 Maurea S, Cuocolo A, Reynolds JC et al. Iodine-131-metaiodobenzylguanidine scintigraphy in preoperative and postoperative evaluation of paragangliomas: comparison with CT and MRI. *J Nucl Med.* 1993;34:173-179.

11 Duet M, Sauvaget E, Petelle B et al. Clinical impact of somatostatin receptor scintigraphy in the management of paragangliomas of the head and neck. *J Nucl Med.* 2003;44:1767-1774.

12 Erickson D, Kudva YC, Ebersold MJ et al. Benign paragangliomas: clinical presentation and treatment outcomes in 236 patients. *J Clin Endocrinol Metab.* 2001;86:5210-5216.

13 Kwekkeboom DJ, van Urk H, Pauw BK et al. Octreotide scintigraphy for the detection of paragangliomas. *J Nucl Med.* 1993;34:873-878.

14 Maurea S, Cuocolo A, Reynolds JC et al. Iodine-131-metaiodobenzylguanidine scintigraphy in preoperative and postoperative evaluation of paragangliomas: comparison with CT and MRI. *J Nucl Med.* 1993;34:173-179.

15 Muros MA, Llamas-Elvira JM, Rodriguez A et al. 111In-pentetreotide scintigraphy is superior to 123I-MIBG scintigraphy in the diagnosis and location of chemodectoma. *Nucl Med Commun.* 1998;19:735-742.

16 Kema IP, Meiborg G, Nagel GT, Stob GJ, Muskiet FA. Isotope dilution ammonia chemical ionization mass fragmentographic analusis of urinary 3O-methylated catecholamine metabolites. Rapid sample clean-up by derivatization and extraction of lyophilic samples. *J Chromatogr Biomed Appl.* 1993;671:181-189.

17 Kema IP, de Vries EG, Slooff MJ, Biesma B, Muskiet FA. Serotonin, catecholamines, histamine, and their metabolites in urine, platelets, and tumor tissue of patients with carcinoid tumors. *Clin Chem.* 1994;40:86-95.

18 Jager PL, Meijer WG, Kema IP et al. L-3-[123I]Iodo-alpha-methyltyrosine scintigraphy in carcinoid tumors: correlation with biochemical activity and comparison with [111In-DTPA-D-

Phe1]-octreotide imaging. *J Nucl Med.* 2000;41:1793-1800.

19 Duet M, Sauvaget E, Petelle B et al. Clinical impact of somatostatin receptor scintigraphy in the management of paragangliomas of the head and neck. *J Nucl Med.* 2003;44:1767-1774.

20 Erickson D, Kudva YC, Ebersold MJ et al. Benign paragangliomas: clinical presentation and treatment outcomes in 236 patients. *J Clin Endocrinol Metab.* 2001;86:5210-5216.

21 Kwekkeboom DJ, van Urk H, Pauw BK et al. Octreotide scintigraphy for the detection of paragangliomas. *J Nucl Med.* 1993;34:873-878.

22 Muros MA, Llamas-Elvira JM, Rodriguez A et al. 111In-pentetreotide scintigraphy is superior to 123I-MIBG scintigraphy in the diagnosis and location of chemodectoma. *Nucl Med Commun.* 1998;19:735-742.

23 Erickson D, Kudva YC, Ebersold MJ et al. Benign paragangliomas: clinical presentation and treatment outcomes in 236 patients. *J Clin Endocrinol Metab.* 2001;86:5210-5216.

24 Kwekkeboom DJ, van Urk H, Pauw BK et al. Octreotide scintigraphy for the detection of paragangliomas. *J Nucl Med.* 1993;34:873-878.

25 van Houtum WH, Corssmit EP, Douwes Dekker PB et al. Increased prevalence of catecholamine excess and phaeochromocytomas in a well-defined Dutch population with SDHD-linked head and neck paragangliomas. *Eur J Endocrinol.* 2005;152:87-94.

26 Erickson D, Kudva YC, Ebersold MJ et al. Benign paragangliomas: clinical presentation and treatment outcomes in 236 patients. *J Clin Endocrinol Metab.* 2001;86:5210-5216.

27 Koopmans KP, de Vries EG, Kema IP et al. Staging of carcinoid tumours with 18F-DOPA PET: a prospective, diagnostic accuracy study. *The Lancet Oncology.* 2006;7:728-734.

28 Brink I, Schaefer O, Walz M, Neumann HP. Fluorine-18 DOPA PET imaging of paraganglioma syndrome. *Clin Nucl Med.* 2006;31:39-41.

29 Hoegerle S, Ghanem N, Altehoefer C et al. 18F-DOPA positron emission tomography for the detection of glomus tumours. *Eur J Nucl Med Mol Imaging.* 2003;30:689-694.

30 Ilias I, Yu J, Carrasquillo JA et al. Superiority of 6-[18F]-fluorodopamine positron emission tomography versus [131I]-metaiodobenzylguanidine scintigraphy in the localization of metastatic pheochromocytoma. *J Clin Endocrinol Metab.* 2003;88:4083-4087.

31 Timmers HJ, Kozupa A, Chen CC et al. Superiority of fluorodeoxyglucose positron emission tomography to other functional imaging techniques in the evaluation of metastatic SDHB-associated pheochromocytoma and paraganglioma. *J Clin Oncol.* 2007;25:2262-2269.

32 van Essen M., Krenning EP, Kooij PP et al. Effects of therapy with [177Lu-DOTA0, Tyr3]octreotate in patients with paraganglioma, meningioma, small cell lung carcinoma, and melanoma. *J Nucl Med.* 2006;47:1599-1606.

Chapter eight

Summary

SUMMARY AND FUTURE PERSPECTIVES

Optimal imaging of neuroendocrine tumors can support patient tailored therapy. Several imaging techniques are available for this purpose, including both morphologic techniques (such as CT or MR) and nuclear medicine techniques. Recently new PET tracers have been developed which take advantage of the metabolic properties of neuroendocrine tumors. The aim of this thesis was to evaluate new tracers for the detection and characterization of neuroendocrine tumors with an emphasis on the metabolic PET tracers ^{18}F-Dihydroxyphenylalanine (^{18}F-DOPA) and ^{11}C-5-hydroxytryptophan (^{11}C-5-HTP).

In **chapter 2** a literature review is presented in which an extensive overview is given of the currently used classical and new metabolic nuclear medicine techniques for the detection of neuroendocrine tumors. This chapter starts by describing the mechanisms, which are responsible for the uptake of these tracers. Thereafter, results of the clinical application of these tracer methods are presented for different neuroendocrine tumor types. With Forest plots, the sensitivities of the different tracers per tracer and tumor type are presented. From these pooled results it becomes clear that the metabolic imaging methods, such as ^{18}F-DOPA PET and ^{11}C-5-HTP PET, have a significantly better sensitivity for the detection of neuroendocrine tumors as compared to the currently used somatostatin receptor scintigraphy (SRS). We concluded therefore that these metabolic PET tracers are very promising, and an indication on their place in algorithms is growing for some NE subtypes, but more studies are needed to better define their precise place in the work-up and follow up of patients with neuroendocrine tumors.

The aim of the study described in **chapter 3** was to test the diagnostic sensitivity of 6-^{18}F-DOPA PET in patients with carcinoid disease. Currently, SRS and morphological imaging (CT, MRI, ultrasound, etc.) are used for the detection of carcinoid tumors. However, these methods have a low sensitivity for the detection of carcinoid tumor lesions. To establish the optimal treatment options for these patients it is essential to know where carcinoid tumor lesions are located. From initial results in smaller studies it has become clear that ^{18}F-DOPA is a tracer with a high potential for the detection of neuroendocrine tumor lesions. In this study the diagnostic sensitivity of ^{18}F-DOPA PET with oral carbidopa pre-treatment was therefore tested in a prospective single center diagnostic accuracy study. ^{18}F-DOPA PET was compared with conventional imaging methods, consisting of SRS and CT.

A group of 53 patients with a metastatic carcinoid tumor was studied. Analysis was performed on a patient, regional and lesional level. PET/CT images were fused to improve localization. Results of cytological and histological findings, all imaging tests, including secondary evaluations for newly found lesions, follow-up and biochemical data served as a composite reference standard.

In a patient based analysis ^{18}F-DOPA PET had a sensitivity of 100% (95%CI 93 – 100), SRS of 93% (95%CI 82 - 98), CT of 87% (95%CI 75 - 95) and the combination of SRS and CT 96% (95%CI 87 - 100) (P=0.45 for PET versus SRS with CT). However, ^{18}F-DOPA PET alone detected

many more lesions, more positive regions and more lesions per region than SRS combined with CT. In regional analysis sensitivity of ^{18}F-DOPA PET was 95% (95%CI 90- 98) versus 66% (95%CI 57 - 74) for SRS alone, 57% (95%CI 48 - 66) for CT and 79% (95%CI 70 - 86) for SRS with CT (P=0.0001, PET versus SRS with CT). In individual lesion analysis, sensitivities were 96% (95%CI 95 - 98), 46% (95%CI 43 - 50), 54% (95%CI 51 - 58) and 65% (95%CI 62 - 69) for PET, SRS, CT and SRS with CT respectively (P<0.0001 for PET versus SRS with CT).

From the results of this study it was concluded that ^{18}F-DOPA PET significantly improves the detection rate of carcinoid tumors and their metastases. ^{18}F-DOPA PET was able to detect an additional tumor positive region in 1 out of 3 patients with an average of 4 additional lesions per patient as compared with the combination of SRS and CT. Combining PET with CT led to some further increase in the number of lesions detected, but the main advantage of this combination is that addition of CT improves the anatomical localization of lesions.

Chapter 4 describes a carcinoid tumor patient with extensive liver metastases and a high catecholamine production by the tumor. This patient developed a carcinoid crisis upon rapid intravenous injection of ^{18}F-DOPA. Symptoms started approximately 3 minutes after injection of ^{18}F-DOPA and consisted of erythema, severe vomiting, shortness of breath and other symptoms. These complaints slowly disappeared approximately 10 minutes after the intravenous administration of the antihistamine clemastine. She was able to continue the scanning procedure. Afterwards blood and urine samples were collected to evaluate for histamine, catecholamine and serotonin metabolites. These values were compared with the blood and urine samples collected just prior to the PET scan.

We concluded from these data that the rapid tracer injection of ^{18}F-DOPA had resulted in a massive serotonin release by the tumor, which had resulted in a carcinoid crisis. Based on this finding we recommend that patients with carcinoids should receive ^{18}F-DOPA as a slowly administered intravenous injection, in order to avoid the development of a carcinoid crisis. Furthermore, somatostatin analogs and ketanserin should be at hand in the scanning facility to treat this condition immediately when it develops.

The study described in **chapter 5** evaluated the diagnostic sensitivity of PET scanning in patients with a carcinoid or islet cell tumor with the tracers ^{11}C-5-HTP, a precursor of the serotonin pathway, in direct comparison with the catecholamine precursor^{18}F-DOPA. Only recently the synthesis of ^{11}C-5-HTP has become operational for clinical use in our institution, as the second institution worldwide. The synthesis of this tracer has been developed in Uppsala, Sweden, which has been the only place where this tracer was available worldwide. From the Swedish results with this tracer in patients with neuroendocrine tumors, it became clear that ^{11}C-5-HTP is superior to SRS imaging and CT for the detection of numerous neuroendocrine tumor types, including foregut and islet cell tumors. However, no comparison has been made between ^{18}F-DOPA and ^{11}C-5-HTP PET scanning in patients with neuroendocrine tumors thus far. A total of 24 patients with a carcinoid tumor and 23 patients with a pancreatic islet cell

tumor were included. All patients had at least one lesion detected on conventional imaging and underwent ^{11}C-5-HTP PET, ^{18}F-DOPA PET, SRS and CT scan.

^{18}F-DOPA PET and ^{11}C-5-HTP PET showed more carcinoid tumor positive regions than SRS, as ^{18}F-DOPA PET sensitivity was 81%, and ^{11}C-5-HTP PET sensitivity was 77% Sensitivity of SRS was 58% (P=0.001 and 0.0004 for comparison with SRS respectively) and CT 70% (P=ns for the comparison of both PET scans with CT). In islet cell tumors ^{11}C-5-HTP PET detected more tumor positive regions (sensitivity 70%) than ^{18}F-DOPA PET (sensitivity 44%, P= 0.0001 for the comparison of ^{11}C-5-HTP PET with ^{18}F-DOPA PET). In carcinoid patients, both ^{11}C-5-HTP PET and ^{18}F-DOPA PET revealed more tumor positive lesions (sensitivity 78% and 87%) then SRS (sensitivity 49%, $P\leq$ 0.001 for the comparison of both ^{11}C-5-HTP PET and ^{18}F-DOPA PET with SRS) in carcinoid patients.

From these results we concluded that for carcinoid tumors ^{18}F-DOPA PET is superior to SRS and CT for the detection of carcinoid tumor lesions. ^{11}C-5-HTP PET has a better lesion detection capability than SRS and CT for carcinoid tumors, but is not as good as ^{18}F-DOPA PET. However, for the detection of islet cell tumors, ^{11}C-5-HTP PET is superior to SRS and ^{18}F-DOPA PET. CT detects an equal number of lesions as ^{11}C-5-HTP PET, but is complementary to ^{11}C-5-HTP PET. For staging patients with either carcinoid or pancreatic islet cell tumors, the combination of PET with CT combines anatomical localization with functional characterization and results in the best currently possible staging of patients.

Chapter 6 describes the study on the application of ^{18}F-DOPA PET in medullary thyroid cancer patients. In patients with recurrent disease after resection of the primary tumor, localization of tumor metastasis is essential. Surgery is the only curative treatment option for these patients. However, the currently used methods consisting of ^{18}F-deoxyglucose PET (^{18}FDG PET), ^{99m}Tc-V-di-mercapto-sulphuric acid (DMSA) and the morphologic imaging methods have a low sensitivity for the detection of recurrent medullary thyroid tumor lesions. Therefore we compared the new PET tracer ^{18}F-DOPA with the currently used imaging methods for medullary thyroid carcinoma to establish whether this new method is better able to detect recurrent medullary thyroid carcinoma. Calcitonin, carcino-embryonic antigen (CEA) and Chromogranin-A are used as tumor markers for the detection of recurrent medullary thyroid carcinoma. In case of elevated tumor markers surgery may be indicated but medullary thyroid carcinoma is often difficult to detect. We examined the value of ^{18}F-DOPA PET compared to ^{18}FDG PET, DMSA scintigraphy and morphologic imaging methods (MRI and/or CT) for the detection of medullary thyroid carcinoma in this patient group. Secondary aim was to evaluate whether there was a relation between tumor markers and imaging results.

We included 21 patients with biochemical evidence of medullary thyroid carcinoma as characterized by rising CEA, calcitonin or Chromogranin-A. Patients underwent ^{18}F-DOPA PET, ^{18}FDG PET, ^{99m}Tc-V-DMSA scintigraphy and morphologic imaging (CT or MRI). Patient- and lesion based sensitivities were calculated using a composite reference consisting of all imaging

modalities and, when available, histology. Imaging results were compared with biochemical markers consisting of Chromogranin-A, calcitonin and CEA. The calcitonin and CEA doubling times were calculated as markers for tumor dedifferentiation. The imaging findings were validated by histology when available or with other imaging studies during clinical follow-up.

In 15 patients with positive imaging results, ^{18}F-DOPA PET detected 13 (sensitivity 62%, with 4.6 lesions per patient [lpp]), morphologic imaging (n=19) was positive in 7 (sensitivity 37%, 4.7 lpp), DMSA (n=18) in 5 (sensitivity 28%, 1.1 lpp) and ^{18}FDG PET (n=17) in 4 (sensitivity 24%, 1.6 lpp). In a lesion based analysis ^{18}F-DOPA PET detected 95 of 134 lesions (sensitivity 71%), morphologic imaging 80 of 126 (sensitivity 64%), DMSA 20 of 108 (sensitivity 19%) and ^{18}FDG PET 48 of 102 (sensitivity 30%). In 2 of 3 patients with a calcitonin/CEA doubling time of $\leq$12 months ^{18}FDG PET performed better than ^{18}FDOPA PET, in the third patient ^{18}FDG PET was not performed. However, in 6 out of 8 patients with a calcitonin level < 500 ng/L imaging results were negative.

We concluded that in patients with well-differentiated medullary thyroid carcinomas, with a characteristically slow calcitonin doubling time (>12 months), ^{18}F-DOPA PET seems to be superior to ^{18}FDG PET, DMSA and morphologic imaging studies. Dedifferentiated tumors are characterized by short calcitonin doubling times (< 12 months). In these tumors, ^{18}FDG PET may be the best imaging method for staging medullary thyroid carcinoma, but there were only 3 patients. Calcitonin levels $\leq$ 500 ng/l are associated with a small tumor mass resulting in negative imaging results in 88% of the patients.

The aim of the study described in **chapter 7** is to establish the value of SRS and MIBG for the detection of head and neck paragangliomas. Head and neck paragangliomas are rare tumors and until now only small studies have been published in which the value of either SRS and/or MIBG was evaluated. In this relatively large study, a homogeneous group of patients with a head and neck paraganglioma is studied. Additionally, plasma and urinary catecholamines and their metabolites were determined to evaluate a possible relationship between tumoral hormonal activity and imaging results.

Twenty nine consecutive patients (F:M 17:12) with suspected or recurrent head and neck paraganglioma were included. Morphologic imaging as well as SRS imaging was positive in 27 patients (sensitivity of 93%, 95% CI 77-98%), whereas MIBG was positive in 13 patients (44%, 95% CI 23-61%). On a lesion-based analysis, morphologic imaging detected 31 lesions (sensitivity 82%, 95% CI 65-92%), SRS 34 (89%, 95% CI 75-97%) and MIBG 15 lesions (42%, 95% CI 26-59%). SRS was superior to MIBG (P=0.0001). SRS detected an unknown carcinoid tumor in 2 patients; MIBG detected an additional adrenal pheochromocytoma in 1 patient. Elevated urinary metanephrine and/or normetanephrines excretion was found in 6 patients. The number of lesions on SRS and MIBG correlated with metanephrine and/or normetanephrines excretion (P=0.005 and P=0.02 respectively).

From these data we concluded that SRS is superior to MIBG, but equal to morphologic

imaging for the detection of head and neck paraganglioma. SRS is of clinical significance for a better characterization of head and neck paraganglioma and may be useful to detect additional but previously unknown neuroendocrine tumors. Our study suggests that MIBG imaging should be restricted to those patients in whom a concomitant (adrenal) pheochromocytoma is suspected.

FUTURE PERSPECTIVES

The studies described in this thesis show that the use of the metabolic PET tracers ^{18}F-DOPA and ^{11}C-5-HTP considerably improve staging of neuroendocrine tumors. We found that for carcinoids ^{18}F-DOPA PET is superior to the combination of SRS and CT, which is the current standard (chapter 2, 3 and 5). An explanation for the high uptake of these tracers is a high metabolic need of neuroendocrine tumor cells for precursors, which results in overexpression of large amino acid transporters (LAT) on the cellular membrane.

Studies performed sofar by others and by ourselves have only included patients with known metastatic neuroendocrine tumors.(*1-4*) ^{18}F-DOPA PET and ^{11}C-5-HTP PET are very powerful tools for the detection of neuroendocrine tumors. Their value in new patients who are suspected of a neuroendocrine tumor however still has to be formally analyzed. Most likely the sensitivity of these scans will be good. For further studies however also the risk of false positive scans in case of uncertainty concerning neuroendocrine disease has to be determined.

In addition new tracer developments are continuously taking place. Somatostatin analogs for example, can now been labeled with positron emitting isotopes.[5-8] Thus far published results are very good, but no comparison is yet being made with metabolic PET tracers. This would be a fair comparison, since both tracers can profit from the increased resolution of PET camera systems. A comparison of metabolic and receptor based approaches is not only interesting for determining which method gives the best tumor detection, but this would also give insight in inter as well as intra-patient heterogeneity of receptor expression and metabolic activity within tumor lesions.

For the individual assessment of imaging and treatment options in patients with neuroendocrine tumors, knowledge of the biologic behavior of the tumor might become essential. As we have shown in chapter 5, dedifferentiation of neuroendocrine tumors leads to an increase in glucose metabolism. Dedifferentiation in neuroendocrine tumors will likely result in the loss of their ability to synthesize complex peptides.[9] Instead, these dedifferentiated tumors will show a higher glucose need to satisfy the increased tumoral energy hunger. Repeated biochemical testing prior to imaging might give an idea of the differentiation grade of the tumor involved. This knowledge will help the clinician in assessing which imaging method should be chosen for the individual patient, or conversely, scanning results may give an idea of tumor

type and differentiation. New targeted drug therapies for neuroendocrine tumors are currently being developed. Until now, no nuclear medicine techniques have been exploited to test their value for drug treatment monitoring in neuroendocrine tumors. The superior lesion detection of ^{18}F-DOPA PET and ^{11}C-5-HTP PET which visualize metabolic activity makes these methods very good candidates for the evaluation of therapy response of neuroendocrine tumors.

In this thesis it has been clearly shown that ^{18}F-DOPA PET and ^{11}C-5-HTP PET are superior compared to SRS for staging patients with neuroendocrine tumors. There are many possible new indications for the use of these tracers, ranging from staging patients with neuroblastoma to the follow-up of patients with hereditary MEN syndromes. However, new tracers for the detection of neuroendocrine tumors are developed, which include receptor based tracers for PET imaging such as ^{68}Ga-DOTA-Tyr3-octreotide. Therefore, head to head comparisons between metabolic imaging methods and receptor based imaging methods for the detection of neuroendocrine tumors are warranted in the near future.

REFERENCES

1. Hoegerle S, Altehoefer C, Ghanem N et al. Whole-body 18F dopa PET for detection of gastrointestinal carcinoid tumors. *Radiology.* 2001;220:373-380.
2. Hoegerle S, Altehoefer C, Ghanem N et al. 18F-DOPA positron emission tomography for tumour detection in patients with medullary thyroid carcinoma and elevated calcitonin levels. *European journal of nuclear medicine.* 2001;28:64.
3. Orlefors H, Sundin A, Garske U et al. Whole-body (11)C-5-hydroxytryptophan positron emission tomography as a universal imaging technique for neuroendocrine tumors: comparison with somatostatin receptor scintigraphy and computed tomography. *J Clin Endocrinol Metab.* 2005;90:3392-3400.
4. Becherer A, Szabo M, Karanikas G et al. Imaging of Advanced Neuroendocrine Tumors with (18)F-FDOPA PET. *J Nucl Med.* 2004;45:1161-1167.
5. Hofmann M, Maecke H, Borner R et al. Biokinetics and imaging with the somatostatin receptor PET radioligand (68)Ga-DOTATOC: preliminary data. *Eur J Nucl Med.* 2001;28:1751-1757.
6. Pettinato C, Sarnelli A, Di DM et al. (68)Ga-DOTANOC: biodistribution and dosimetry in patients affected by neuroendocrine tumors. *Eur J Nucl Med Mol Imaging.* 2007;.
7. Seemann MD. Detection of metastases from gastrointestinal neuroendocrine tumors: prospective comparison of 18F-TOCA PET, triple-phase CT, and PET/CT. *Technol Cancer Res Treat.* 2007;6:213-220.
8. Win Z, Al-Nahhas A, Rubello D, Gross MD. Somatostatin receptor PET imaging with Gallium-68 labeled peptides. *Q J Nucl Med Mol Imaging.* 2007;51:244-250.
9. Timmers HJ, Kozupa A, Chen CC et al. Superiority of fluorodeoxyglucose positron emission tomography to other functional imaging techniques in the evaluation of metastatic SDHB-associated pheochromocytoma and paraganglioma. *J Clin Oncol.* 2007;25:2262-2269.

Chapter nine

Nederlandse samenvatting

NEDERLANDSE SAMENVATTING, CONCLUSIE EN VOORUITBLIK

Om patiënten met neuroendocriene tumoren zo goed mogelijk te kunnen behandelen is optimale beeldvorming nodig. Er zijn verschillende beeldvormende technieken beschikbaar voor dit doel. Er zijn grofweg twee soorten beeldvormingstechnieken: anatomische met behulp van röntgenologische technieken zoals CT of MRI en functionele afbeeldingstechnieken zoals de nucleaire geneeskunde levert dwz PET en SPECT. Neuroendocriene tumoren produceren vaak allerlei stoffen, zoals serotonine en dopamine. Recent zijn er voor neuroendocriene tumoren nieuwe tracers ontwikkeld voor gebruik met PET camera's. Deze tracers kunnen door neuroendocriene tumoren gebruikt worden als bouwstof voor de productie van deze hormonen en hormoon achtige stoffen In dit proefschrift worden de metabole PET tracers ^{18}F-Dihydroxyphenylalanine (^{18}F-DOPA) en ^{11}C-5-hydroxytryptophan (^{11}C-5-HTP) geëvalueerd voor gebruik bij het opsporen van neuroendocriene tumoren.

In **Hoofdstuk 2** wordt op basis van literatuur onderzoek een overzicht gegeven over de huidige stand van zaken met betrekking tot klassieke en nieuwe metabole tracer methoden voor het opsporen van neuroendocriene tumoren. In dit hoofdstuk wordt een overzicht gegeven van de mechanismen achter de opname van deze tracers, gevolgd door een overzicht van de toepasbaarheid van deze tracers bij de verschillende subtypen van neuroendocriene tumoren. De sensitiviteit van de verschillende tracers wordt per tracer en per tumor grafisch weergegeven middels Forest Plots. Uit deze analyse volgt dat de metabole tracers ^{18}F-DOPA ^{11}C-5-HTP beter presteren dan de standaard gebruikte octreotide scan voor het opsporen van neuroendocriene tumoren. Concluderend stellen we dan ook dat deze tracers in de toekomst waarschijnlijk een grote rol zullen gaan spelen, zowel voor het stadieren als voor de follow-up, van patiënten met neuroendocriene tumoren .

In **hoofdstuk 3** wordt de studie beschreven waarin de waarde van ^{18}F-DOPA PET voor het opsporen van carcinoid tumoren wordt onderzocht. Voor de detectie van carcinoid tumoren wordt in de kliniek gebruik gemaakt van de octreotide scan en CT. Deze twee technieken hebben echter een lage sensitiviteit voor het opsporen van deze tumoren, of met andere woorden, deze technieken missen tumorhaarden. Uit andere studies in kleine groepen patiënten was al bekend dat ^{18}F-DOPA PET een hoge sensitiviteit heeft voor het opsporen van carcinoid tumorhaarden in patiënten. Daarom hebben wij in deze prospectieve studie de sensitiviteit van ^{18}F-DOPA PET onderzocht in een groep van 53 patiënten met een gemetastaseerd carcinoid. Al onze patiënten werden voorbereid met carbidopa om de beeldkwaliteit te verbeteren. ^{18}F-DOPA PET werd vergeleken met de octreotide scan en CT. We hebben de resultaten geanalyseerd op 3 niveaus; namelijk op patiënt niveau, regio niveau en op het niveau van de tumorhaarden. Voor het verifieren van gevonden haarden gebruikten we een samengestelde gouden standaard. Deze bestaat uit de resultaten van alle verschillende scans, histologie en follow-up. Bij de analyse op patiënt nivo wordt

gekeken of een techniek in een patiënt tumor aan kan toenen. Bij een regioanalyse, wordt er gekeken hoeveel (van te voren gedefinieerde) regio's per techniek tumorpositief zijn. En tot slot, bij de lesie analyse, wordt per techniek beoordeeld welke techniek de meeste tumorhaarden kan aantonen.

Bij analyse op patient niveau, vonden we een sensitiviteit van 100% (95%CI 93 – 100) voor ^{18}F-DOPA PET, 93% (95%CI 82 - 98) voor SRS, 87% (95%CI 75 - 95) voor CT en voor de combinatie van SRS en CT 96% (95%CI 87 - 100) ?) de analyse op patiënt niveau. ^{18}F-DOPA PET alleen detecteerde meer tumorpositieve regio's en laesies per regio dan de combinatie SRS met CT. In de regio analyse vonden we een sensitiviteit van 95% (95%CI 90-98) voor ^{18}F-DOPA PET versus 66% (95%CI 57 - 74) voor de SRS scan, 57% (95%CI 48 - 66) voor CT en voor de combinatie SRS met CT 79% (95%CI 70 – 86, P=0.0001, PET versus SRS plus CT). In de individuele laesie analyse werden sensitiviteiten van 96% (95%CI 95 - 98), 46% (95%CI 43 - 50), 54% (95%CI 51 - 58) en 65% (95%CI 62 - 69) voor PET, SRS, CT en SRS gecombineerd met CT respectievelijk (P<0.0001 voor PET versus SRS in combinatie met CT).

Uit de resultaten van onze studie concludeerden we dan ook dat ^{18}F-DOPA PET een significante verbetering oplevert voor het opsporen van carcinoid tumoren en hun metastasen ten opzichte van de huidige technieken. Ten opzichte van de combinatie van octreotide scan met CT, detecteerde ^{18}F-DOPA PET een extra tumor positieve regio in 1 op 3 patiënten. Daarbij werden gemiddeld 4 extra tot dan toe onbekende tumorhaarden per patiënt gevonden (oftewel gemiddeld 50% meer afwijkingen) met ^{18}F-DOPA PET. Als ^{18}F-DOPA PET gecombineerd wordt met CT, levert dat nog een kleine verbetering op van de sensitiviteit. Het grootste voordeel van deze combinatie is echter dat de tumorhaarden preciezer gelokaliseerd kunnen worden.

In **hoofdstuk 4** wordt een zeldzame reactie op injectie van ^{18}F-DOPA beschreven bij een patiënt met een uitgebreid gemetastaseerde carcinoidtumor. Na de intraveneuze bolusinjectie met ^{18}F-DOPA ontwikkelde deze patiënt een carcinoid crisis. De symptomen begonnen ongeveer 3 minuten na injectie en bestonden uit erythemateuze huidafwijkingen, heftig braken, kortademigheid en andere verschijnselen. Deze klachten verdwenen vervolgens na intraveneuze toediening van het antihistamicum clemastine. Gelukkig kon deze patiente daarna in goede conditie de scanprocedure alsnog afmaken. Na de scan werden bloed en urinemonsters onderzocht op histamine, catecholamine en serotonine afbraakproducten. De resultaten hiervan werden vergeleken met haar bloed en urine waarden van de monsters die 's ochtends voor de scan waren afgenomen.

De resultaten van het urine en bloedonderzoek wezen erop dat de snelle injectie van ^{18}F-DOPA een hele heftige uitstorting van serotonine uit de tumor tot gevolg had. Deze plotselinge uitstortingheeft geleid tot het ontstaan van de carcinoid crisis. Op basis van deze bevindingen adviseren wij om bij alle patiënten met carcinoid tumoren ^{18}F-DOPA langzaam in te spuiten om het ontstaan van een carcinoid crisis te voorkomen. Bovendien

is het aan te bevelen om somatostatine analoga en ketanserine op voorraad te hebben in de voorbereidingsruimte van PET centra waar ^{18}F-DOPA wordt toegediend aan patiënten met carcinoid tumoren om een eventueel ontstane carcinoid crisis adequaat te kunnen bestrijden.

In **Hoofdstuk 5** wordt de studie beschreven waarin de gevoeligheid van PET technieken wordt getest bij patiënten met een carcinoid of eilandjesceltumor. In deze studie werden de tracers ^{11}C-5-HTP (dit is een precursor voor de serotonine pathway) en ^{18}FDOPA met elkaar vergeleken. ^{11}C-5-HTP is pas recent in ons centrum beschikbaar gekomen voor klinisch gebruik, als tweede centrum wereldwijd. In Uppsala, Zweden, is de synthese van deze tracer oorspronkelijk ontwikkeld. Het is een moeilijke synthese. Uit Zweeds onderzoek met deze tracer blijkt dat deze tracer beter is dan de octreotide scan en de CT scan voor het opsporen van verschillende subtypen neuroendocriene tumoren, waaronder ook eilandjesceltumoren en carcinoiden. Tot nu toe is er nog geen vergelijkende studie gepubliceerd waarin ^{11}C-5-HTP en ^{18}FDOPA PET met elkaar werden vergeleken. Daarom hebben wij deze studie opgezet, waarin we ^{11}C-5-HTP en ^{18}FDOPA PET met elkaar vergeleken hebben bij 24 patiënten met een carcinoid tumor en 23 patiënten met een eilandjesceltumor.

^{11}C-5-HTP en ^{18}FDOPA PET detecteerden beide meer carcinoid tumor positieve regio's dan de octreotide scan. De sensitiviteit van ^{18}FDOPA PET was 81% en van ^{11}C-5-HTP 77%. De sensitiviteit van de octreotide scan was 58% (dit was significant slechter dan de ^{18}FDOPA PET en de ^{11}C-5-HTP PET, waarbij p=0.001 en respectievelijk p=0.0004 voor de vergelijking tussen PET scan en octreotide scan) en de sensitiviteit van de CT scan was 70% (p=niet significant voor de vergelijking tussen PET scans en CT). Bij eilandjesceltumoren lag dit anders, hier detecteerde de ^{11}C-5-HTP PET meer tumorpositieve regio's (sensitiviteit 70%) dan ^{18}FDOPA PET (sensitiviteit 44%, p=0.0001 voor de vergelijking tussen ^{11}C-5-HTP en ^{18}FDOPA PET).

Op basis van deze resultaten concludeerden wij dat voor het aantonen van carcinoid tumoren ^{18}FDOPA PET beter is dan de octreotide scan en de CT. ^{11}C-5-HTP PET is weliswaar beter dan de octreotide scan en de CT, maar is iets minder goed in staat carcinoid tumorhaarden op te sporen dan ^{18}FDOPA PET. Voor eilandjesceltumoren is ^{11}C-5-HTP PET superieur ten opzichte van de octreotide scan en ^{18}FDOPA PET. CT toont qua aantal wel evenveel eilandjescel tumorhaarden aan, maar is complementair, hetgeen wil zeggen dat de CT en de ^{11}C-5-HTP PET verschillende haarden aantonen. Daarom is zowel voor carcinoid tumoren als voor eilandjesceltumoren stadiering met de combinatie PET/CT optimaal. Dit combineert de anatomische informatie van de CT met de functionele informatie van de PET.

In **Hoofdstuk 6** wordt een studie beschreven waarin de waarde van ^{18}FDOPA PET voor het opsporen van recidief medullair schildkliertumor werd onderzocht. Het opsporen

van deze haarden is van groot belang omdat chirurgie de enige curatieve optie is voor deze patienten. De huidige technieken die hier tot nog toe voor gebruikt worden, bestaande uit de ^{18}F-deoxyglucose PET (^{18}FDG PET), ^{99m}Tc-V-di-mercapto-sulphuric acid (DMSA), octreotide, en radiologische technieken, maar deze hebben allen een vrije lage sensitiviteit voor het opsporen van recidief medullair schildkliercarcinoom. Als tumormarkers voor het aantonen van een recidief van het medullair schildklier carcinoom worden calcitonine, carcino-embryogeen antigen (CEA) en chromogranine A gebruikt. In deze studie werden ^{18}FDOPA PET, FDG PET, DMSA scintigrafie en CT of MRI met elkaar vergeleken voor het opsporen van recidief medullair schildkliercarcinoom bij patienten met verhoogde tumormarkers. Daarnaast wilden we onderzoeken of er een relatie bestond tussen tumormarkers en scan resultaten.

In onze studie werden 21 patienten geincludeerd die op grond van verhoogd calcitonine, CEA, en / of chromogranine A verdacht werden van een recidief medullair schildkliercarcinoom. De patienten kregen een ^{18}FDOPA PET, FDG PET, DMSA scintigrafie en CT of MRI. Voor deze patienten werden de sensitiviteiten van deze verschillende technieken berekend op patient en lesienivo. Hiervoor werd een composite referencestandard gebruikt, bestaande uit alle beeldvormende technieken bij elkaar, en indien beschikbaar, histologie. De resultaten van de beeldvormende technieken werden vergeleken met calcitonine, CEA, en chromogranine A spiegels. Daarnaast werden calcitonine en CEA verdubbelingstijden uitgerekend als maat voor tumor dedifferentiatie. Indien mogelijk werden de resultaten van beeldvorming vergeleken met histologie of met resultaten van beeldvorming uit de follow-up.

Bij 15 patienten werden met behulp van beeldvormende technieken afwijkingen verdacht voortumor gevonden. Van deze 15 patienten, detecteerde ^{18}F-DOPA PET 13 (sensitiviteit 62%, met 4.6 lesies per patient [lpp]), radiologische technieken (verricht in n=19 patienten) waren positief in 7 (sensitiviteit 37%, 4.7 lpp), DMSA (n=18) in 5 (sensitiviteit 28%, 1.1 lpp) en ^{18}FDG PET (n=17) in 4 (sensitiviteit 24%, 1.6 lpp). In de lesie analyse, detecteerde ^{18}F-DOPA PET 95 van in totaal 134 lesies (sensitiviteit 71%), radiologische technieken 80 van 126 (sensitiviteit 64%), DMSA 20 van 108 (sensitiviteit 19%) en ^{18}FDG PET 48 van 102 (sensitiviteit 30%). Bij 2 van de 3 patienten met een calcitonin/CEA verdubbelingstijd van $\leq$12 maanden, toonde ^{18}FDG PET een beter resultaat dan ^{18}FDOPA PET. Bij de derde patient was de ^{18}FDG PET niet verricht. Daarentegen werden in 6 van de 8 patienten met een calcitonin waarde van < 500 ng/L geen tumorhaarden gevonden met beeldvormende technieken.

Uit onze resultaten concludeerden wij dat bij patienten met een goed gedifferentieerd medullair schildkliercarcinoom, met een lange calcitonine verdubbelingstijd van >12 maanden, ^{18}FDOPA PET superieur is aan ^{18}FDG PET, DMSA scintigrafie en CT of MRI. Bij gedediffentieerd medullair schildkliercarcinoom (met als kenmerk een korte calcitonine verdubbelingstijd van <12 maanden) lijkt het erop dat ^{18}FDG PET de beste beeldvormende techniek is om deze

tumor te stadieren. Maar, deze groep bestond slechts uit 3 patienten. Bij patienten met een calcitonine <500 ng/l is de tumormassa waarschijnlijk te klein om met beeldvormende technieken opgespoord te kunnen worden.

In **Hoofdstuk 7** wordt de waarde van de octreotide scan en de ^{123}I-meta-iodo-benzylgyanidine (MIBG) scan onderzocht voor het opsporen van hoofd-hals paragangliomen. Paragangliomen in het hoofd- en halsgebied zijn zeldzame tumoren, en tot nu toe zijn er alleen studies verricht met kleine groepen patienten waarin de waarde van ofwel de octreotide scan ofwel de MIBG scan wordt onderzocht voor de detectie van deze tumoren. In deze studie met een relatief groot aantal patienten met hoofd/hals paragangliomen werd de waarde van de octreotide scan en de MIBG scan onderzocht voor het aantonen van tumorhaarden. Daarnaast werden plasma en urine catecholaminen en hun metabolieten bepaald om een eventuele relatie tussen tumorale hormoonproductie en scanresultaten te evalueren.

Er werden 29 opeenvolgende patienten (F:M 17:12) met verdenking op een hoofd/hals paraganglioom of een bewezen recidief geincludeerd. Radiologische beeldvorming (CT of MRI) en de octreotide scan waren positief in 27 patienten (sensitiviteit 93%, 95% confidence interval 77-98%), terwijl MIBG positief was in 13 patienten (44%, 95%CI 23-61%), In de analyse op lesie nivo detecteerden CT/MRI 31 lesies (sensitiviteit 82%, 95% CI 65-92%), de octreotide scan 34 (89%, 95% CI 75-97%) en de MIBG scan 15 lesies (42%, 95% CI 26-59%). De octreotide scan was significant beter dan de MIBG scan (P=0.0001). De octreotide scan toonde bij twee patienten een tot dan toe onbekende carcinoid tumor aan; de MIBG scan toonde een tot dan toe onbekend feochromocytoom aan bij 1 patient. Bij 6 patienten werden verhoogde urine metanefrine en of normetanefrine concentraties gevonden. Het aantal haarden op de octreotide en de MIBG scan correleerden met deze metanephrine en of normetanephrine excretie (p=0.005 en p=0.02 respectievelijk).

Wij concludeerden op basis van deze gegevens dat de octreotide superieur is aan de MIBG scan, maar gelijk is aan de CT/MRI voor het aantonen van hoofd/hals paragangliomen. Octreotide blijft klinisch belangrijk omdat het beter in staat is de tumor te karakterizeren als neuroendocrien. Ook kan het gebruik van de octreotide scan leiden tot het aantonen van tot dan toe onbekende andere neuroendocriene tumoren. Het gebruik van de MIBG scan lijkt beperkt tot patienten bij wie het vermoeden bestaat dat er ook een feochromocytoom in de bijnierregio aanwezig is.

Toekomstperspectieven

Uit de in deze thesis beschreven studies blijkt dat het gebruik van de metabole PET tracers ^{11}C-5-HTP en ^{18}FDOPA een aanzienlijke verbetering zijn voor het stadieren van neuroendocriene tumoren in vergelijking met de klassieke technieken. Bij carcinoiden blijkt de ^{18}FDOPA PET superieur te zijn aan huidige standaard, de combinatie van octreotide met CT scan (hoofdstukken 2, 3 en 5). Een verklaring voor de goede opname van deze metabole tracers zou oa kunnen zijn de grote behoefte aan precursors voor hormoon productie ten gevolge van de hoge productiesnelheid van hormonen, wat dan resulteert in overxpressie van onder andere de large amino acid transporters (LAT) op de celmembraan.

Bij de studies die tot nu toe verricht zijn door anderen en door onszelf zijn alleen patienten geincludeerd met bekende gemetastaseerde neuroendocriene tumoren. [1-4] ^{11}C-5-HTP PET en ^{18}FDOPA PET zijn echter waarschijnlijk uitstekende technieken om neuroendocriene tumoren op te sporen. De waarde van deze technieken in patienten waarbij er alleen een verdenking is op de aanwezigheid van een neuroendocriene tumor moet echter nog vastgesteld wroden. Zeer waarschijnlijk zullen ^{11}C-5-HTP en ^{18}FDOPA PET ook in deze patientencategorie uitstekend scoren, maar waarschijnlijk minder dan in bekende tumoren. Hele kleine tumoren kunnen ook met PET nog worden gemist. Ook het risico op fout-positieve uitslagen met deze technieken ten aanzien van neuroendocriene tumoren moet worden uitgezocht.

Er wordt voordurend gewerkt aan nieuwe tracers of verbeteringen in bestaande. Somatostatine analogen kunnen nu bijvoorbeeld ook gelabeld worden met positron emitterende isotopen.[5-8] Tot nu toe is er geen vergelijkende studie geweest waarin de metabole PET tracers ^{11}C-5-HTP en ^{18}FDOPA direct werden vergeleken met deze receptor tracers. Deze vergelijking zou een stuk eerlijker zijn dan de vergelijking met de gewone octreotide scan, omdat beide tracers dan gebruik maken van de superieure resolutie van de PET camera ten opzichte van de gamma camera. De vergelijking metabole tracers en receptor tracers is niet alleen interessant voor het vaststellen welke de beste techniek is voor het opsporen van neuroendocriene tumoren, maar ook om een inzicht te krijgen in de nog niet altijd even duidelijke relatie tussen receptor expressie en metabole activiteit, die ook nog mogelijk eens per haard zou kunnen varieren. van de verschillende tumorhaarden in de individuele patient, en dit te vergelijken met de metabole actiiviteit.

Voor het beoordelen van het nut van beeldvorming en het evalueren van behandelingsopties per patient, zal kennis van het biologische gedrag van de tumor essentieel worden. In hoofdstuk 6 hebben we aangetoond dat dedifferentiatie van neuroendocriene tumoren (in casu het medullair schildkliercarcinoom) leidt tot het verlies van de mogelijkheid om complexe eiwitten te maken.[9] Daarentegen zullen deze gedediffernetieerde tumoren een grotere glucose behoefte hebben om het verhoogde glucosemetabolisme van grondstoffen te kunnen voorzien. Herhaalde biochemische onderzoeken voordat beeldvormend onderzoek verricht wordt kan een idee geven over de mate van dedifferentiatie, om zo de keuze van de

optimale techniek te bepalen. Andersom, scan resultaten kunnen ook inzicht geven in het biologische gedrag van tumoren en zo leiden tot een betere individualisering van therapie.

Er wordt hard gewerkt aan de ontwikkeling van nieuwe middelen voor de behandeling van neuroendocriene tumoren. Tot nu toe zijn er echter nog geen nucleaire beeldvormende technieken die in staat zijn om het effect van deze medicatie bij neuroendocriene tumoren te evalueren. De uitstekende tumordetectie van ^{11}C-5-HTP en ^{18}FDOPA PET maakt dat deze technieken in potentie geschikt lijken te zijn voor het evalueren van therapierespons.

In dit proefschrift is aangetoond dat ^{11}C-5-HTP en ^{18}FDOPA PET superieur zijn ten aanzien van de octreotide scan voor het opsporen van neuroendocriene tumorhaarden. Er zijn veel nieuwe toepassingen te mogelijk voor deze technieken bij neuroendocrien tumoren. Mogelijke toepassingen kunnen varieren van bijvoorbeeld het opsporen van het neuroblastoom, tot de follow-up van patienten met erfelijke MET syndromen. Er worden echter steeds nieuwe tracers ontwikkeld, waaronder ^{68}Ga-DOTA-Tyr3-octreotide. Daarom zullen ook in de toekomst onderzoeken moeten worden verricht waarbij de metabole technieken (^{11}C-5-HTP en ^{18}FDOPA PET) worden vergeleken met de andere technieken.

REFERENCES

1. Hoegerle S, Altehoefer C, Ghanem N et al. Whole-body 18F dopa PET for detection of gastrointestinal carcinoid tumors. *Radiology*. 2001;220:373-380.
2. Hoegerle S, Altehoefer C, Ghanem N et al. 18F-DOPA positron emission tomography for tumour detection in patients with medullary thyroid carcinoma and elevated calcitonin levels. *European journal of nuclear medicine*. 2001;28:64.
3. Orlefors H, Sundin A, Garske U et al. Whole-body (11)C-5-hydroxytryptophan positron emission tomography as a universal imaging technique for neuroendocrine tumors: comparison with somatostatin receptor scintigraphy and computed tomography. *J Clin Endocrinol Metab*. 2005;90:3392-3400.
4. Becherer A, Szabo M, Karanikas G et al. Imaging of Advanced Neuroendocrine Tumors with (18)F-FDOPA PET. *J Nucl Med*. 2004;45:1161-1167.
5. Hofmann M, Maecke H, Borner R et al. Biokinetics and imaging with the somatostatin receptor PET radioligand (68)Ga-DOTATOC: preliminary data. *Eur J Nucl Med*. 2001;28:1751-1757.
6. Pettinato C, Sarnelli A, Di DM et al. (68)Ga-DOTANOC: biodistribution and dosimetry in patients affected by neuroendocrine tumors. *Eur J Nucl Med Mol Imaging*. 2007;.
7. Seemann MD. Detection of metastases from gastrointestinal neuroendocrine tumors: prospective comparison of 18F-TOCA PET, triple-phase CT, and PET/CT. *Technol Cancer Res Treat*. 2007;6:213-220.
8. Win Z, Al-Nahhas A, Rubello D, Gross MD. Somatostatin receptor PET imaging with Gallium-68 labeled peptides. *Q J Nucl Med Mol Imaging*. 2007;51:244-250.
9. Timmers HJ, Kozupa A, Chen CC et al. Superiority of fluorodeoxyglucose positron emission tomography to other functional imaging techniques in the evaluation of metastatic SDHB-associated pheochromocytoma and paraganglioma. *J Clin Oncol*. 2007;25:2262-2269.

Chapter ten

Dankwoord

DANKWOORD

De laatste loodjes... Het voor velen favoriete deel van dit proefschrift is nu aan de beurt om inhoud te krijgen. Ik heb met heel veel plezier aan dit promotieonderzoek gewerkt, vooral ook door de inzet van de vele betrokkenen. Dankzij de bijdrage van diverse afdelingen binnen en buiten het UMCG is het mogelijk geweest om zo'n groot aantal patiënten met een zeldzaam type tumor te motiveren om mee te doen aan dit onderzoek. Dat roept natuurlijk om een heel uitgebreid dankwoord... Ik vrees dat ik niet in staat zal zijn iedereen te bedanken die dit werk mogelijk heeft gemaakt, daarvoor waren er teveel mensen die hun steentje hebben bijgedragen. Weet dat dat niet met opzet is!!!

Om bij de basis te beginnen: zonder de donateurs en de collectanten van het KWF was er nooit een financiering geweest om dit project af te kunnen ronden.
Uiteraard wil ik ook alle patiënten die mee hebben gedaan aan de in dit boekje beschreven studies van harte bedanken!

Mijn promotoren. Allereerst Prof dr. P.L. Jager, oftewel Piet. Prof in de radiology, in Canada, wie had dat gedacht toen wij elkaar ontmoetten in 2003... Tijdens mijn studie had ik niet verwacht dat ik ooit zou promoveren, maar nu is het dan dankzij jou enthousiasme (bijna) zover. Ik heb altijd erg genoten van jouw heerlijk frisse blik op schrijven, data analyseren, PET scans beoordelen, etc. Ook het gemak waarmee ik bij je terecht kon met vragen, enthousiaste en minder enthousiaste verhalen heeft me altijd bijzonder vele plezier gedaan. Ook de huidige 6000 kilometer afstand tussen Groningen en Hamilton blijken geen enkel beletsel voor een heel plezierig contact. Zonder jou had ik niet op deze plek kunnen staan!
Prof dr E.G.E. de Vries, beste Liesbeth, ik heb je leren kennen als een zeer gedreven persoon met een warm hart. Je scherpe blik en kritische vragen werkten soms wel eens ontnuchterend, maar leidden altijd tot een beter resultaat. Je wist daarmee, vaak met revisies in recordtijd en soms ook vanaf unieke locaties, stukken te polijsten tot prachtproducten. Ik heb heel veel van je geleerd en ook heel veel aan je gehad met betrekking tot wetenschap bedrijven en alles wat zich daarom heen afspeelt.

Mijn Copromotoren. Dr. P.H. Elsinga, Beste Philip, jij was toch altijd min of meer de nuchtere noorderling binnen het project. Je zag de (on-)mogelijkheden en ging er rustig op af. Persoonlijk hebben wij wat minder met elkaar te maken gehad, indirect via Oliver des te meer. Ik ben je zeer erkentelijk voor alles wat je voor het project hebt gedaan.
Dr. I.P. Kema, Ido. Jij hebt ons allen altijd weer versteld laten staan door jou inzicht en kennis in de biochemie van neuroendocriene tumoren. We konden altijd bij je terecht met vragen over leuke biochemische puzzels. Ik heb altijd erg genoten van deze 'onderonsjes'!

En voor dit project onmisbaar: mijn partner in crime, Oliver Neels: zonder jou zou het nucleaire adagium "no tracer no fun" wel erg waar zijn geworden in dit project... Het unieke van dit project was toch wel de combinatie 'harde' scheikunde met 'softe' geneeskunde. Ik bewonder het dan ook zeer hoe jij je de wereld van de geneeskunde eigen hebt gemaakt in deze 4 jaar, zodat we nu allemaal als volwaardig gesprekspartner met elkaar in vloeiend Nederlands (!) over alle facetten rondom een nucleair geneeskundige afdeling kunnen praten.

De leden van de beoordelingscommissie: prof. dr. C.J. Lips, prof. dr. W.J.G. Oyen en prof. dr. M.J.H. Slooff dank ik voor het beoordelen van het proefschrift.
Dr. T.P.Links, beste Thera, het was altijd erg leuk zaken met je doen! Het is erg leuk om samen te werken met iemand die zo van haar vak houdt en dat ook weet uit te stralen.

Dr. R. Dullaart. Beste Robin, dankzij jou heb ik me kunnen verdiepen in een nog wat zeldzamer type neuroendocriene tumor, het paraganglioom. We hebben in een gezamenlijke eindspurt een mooi resultaat neergezet.

Dr. W.J. Sluiter, beste Wim, de statistiek is altijd in hele goede handen geweest bij jou! Ik heb er elke keer dat ik bij je kwam weer van genoten hoe jij, na een uiteenzetting van ons over onze data, daar weer met een heldere blik een mooie statistische analyse op los kon laten. Waar ik me nog altijd het meest over verwonder is hoe jij toch elke keer weer in staat bent om het juiste excelbestandje uit die lange lijst analyses in jouw computer te halen.

Dr. J. Th. Plukker, beste John, van jou heb ik geleerd hoe de chirurg naar het medullair schildkliercarcinoom kijkt. De hartelijke begroetingen van jouw heb ik altijd erg gewaardeerd! Van jou heb ik geleerd hoe je kort en bondig een METc aanvraag in elkaar draait met chirurgische precisie.

Drs. Koen Vanghillewe, beste Koen, ik heb veel geleed van alle CT's die we samen bestudeerd en herbeoordeeld hebben. Het was naast nuttig ook nog eens leuk!

Dr. C. Nijdam, beste Cees, via jou hebben we een hele andere toepassing van de FDOPA PET leren kennen; namelijk die voor kindertjes met congenitale persisterende hyperinsulinemie. Het was elke keer weer een uitdaging de scans van deze hele jonge patientjes te plannen en te coördineren, maar het was een heel leuk zijspoor!

Kamergenoten achtereenvolgens dr. A.H. Brouwers, dr. R.H.J.A. Slart, Liesbeth Ruytjens, en Simone Reinders. Allereerst Adrienne. Toen ik begon had ik de eer om een hoekje van jou bureau te mogen gaan gebruiken. Wie had toen gedacht dat jij het stokje van dit project ooit over zou nemen van Piet... Ik ben erg blij dat jij dit project voortzet!
Riemer, ja, wij zullen nog steeds eens samen gaan touren op de motor, he? Ik ben jouw uitnodiging niet vergeten! Na het kamertje van Adrienne verruilde ik dat kleine hoekje voor een iets groter hoekje in jouw kamer. Ik heb het verloop van de laatste fase van jouw promotie van dichtbij mogen meemaken en heb daar nu veel aan. Ik heb veel over de cardiologie geleerd tijdens onze gezamenlijke speurtochten naar mogelijkheden om de software naar onze hand te zetten.
Liesbethhelaas moest ik je promotie missen, maar de EANM was wel erg leuk... Simone, wij hebben slechts kort de kamer gedeeld. Vond het zeer plezierig.

Mijn opleiders. Prof dr R.A.J.O. Dierckx en dr J. Pruim. Beste Rudi, beste Jan, in plaats van werken aan mijn opleiding hebben jullie mij de mogelijkheid geboden mijn promotie onderzoek 'in de baas zijn tijd' af te ronden. Daar ben ik jullie heel erkentelijk voor!

Collega arts-assistenten. Beste Niels en Silvia, we zitten allemaal in hetzelfde schuitje. Ik heb mijn project nu afgerond, Silvia bijna en Niels, jij staat aan het begin van een leuk traject. Ik heb erg genoten van het onderzoekswerk. De combinatie met de opleiding was niet altijd even gemakkelijk. Vooral het me elke avond weer opnieuw opladen om de strijd met mijn laptop aan te gaan viel niet altijd mee. Maar, het is het waard geweest! Ik hoop dat ik jullie straks, als ik weer terug ben op onze afdeling, net zo kan steunen als jullie mij. Vooral ook bij die laatste loodjes!

Medewerkers NGMB. Oooh, wat zijn jullie met velen... Allereerst wil ik uiteraard Erna en Arja bedanken voor al het werk dat ze hebben gedaan om al die FDOPA, HTP en combinatie van beide in te plannen. Geweldig werk! Van groot belang zijn natuurlijk ook alle medewerkers van de radiofarmacie. Al die FDOPA en later HTP scans op soms gekke tijden heb ik toch aan jullie te danken. Tsja, zonder MNW-ers geen PET scan. Johan, Hans, Judith, Remco, Yvonne (2x), Sabine, Annemiek, Bregtsje, (sorry, als ik iemand van jullie vergeten heb ligt dat niet aan jullie inzet, maar aan mijn brein) jullie hebben allemaal geweldig werk verricht met al die FDOPA en HTP scans die vaak net allemaal wat anders verricht moesten worden. Uiteraard geldt dit ook voor alle MNW-ers van de SPECT kant. Aan jullie dank ik al die octreotide, Tc-V-DMSA en MIBG scans die voor de diverse projecten nodig waren. Clara, jij bent altijd een geweldige steun geweest, ook bij het mij op weg helpen op de afdeling!
Thys van der Molen. Beste Thys, ik weet niet of ik zonder jouw adviezen en de gesprekken met jou ooit aan dit promotie onderzoek zou zijn begonnen... Ik ben heel erg blij dat je mij over

de streep hebt weten te trekken! Ik vind het heel erg jammer dat je niet bij mijn promotie aanwezig kan zijn. Overigens, die gezamenlijke wandeling is me erg goed bevallen, dat moeten we nog eens overdoen.

Dr. Ir. Ing. J.J. Dijkstra, beste neefelijkheid, ook jou ben ik erg dankbaar voor jouw aanstekelijke woorden met betrekking tot promotieonderzoek. Ik heb ook altijd erg genoten van jouw verhalen en ervaringen over je onderzoek met betrekking tot het gedrag van vliegas in de bodem (niet dat ik er nu veel van snap, als jij dat maar doet). In mei ben jij gepromoveerd, nu ben ik aan de beurt.

Wil Snitjer: beste Wil, eindelijk een plaats waar ik je toepasselijk kan danken voor alle hulp! Tijdens dit promotieonderzoek heb ik veel profijt gehad van de adviezen en verhalen mbt onze hobby, modelvliegen/bouwen etc. Dankzij jouw hulp heb ik slechts weinig crashes mee hoeven maken van mijn helivloot. Het wordt weer tijd voor het geluid van kleine verbrandingsmotortjes, turbines en klappende rotors. En ooit moet mijn volgende project ingevlogen worden!

Paranimfen. Beste Jeroen, we hebben veel samen beleefd en gedaan. Ik heb altijd erg genoten van onze gesprekken tijdens keuzeprojecten, het ontwikkelen van foto's, tutorgroepen, etentjes, feestjes, halklim-uren, als chauffeur, etc. Ik vind het erg fijn dat je mijn paranimf wil zijn!
Beste Ali, we zijn tegelijk begonnen in het UMCG, jij als AIOS nucleaire, ik als arts-onderzoeker nucleaire geneeskunde. Ik heb bewondering voor wat jij allemaal hebt gedaan en hebt meegemaakt in je leven. Heb altijd genoten van onze gezamenlijke lunches en onze gezamenlijke uitstapjes. Je bent een geweldige kerel en ik ben dan ook erg blij dat jij mij wil bijstaan als paranimf.

Familie
Zonder jullie steun was dit project lang zo leuk niet geweest. Ik weet 't, mijn congresbezoekjes waren erg inspannend voor jou, Arrienne. En elke keer mijn zwijgen maar weer moeten accepteren als ik weer eens achter de laptop kroop. Ja, erg spraakzaam word ik niet van schrijven... Alleen met 3 van die schatjes, alles mogen opknappen en ondertussen je eigen praktijk blijven runnen. Ik heb ontzettend veel bewondering voor deze prestatie! Ook nu, nu ik van die lange dagen maak in het Martini Ziekenhuis weet je toch het gezin draaiende te houden en de ukjes op tijd van eten te voorzien. Simon, Sophie en Sarah, wat zijn jullie toch een schatjes... Ik weet 't ukjes, jullie vinden het maar niks als papa of mama weer eens achter de computer kruipt om zogenaamd nuttige dingen te doen in plaats van met jullie te bouwen, rennen, tekenen wat dan ook. Gelukkig heb ik dít project af en heb ik nu in de weekenden een excuus minder om *niet* met jullie te spelen!

Chapter eleven

Curriculum Vitae

CURRICULUM VITAE

Klaas Pieter Koopmans was born on 11 mei 1973 in LeeuwardenHe grew up in a small village in Friesland, Ferwerd. In 1991 graduated at the Gymnasium in Leeuwarden. Thereafter he moved to Gent for three years to study medicine at the Rijks Universiteit Gent (RUG) In 1997 his father died suddenly. 2000 was a busy year: he married with Arrienne in august, october 26th he graduated in medicine (just two hours after buying their current house) and november 12 Simon was born.

In februari 2001 he started working in the Delfzicht hospital in Delfzijl. This was followed by a major switch later that year: just after the terrible events of September 9th 2001, he started a training to become a professional pilot (ATPL). In October 19, 2002 their second child was born: Sophie. Due to circumstances, Klaas Pieter was forced to stop the ATPL training to think nuclear and to apply a PhD project. Thys van der Molen and Joris Dijkstra made this choice a lot easier and thanks to them started in october 2003 as a research physicion on the KWF project "Metabolic characterization of Neuroendocrine tumors" which led to this these. September 9 2004 3rd child, Sarah, was born. A new phase in life started Oktober 1st, 2006

Klaas Pieter Koopmans, november 2007

Chapter twelve

List of publications

PUBLICATIONS

van Assen S, Houwerzijl EJ, van den Dungen JJ, **Koopmans KP**. Vascular graft infection due to chronic Q fever diagnosed with fusion positron emission tomography/computed tomography. J Vasc Surg. 2007 Aug;46(2):372.

Neels OC, Jager PL, **Koopmans KP**, et al. Development of a reliable remote-controlled synthesis of β-$^{[11C]}$-5-hydroxy-L-tryptophan on a Zymark robotic system. J Labelled Comp Radiopharm 49:889-895, 2006

Jager PL, **Koopmans KP**, de Vries EG. [Gastroenteropancreatic neuroendocrine tumours (carcinoid tumours): definition, clinical aspects, diagnosis and therapy]
Ned Tijdschr Geneeskd. 2006 Oct 28;150(43):2401-3; author reply 2403.

Mohnike K, Blankenstein O, Christesen HT, De Lonlay J, Hussain K, **Koopmans KP**, Minn H, Mohnike W, Mutair A, Otonkoski T, Rahier J, Ribeiro M, Schoenle E, Fékété CN. Proposal for a standardized protocol for 18F-DOPA-PET (PET/CT) in congenital hyperinsulinism. Horm Res. 2006;66(1):40-2.

Slart RH, **Koopmans KP**, Gunneweg P, Luijckx GJ, de Jong BM. Persistent aseptic meningitis due to post-surgical spinal CSF leakage: value of fused (111m)In-DTPA SPECT-CT cisternography. Eur J Nucl Med Mol Imaging. 2006 Jul;33(7):856.

Koopmans KP, de Vries EG, Kema IP, Elsinga PH, Neels OC, Sluiter WJ, van der Horst-Schrivers AN, Jager PL. Staging of carcinoid tumours with 18F-DOPA PET: a prospective, diagnostic accuracy study. Lancet Oncol. 2006 Sep;7(9):728-34.

Jager PL, de Korte MA, Lub-de Hooge MN, van Waarde A, **Koopmans KP**, Perik PJ, de Vries EG. Molecular imaging: what can be used today. Cancer Imaging. 2005 Nov 23;5 Spec No A: S27-32.

Koopmans KP, Brouwers AH, De Hooge MN, Van der Horst-Schrivers AN, Kema IP, Wolffenbuttel BH, De Vries EG, Jager PL. Carcinoid crisis after injection of 6-18F-fluorodihydroxyphenylalanine in a patient with metastatic carcinoid. J Nucl Med. 2005 Jul;46(7):1240-3

ABSTRACTS

J. T. Plukker, L. M. Schreurs, B. B. Pultrum, **K. P. Koopmans**, C. C. Verhoef, P. L. Jager, G. M. Van Dam, H. Groen, E. J. Van der Jagt. PET/CT fusion is more accurate than side-by-side PET/CT judgment in staging cancer of the esophagus and gastro-esophageal junction. 2007 Gastrointestinal cancers symposium.

K. P. Koopmans, Jan Willem de Groot, Ido Kema, John Plukker, Thera Links and Piet Jager. Value of 18Fluor-L-DOPA (DOPA) PET in the follow up of patients with biochemical evidence of medullary thyroid cancer. 2007 SNM annual congress Washington DC. *Oral presentation*.

K.P. Koopmans, E.G.E. de Vries, I.P. Kema, P.H. Elsinga, O.C. Neels, W.J. Sluiter, K Vanghillewe, A.H. Browers and P.L. Jager. 11C-5-HTP and 18F-DOPA PET superior for staging carcinoid and islet cell tumors. 2007 SNM annual congress Washington DC. *Oral presentation*.
K. P. Koopmans, E. G. E. de Vries, I. P. Kema, P. H. Elsinga, O. Neels, W. J. Sluiter, A. N. A. van der Horst - Schrivers, P. L. Jager; 18-F-DOPA PET for staging neuroendocrine tumors. 2006 EANM annual congress Athens. *Oral presentation*.

P.L.Jager, **K.P. Koopmans**, J.W.B. de Groot, I.P. Kema, JTM Plukker, T.P. Links
Value of 18Fluor-L-DOPA (DOPA) PET in the follow up of patients with biochemical evidence of medullary thyroid cancer. World Men Congress Marseille 2006.

K.P. Koopmans, E.G.E. de Vries, O. Neels, I.P. Kema, A.N. A. Van der Horst-Schrivers, P.H. Elsinga, P.L. Jager. 18-F-DOPA PET superior for staging of neuroendocrine tumors. 2004 SNM annual congress Toronto. *Oral presentation*.

K.P. Koopmans, F.W. Albers, I.P. Kema, M.N.Kerstens, P.L.Jager, R.P.Dullaart
Value of ^{111}-In-octreotide and ^{123}-I MIBG for the detection of paragangliomas – influence of serum and urine dopamine, metanefrine and normetanefrine levels on tracer uptake. 2004 SNM annual congress Toronto.